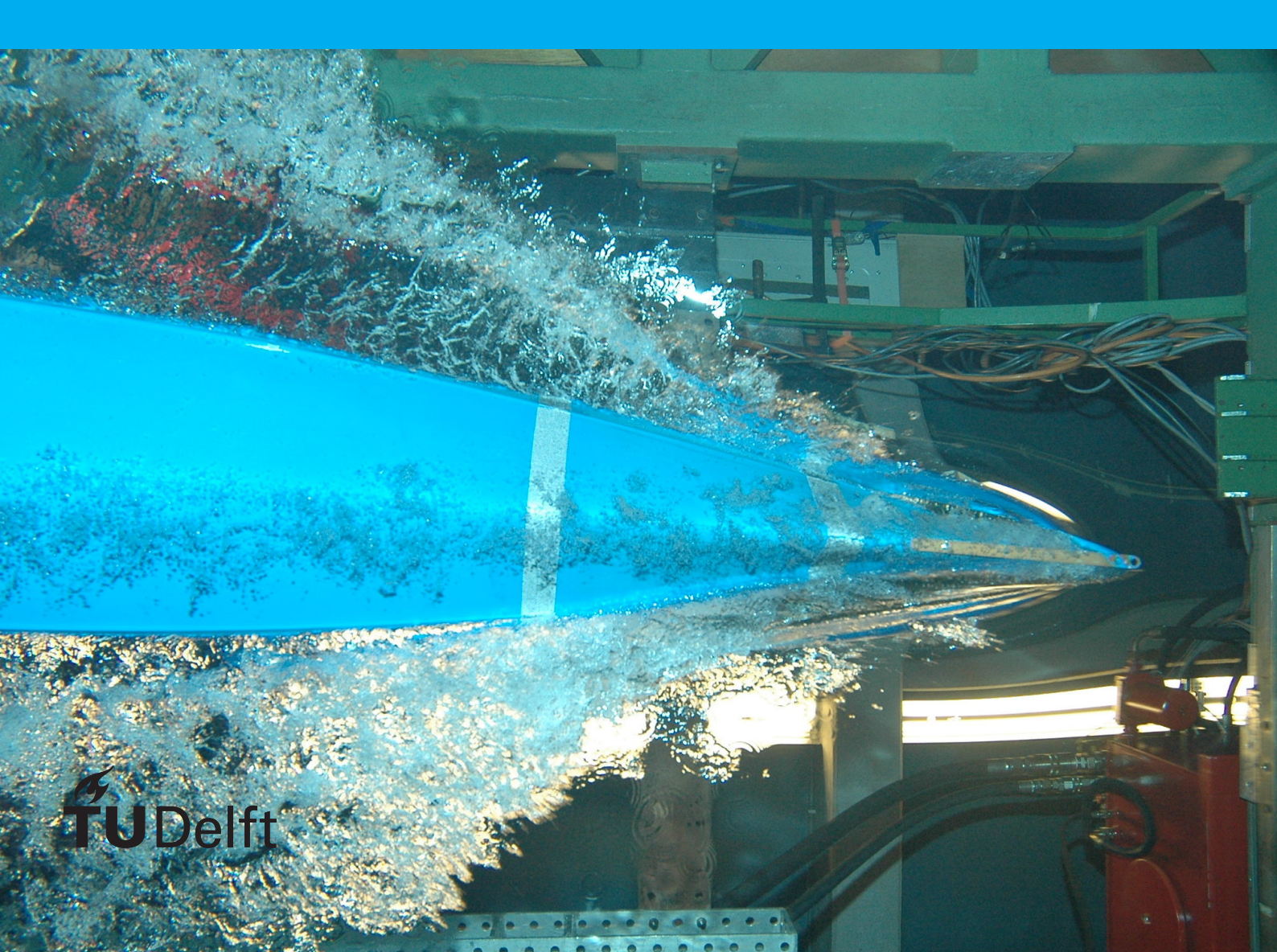
Vapors Transport in the Anode Baking Process

Master's Thesis

Master's program: Applied Mathematics

Specialization: CSE



Transport in the Anode Baking Process

by Narken Aimambet

to obtain the degree of Master of Science at the Delft University of Technology, to be defended publicly on March 28, 2019 at 9:00 AM.

Student number: 4626567

Project duration: April, 2018 – February, 2019

Thesis committee: Prof. dr. ir. Domenico Lahaye, TU Delft, supervisor

Prof. dr. ir. Arnold W. Heemink, TU Delft Prof. dr. ir. Kees Vuik, TU Delft

An electronic version of this thesis is available at http://repository.tudelft.nl/.



Abstract

Anode baking is a huge part of the Aluminum industry. The quality and characteristics of the anode blocks will be formed in the anode baking furnaces. The process itself is very expensive, time consuming and ecologically unfriendly. From the other hand, anode baking process can use its own waste as a secondary fuel source. Here, by waste we mean volatile gases from the baking process. In the factories, raw anode and baked anode are weighted before and after baking process. The difference in the weight counted as a released gas. In this work we will try to build a model and solve it that can find volume of the volatiles. Different parameters of the anode material will be included into the model, and analyzed to find insights how it can be used for future investigations. The results of this work will be compared with experimental results. Finally, recommendations for further works will be given.

Preface

This thesis is the compulsory part of my masters program in applied mathematics at TU Delft.

The topic 'Vapors Transport in the Anode Baking Process' was chosen because of my interest: how can we apply mathematics to solve real life problems. Fortunately, Prof. Lahaye leads PhD students who work in cooperation with AluChemie. So, he had good topic for me too.

First of all, I want to thank my supervisor Prof. Lahaye, for being patient and always guiding me. Moreover, thanks for time and consideration to professors who decided to be in my thesis committee. Furthermore, I am happy that I could present in front of Combustion group.

The last but not the least, I am grateful to my mother who gave me the opportunity to study abroad and travel. Also, I am thankful to my significant other for supporting me all the time.

Narken Aimambet Delft, February 2019

Contents

1	Intro	oduction	1
	1.1	Anode Baking	2
	1.2	The goal of the thesis	3
	1.3	Structure of the thesis	5
2	Prol	blem Formulation	7
	2.1	Mathematical model	7
	2.2	Boundary conditions	10
	2.3	Volatile gases	12
3	Dryi	ing of Textile	15
	3.1	Drying process	15
	3.2	Case 1	17
	3.3	Case 2	22
4	Hea	t Equation	25
	4.1	Analytical solution	25
	4.2	Thermal diffusivity	28
	4.3	Sigmoid Function	33
5	Hea	t Transfer through Anode Material	37
	5.1	Numerical solutions	38
		5.1.1 Robin Boundary Condition	47
		5.1.2 Homogeneous Neumann Boundary Condition	53
		5.1.3 Radiation factor	54
		5.1.4 Non-constant boundary condition	56
6	Con	clusion - Discussion - Recommendation for Future Work	61
Bi	blioa	ıraphy	69

1

Introduction

Aluminum is produced by electrolysis. The anodes used in the process wear over time and need to be replaced regularly. Anodes are manufactured by baking raw material in industrial furnaces. Heat is produced in the furnace by the combustion of the natural gas and air. This combustion is similar as in a bunsen burner or a gas cooker. The heat transferred indirectly to the raw material through a hot wall as schematically represented in Figure 1.4. During baking, the anode acquires its desired properties of strength, hardness, density and electrical conductivity. The anode raw material also looses an amount of liquid fraction during baking. The chemical composition of these vapors makes then suitable a fuel for the combustion in the furnace. The objective of this thesis is to contribute to the quantification of the infiltration of these vapors in the furnace.

2 1. Introduction

1.1. Anode Baking

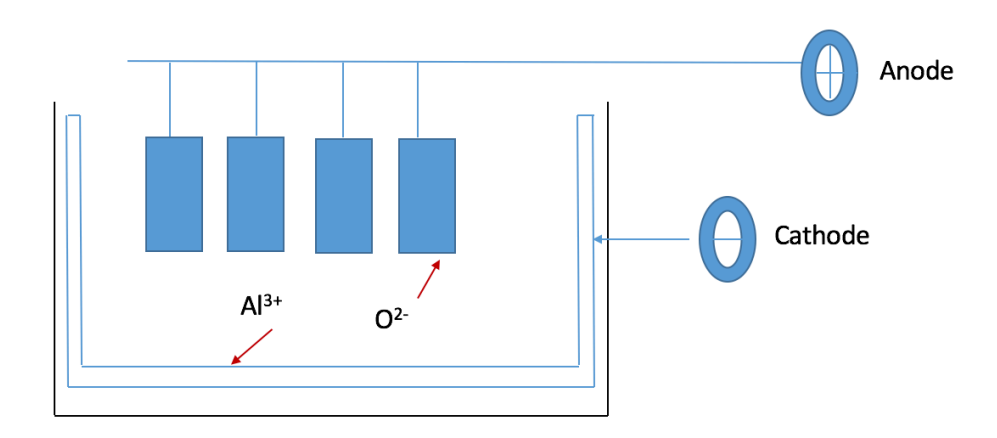


Figure 1.1: Schematic representation of the electrolyze process used in the production of aluminum. The figure shows the deposition of O_2 at the anode and of Al_3 at the cathode.

Aluminum is not naturally occurring element (only in very rare circumstances). However, in the nature it is circulated as Aluminum Oxide (Al_2O_3) . In order to get pure metal from its Oxide, electrolyze process must be done. Electrolyze is the process where substance will be separated into an anions and cations. While, for the electrolyze process anode is needed, and it is used for oxidation. Whereas, after oxidation, anode can not be used again. Thus, you may imagine the amount of anode production, and its importance in Aluminum industry. For the production of one ton of aluminum, approximately 400 kg of anode is needed [14]. As shown in Figure 1.1, anodes are a carbon blocks, which has specific physical and chemical properties. To acquire right properties, there are some important things need to be considered, such as:

- 1. Appropriate (smooth or homogeneous) temperature distribution in the pit to have stable anode characteristics
- 2. Control volatile gases to save in energy costs
- 3. Regulate cooling process and minimize packing coke amount

More than four decades, R&D scientists try to research, understand and improve backed anode quality, reduce carbon emission and make the anode baking cheaper [19], [24], [25]. In order to get good properties, raw carbon paste will be placed into rectangular blocks and baked around 14 days. These 14 days consist of pre-heating, heating and cooling phases. Furthermore, interest of this work is the first 240 hours, when pre-heating and heating phases occur.

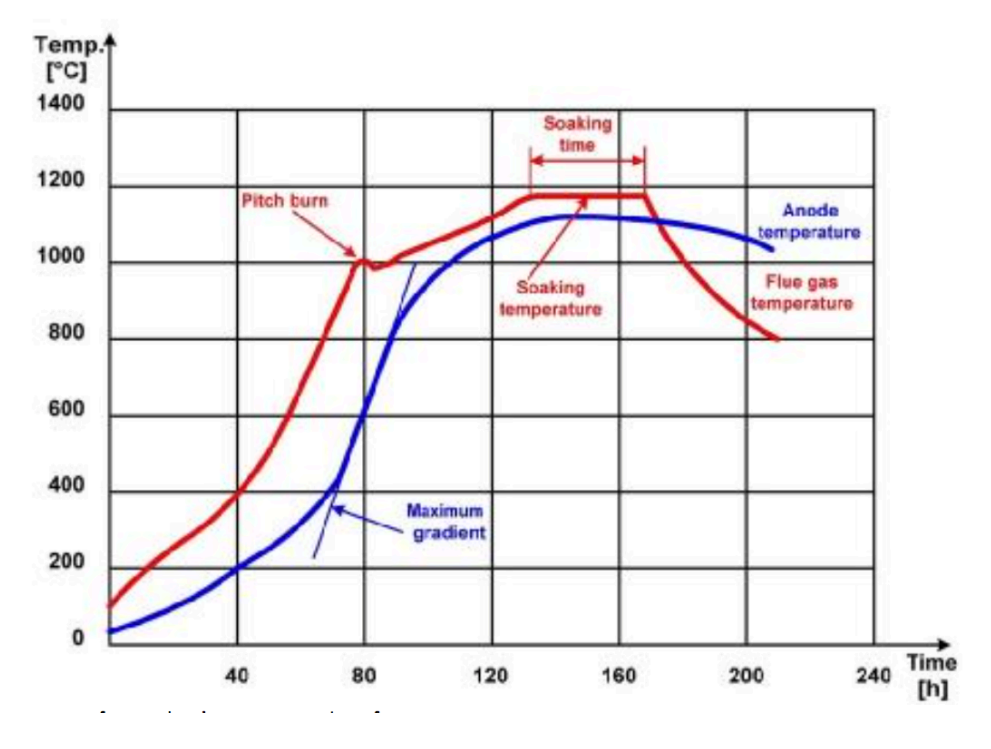


Figure 1.2: Temperature of the anode and the flue gas as a function of time in the pre-heating and heating phase. The figure shows how the anode heats up due to the hot flue gas [4].

According to the Figure 1.2 we can assume that heating phase lasts for approximately 120 hours and max temperature rises to 1473 Kelvin.

1.2. The goal of the thesis

It is essential to investigate and understand the vapor transport during the anode baking process. During the anode baking process there are different processes occur, such as combustion, chemical reactions and heat exchange between surrounding and anode. In the anode baking process, there are three types of heat sources. First one is fuel in the furnace from outside, which is for heating the furnace. Second is the gases released from anode itself. Finally, heat from packing coke. However, the goal of this work is to model the transition of gaseous vapors from the anode material into the furnace. This transition occurs through the walls of the furnace. According to Figures 1.4 and 1.5, anode material placed between two hot walls. The vapors act as a secondary fuel for the combustion process. Thus, it is essential to calculate the volume of these gases, and look at the dynamics of desired gases in time and location dimensions.

4 1. Introduction



Figure 1.3: View of the anode baking furnace in operation the factory. The front view show the packing coke covering the anodes. The rear view shows empty pits [12].

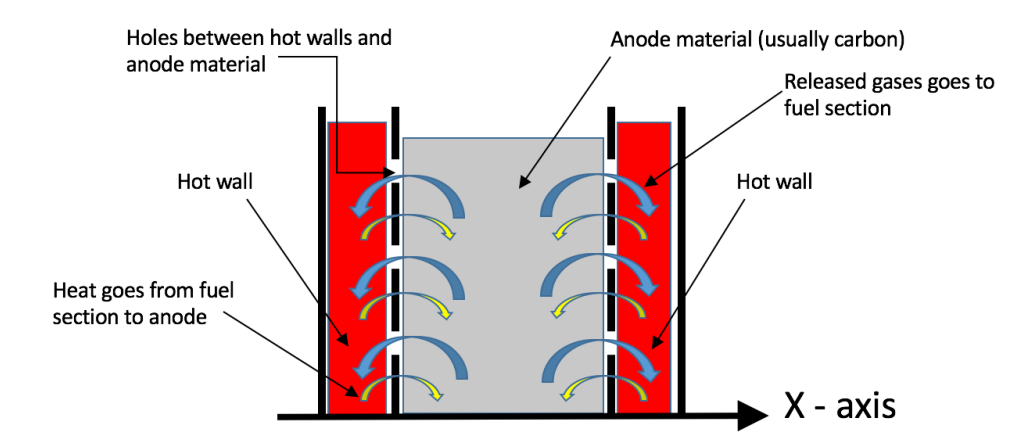


Figure 1.4: Anode baking furnace, sliced view. The grey area stands for anode block and the red areas mean heating source, which is inside the wall. Also, you may notice holes between anode block and furnace.

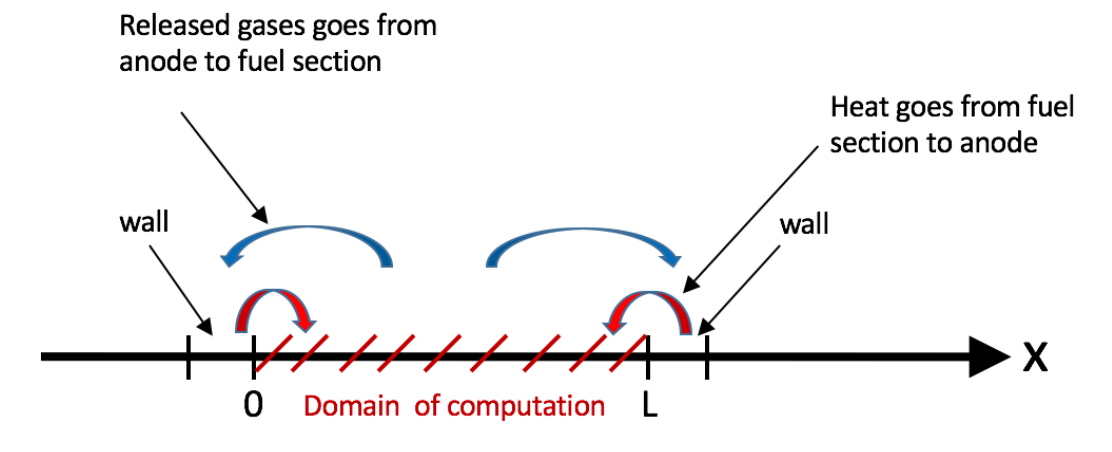


Figure 1.5: Anode baking furnace, sliced view (1D case).

TU Delft cooperates with AluChemie (producer of high-quality anodes for the aluminum industry)

in order to optimize anode baking process. Moreover this work occurs to be the subset of the context of PhD project of Prajakta Nakate. Her thesis focuses on the combustion in the furnace (in the hot walls), without concern of the pit. While, my work directed to volatile gases in the pit, without consideration of combustion in the furnace.

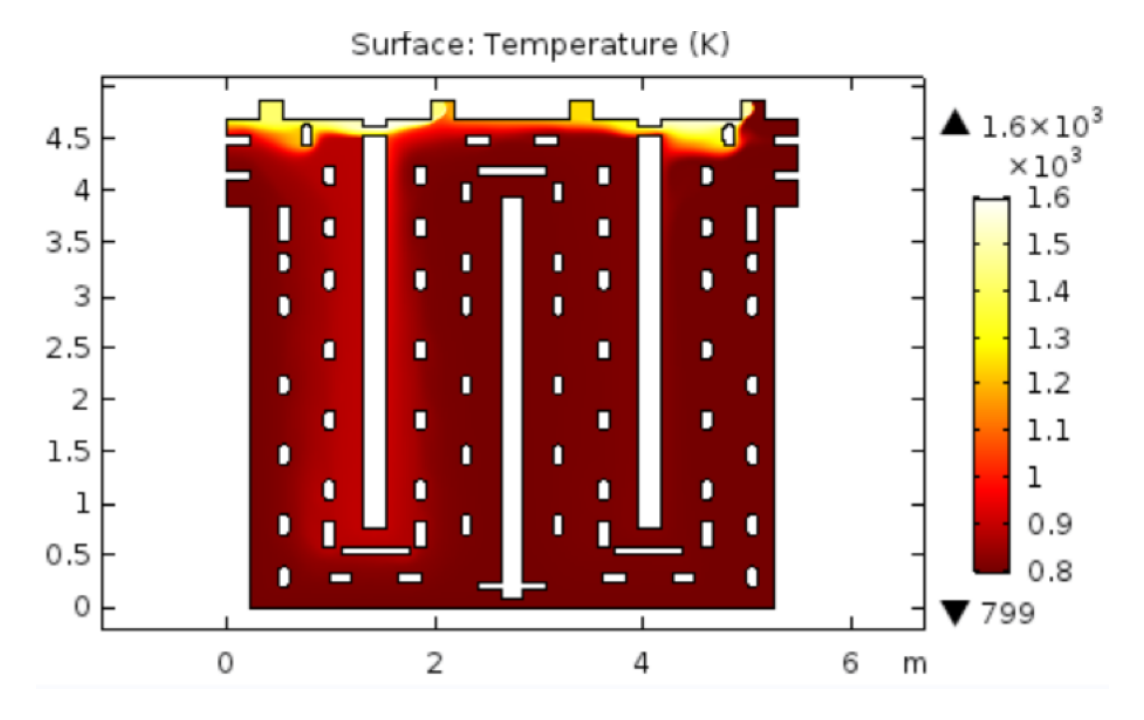


Figure 1.6: Structure of the wall. The picture shows, how the wall is constructed from inside.

The Figure 1.6 taken from Prajakta's presentation, where the yellow color stands for fire. From the graph, the fire arises only at the top of the furnace. However, taking into account released gases from the pit, we expect additional source of fire from the bottom part. Consequently, this work is complementary research to Prajakta's PhD thesis. Please note that in this project we will not consider chemical composition of the volatile gases and combustion in the furnace.

1.3. Structure of the thesis

The outline of this project will be as following. First, the formulation of the mathematical model will be presented, where the system of equations and its parameters going to be described. Also, different boundary conditions will be introduced. The next chapter is about drying of textile. Here, we will reproduce the results from the paper [21], and compare them with the paper's outcome. In order to check how works the model, and to be sure about up-coming results in anode baking. Chapter 4 will be about heat equation only. Due to the reason that, the domination factor of the baking process is a heat exchange. We are going to solve heat equation analytically and apply non-constant diffusion coefficients. Then, chapter 5 is about heat and vapor transfer through the anode material. Mostly, numerical results and their explanations will be shown in this chapter. Finally, we have conclusion, discussion and recommendations, where we will finalize this work.

Problem Formulation

2.1. Mathematical model

Henry described heat and moisture conservation with a system of nonlinear differential equations [17]. First two equations contain mass and heat diffusion, third is the equation of the moisture in the material fibers. In order to derive the solution, he proposed several assumptions to simplify the non-linear problem [16]. The conservation of heat and moisture can be expressed by the following equations:

$$\begin{cases} \epsilon \frac{\partial C_A}{\partial t} = \frac{D\epsilon}{\tau} \frac{\partial^2 C_A}{\partial x^2} + v \frac{\partial C_A}{\partial x} & \underbrace{-(1-\epsilon) \frac{\partial C_F}{\partial t}}_{\text{extract moisture}} \\ \rho C_v \frac{\partial T}{\partial t} = K \frac{\partial^2 T}{\partial x^2} & + \lambda \frac{\partial C_F}{\partial t}_{\text{latent heat sink}} \end{cases}$$
(2.1)

 $_{
m where}$

- 1. C_A is a moisture content in the air pores of the material
- 2. T is the temperature
- 3. C_v and λ can be considered as a functions of moisture content in a matter or as a constant values. Also, these two equations are nonlinear and has three unknowns. Thus, third equations (so called rate equation) must be constructed in order to solve the system. According to David and Nordon, the rate of moisture exchange is proportional to the relative humidity difference [23]. The third equation is [15]:

$$\frac{1}{\rho(1-\epsilon)}\frac{\partial C_F}{\partial t} = k(y_A - y_F) \tag{2.2}$$

Where C_F is a moisture content in the material fibers, $y_A = \frac{C_A RT}{P_S}$ is a relative humidity of the air, $y_F = \frac{C_F}{\rho(1-\epsilon)}$ is the equilibrium relative humidity of the fiber and k is so called the constant between 0.01 and 10. As we can see, rate equation depends on several parameters, such as saturation vapor pressure,

8 2. Problem Formulation

ideal gas constant and temperature.

Further, let us consider relation between humidity of the air and saturation vapor pressure. To be specific, relative humidity of the air is inversely proportional to saturation vapor pressure $y_A \sim \frac{1}{P_s}$. Accordingly, the higher saturation vapor pressure is, the lower relative humidity of the air is; or the lower saturation vapor pressure is, the higher relative humidity of the air is. Which make sense, if the vapor pressure is high in the air pores, then the water drops has a transition difficulties from the fibers into the air pores, because high pressure presses the walls of the pores. On the other hand, humidity of the air proportional to the temperature $y_A \sim T$. Again, it is reasonable fact, because high temperature pushes the water in the fibers to leave the fibers, and these water drops goes into the air pores of the material. Moreover, we may ask why there is no diffusion term in the rate equation? It is due to the fact that the mass transport occurs in air pores, but not in the fibers. The reason is that water vapor first of all goes into the air pores of the material and then moves further. Thus, there is no diffusion in the fibers of the material.

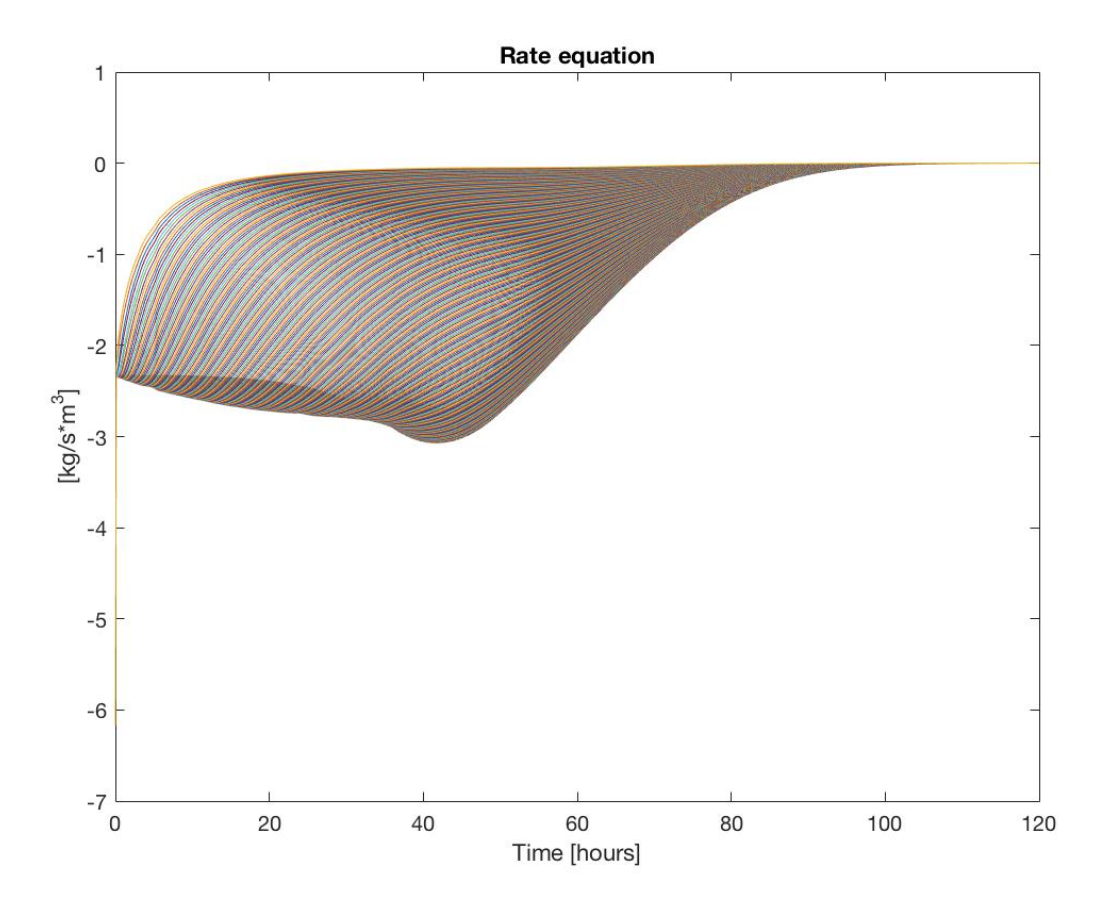
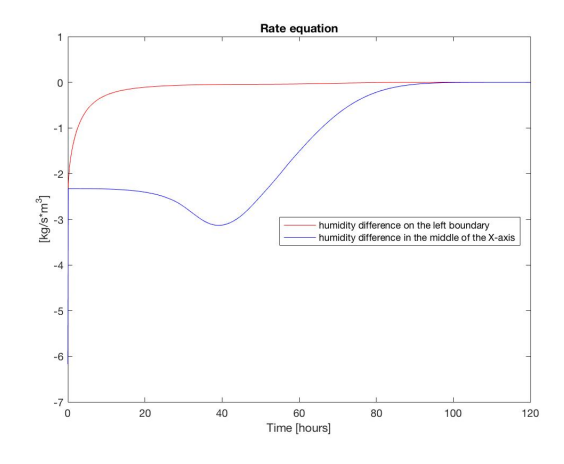
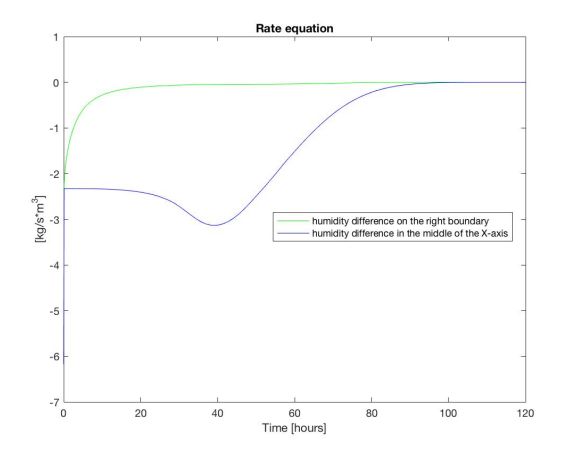


Figure 2.1: The rate equation. Image of $\frac{1}{\rho(1-\epsilon)}\frac{\partial C_F}{\partial t}=k(y_A-y_F)$

2.1. Mathematical model 9





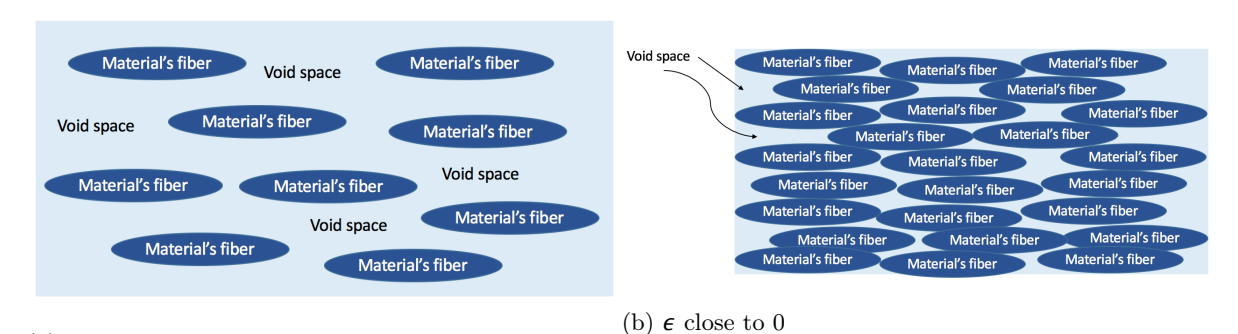
- (a) Rate equation in the left boundary and middle
- (b) Rate equation in the right boundary and middle

Figure 2.2: Rate equation

The Figure 2.1 is the representation of the third equation from the model. As we know, rate equation is a difference of two relative humidities. The Figure 2.2 is also the humidity difference, but here we can see behavior of humidity difference in exact points along the length of the domain. In the Figure 2.1 it is shown that after long time, difference of two humidities is zero. Which means that finally humidity conditions of two environments (environment of air pores and fibers) are the same, and there is no need of transport of water vapors from fibers into void space.

Furthermore, ϵ (porosity) plays not the last role in this mathematical model [8], [9]. Porosity appeared twice in the mass transfer equation and in the the rate equation. By definition, porosity is the fraction of the volume of the empty space (pores or void space) over the entire volume of the body (material, bulk) $\epsilon = \frac{V_{emptyspace}}{V_{entirebody}}$. Thus, porosity can be between 0 and 1. If porosity is zero, there are no air pores in the material. As well as, if the value of ϵ close to one, there are a lot of void space and a little fibers. Consequently, water vapor diffusion depends on porosity. The water vapor diffusion goes faster in air pores, thus in the materials with high porosity mass transport is rapid. The Figure 2.3 shows schematic view of the material with two different porosity. Obviously, void space provides all the convenient conditions for mass diffusion. In this model we assume that any amount of released moisture can be observed by the void space of the body. Thus, theoretically our model is linear. However, sometimes there could be limitations of the empty space and some part of vapor could stuck in the material fibers. Of course, it will affect on the time of baking process. To be specific, it is going to slow down the process.

10 2. Problem Formulation



(a) ϵ close to 1

Figure 2.3: Two types of material, (a) with plenty of void space and (b) with few void space. In (a) water drops will move freely and fast, in (b) it will take a time to transport the mass.

2.2. Boundary conditions

In this work different types of boundary conditions were applied. As it was mentioned before, the anode paste located between two hot walls. According to this information, the simplest boundary condition which can be applied is Dirichlet boundary condition for temperature equation.

$$\begin{cases} \frac{\partial C_A(L,t)}{\partial x} = -h_m(C_A - C_e) \\ T(L,t) = -T_{wall} \\ \frac{\partial C_F(L,t)}{\partial x} = 0 \\ \frac{\partial C_A(0,t)}{\partial x} = h_m(C_A - C_e) \\ T(0,t) = T_{wall} \\ \frac{\partial C_F(0,t)}{\partial x} = 0 \end{cases}$$
(2.3)

The boundary conditions of C_A represents proportionality of the mass flux on the boundaries to the difference in the moisture concentration between surrounding environment and the material surface [16]. Here, $T_{wall} = 1473$ Kelvin and $C_e = 0$. The initial conditions are $C_A = 0$, $C_F = 0.15$ and $T_{initial} = 350$ Kelvin, and we will keep these initial conditions for further cases.

After that, the Robin boundary condition will be used in heat equation.

$$\begin{cases} \frac{\partial C_A(L,t)}{\partial x} = -h_m(C_A - C_e) \\ \frac{\partial T(L,t)}{\partial x} = -h_{heat}(T - T_{wall}) \\ \frac{\partial C_F(L,t)}{\partial x} = 0 \\ \frac{\partial C_A(0,t)}{\partial x} = h_m(C_A - C_e) \\ \frac{\partial T(0,t)}{\partial x} = h_{heat}(T - T_{wall}) \\ \frac{\partial C_F(0,t)}{\partial x} = 0 \end{cases}$$

$$(2.4)$$

The boundary conditions above represents proportionality of the heat flux on the boundaries to the difference in the temperature between surrounding environment and the material surface, as well as

mass flux to the difference in moisture concentration between surrounding environment and the material surface [16]. As you may notice, the boundary conditions for moisture of the air pores (C_A) and the material fibers (C_F) have not changed, because these are the most appropriate boundary conditions for them. Specially, Neumann boundary condition for C_F was chosen by us. Due to the reason that in the most of the cases, Neumann boundary condition is a natural boundary condition.

For instance, $-\frac{\partial^2 u}{\partial x^2} = f$ $\frac{\partial u}{\partial x}|_0 = 0$ $u|_1 = 0$ In order to get weak form, we need to multiply both sides of the differential equation by the test function v and integrate it over the computation domain. Then we get $\int_0^1 v(\frac{\partial^2 u}{\partial x^2} + f) dx = |applying| integration by parts| = <math>v \frac{\partial u}{\partial x}|_0^1 - \int_0^1 \frac{\partial v}{\partial x} \frac{\partial u}{\partial x} dx + \int_0^1 v f dx = 0$. We get $v \frac{\partial u}{\partial x}|_0 = 0$ and $v \frac{\partial u}{\partial x}|_1 = 0$ because test function v satisfies the Dirichlet boundary condition. Thus, we do not need to do anything further, because we have exactly $-\int_0^1 \frac{\partial v}{\partial x} \frac{\partial u}{\partial x} dx + \int_0^1 v f dx = 0$ weak form of the PDE. In this case, linear space $\chi = \{u \in H^1, u|_1 = 0\}$. Accordingly, we can have a weak form satisfied Neumann boundary condition without enforcing it [18].

The next is homogeneous Neumann boundary condition applied on the heat equation. This is a little bit unusual, but it was done for the following reason. We wold like to isolate anode block, to check the role of parameter λ .

$$\begin{cases} \frac{\partial C_A(L,t)}{\partial x} = -h_m(C_A - C_e) \\ \frac{\partial T(L,t)}{\partial x} = 0 \\ \frac{\partial C_F(L,t)}{\partial x} = 0 \\ \frac{\partial C_A(0,t)}{\partial x} = h_m(C_A - C_e) \\ \frac{\partial T(0,t)}{\partial x} = 0 \\ \frac{\partial C_F(0,t)}{\partial x} = 0 \end{cases}$$

$$(2.5)$$

Fours boundary conditions for temperature equation is still Robin, but with radiation term.

$$\begin{cases} \frac{\partial C_A(L,t)}{\partial x} = -(C_A - C_e) \\ \frac{\partial T(L,t)}{\partial x} = -(h_{heat}(T - T_{wall}) + h_e(T^4 - T_{wall}^4)) \\ \frac{\partial C_F(L,t)}{\partial x} = 0 \\ \frac{\partial C_A(0,t)}{\partial x} = (C_A - C_e) \\ \frac{\partial T(0,t)}{\partial x} = h_{heat}(T - T_{wall}) + h_e(T^4 - T_{wall}^4) \\ \frac{\partial C_F(0,t)}{\partial x} = 0 \end{cases}$$

$$(2.6)$$

Where h_e stands for radiation constant.

The last boundary condition is the Robin boundary condition with wall temperature as a function of

12 2. Problem Formulation

time.

$$\begin{cases} \frac{\partial C_A(L,t)}{\partial x} = -h_m(C_A - C_e) \\ \frac{\partial T(L,t)}{\partial x} = -T_{wall} \\ \frac{\partial C_F(L,t)}{\partial x} = 0 \\ \frac{\partial C_A(0,t)}{\partial x} = h_m(C_A - C_e) \\ \frac{\partial T(0,t)}{\partial x} = T_{wall} \\ \frac{\partial C_F(0,t)}{\partial x} = 0 \end{cases}$$

$$(2.7)$$

where $T_{wall} = 294 * log(4 + t)$.

One of the most important things are the parameters, which were used in computations. The table below shows numerical values of the parameters.

Table 2.1: Numerical values and the physical units of the anode material [13]

Parameter	Formula	Unit
K	3.5 – 5	$kg * m/s^3K$
C_v	$175.03 + 20.04T - 6 * 10^{-4}T^{2}$	m^2/s^2K
λ	2260	m^2/s^2
ϵ	0.2	-
ρ	1600	kg/m^3
τ	1.5	-
D	2.49e – 5	m^2/s
P_{S}	$exp(20.386 - \frac{5132}{T})$	$kg/m * s^2$ $m^2/K * s^2$
R	461	$m^2/K * s^2$

2.3. Volatile gases

Finally, the aim of this work is find an amount of released gases. Hence, somehow the volume of volatile vapors should be quantified. Thus, let us start from finding a mass flux. If the equation has the form:

$$\frac{\partial c}{\partial t} = \nabla \cdot (D\nabla c) - \nabla \cdot (vc) + Q \tag{2.8}$$

where

c is desired variable (in our case \mathcal{C}_A moisture content in void space)

D is diffusion coefficient

v is the velocity of c

Q is a sources or sinks of the c

Fortunately, equation of C_A is exactly in the form as above. Thus, we can use common formula for total flux, which is:

$$j = j_{diffusive} + j_{advective} = -D\nabla C_A + vC_A \tag{2.9}$$

2.3. Volatile gases

where j is total flux, $j_{diffusive}$ is diffusive flux and $j_{advective}$ is advective flux. Flux in here has the following units:

$$\frac{m^2}{s} \frac{kg}{m^3} \frac{1}{m} - \frac{m}{s} \frac{kg}{m^3} = \frac{kg}{sm^2}$$
 (2.10)

Further, the flux going to be multiplied by the area of the holes, which are adjacent to the anode blocks, and it results in $\frac{kg}{sm^2}*m^2=\frac{kg}{s}$. Moreover, flux flows all the time of the process, so we integrate it over time, and this is how we get amount of released gases in $\frac{kg}{s}*s=kg$. The most important thing is that flux was computed on the boundaries.

3

Drying of Textile

3.1. Drying process

In order to start such a complex model as an anode baking, it is better to look at a given cases. For instance, how drying process goes on in textile industry. Thus, we tried to repeat the results of the paper "An Improved Mathematical Simulation of the Coupled Diffusion of Moisture and Heat in Wool Fabric" by Yi Li and Zhongxuan Luo [21]. Considering, the drying process is an integral part of the anode baking, due to the simple reason that when we apply heat through anode baking, the moisture in the material will evaporate, which is the drying process. We start from drying process.

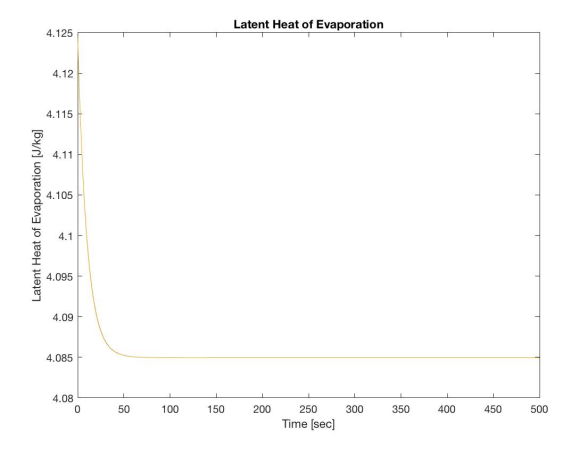
One of the most important processes in the textile industry is a Drying Process. Here, we will consider mathematical model of heat and moisture transfer in the wool fabric, which was proposed by Henry. In simple words, drying implies to decrease amount of moisture or completely de-moisturize. In this work, we use the following as a definition of drying: vaporization of water from a fabric. The drying process has 2 periods: warm-up period and constant rate period. Warm-up period means the beginning period of the process, when the material gains heat. In this period, drying rate is low, sometimes, can be negative due to the liquid gas used for heating. Constant rate period is the last period of heating, when material is heated to its maximum and drying is in its peak level [16].

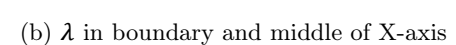
16 3. Drying of Textile

Table 3.1: Numerical values of the fabric and the physical properties

Param.	Formula	Unit
K	$(38.493 - 0.72W_c + 0.113W_c^2 - 0.002W_c^3) \times 10^{-3}$	kJ/m°C
C_v	$373.3 + 4661W_c + 4.221T$	kJ/kg°C
λ	$1602.5 \exp(-11.72W_c) + 2522$	kJ/kg
ϵ	0.925	-
ρ	1320	kg/m^3
h_m	0.137	m/s
h_{heat}	99.4	kJ/m ² °C
τ	1.2	-
D	2.49×10^{-5}	m^2/s
P_{S}	$4.6 + 0.33(T - T_0) + 0.01(T - T_0)^2 + 0.13(T - T_0)^3 + 10^{-3} + 0.42(T - T_0)^5 + 10^{-5}$	kg/m²
R	461	J/kg°C

where $W_c = \frac{c_F}{\rho} = \frac{kg}{m^3} \frac{m^3}{kg}$, which does not have a units [21].





450

100 150

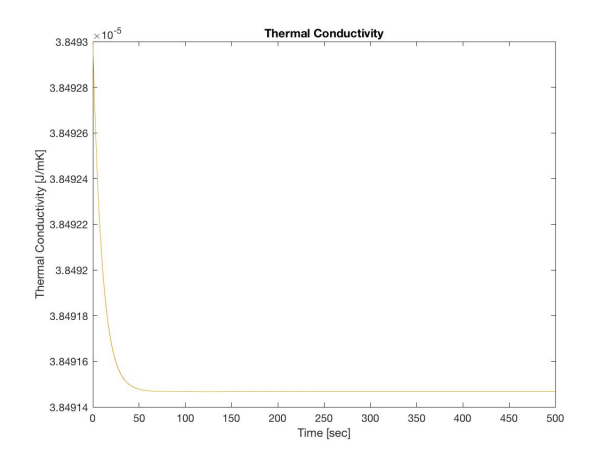
Latent Heat of Evaporation [J/kg] 4.11 4.095

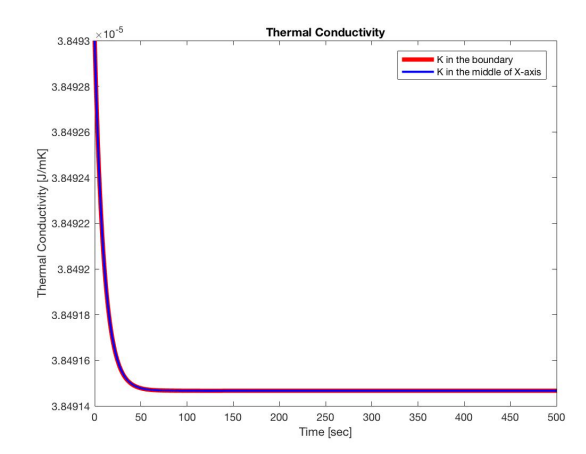
4.085

(a) λ along all the points of the X domain

Figure 3.1: Latent Heat of Evaporation

3.2. Case 1 17

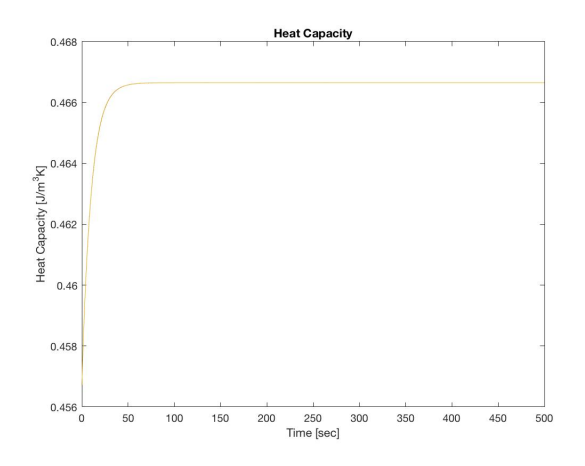


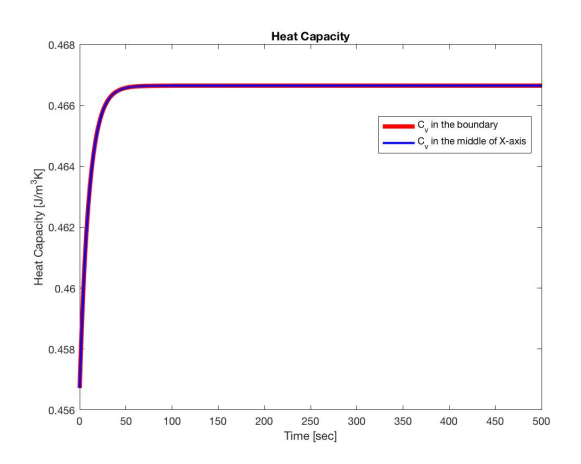


(a) K along all the points of the X domain

(b) K in boundary and middle of X-axis

Figure 3.2: Thermal Conductivity





(a) C_v along all the points of the X domain

(b) C_v in boundary the middle of X-axis

Figure 3.3: Heat Capacity

The Figures 3.1 - 3.3 represents different parameters from the drying model. To be specific, latent heat of evaporation, thermal conductivity and heat capacity are shown. As we can see, these parameters changed with time and position. However, the changes are very small. Especially, these changes are invisible along X domain of the computation, which means, these parameters have the same values, for example on x = 5cm and x = 30cm. Thus, actually we can replace them by constant values. Moreover, it would not make obvious effect on the final result of the model.

3.2. Case 1

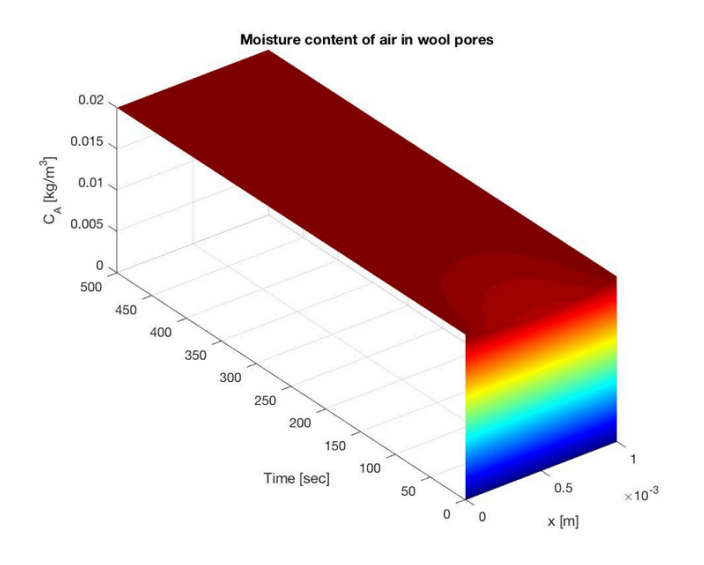
Computations were done by Matlab PDE solver, the details given in Appendix 1. As initial conditions, we take $T(x,0) = 20^{\circ}C$, $C_A = 0$ and $C_f = 0$. Boundary conditions are the same as in equation 2.4. The figures below are comparison between our results and results from the paper. We observed that

18 3. Drying of Textile

the profiles of all three variables have the same shape. However, the values are not equal. This could be because of our equation 2.2, which is from the paper [15], while, here we are trying to re-do the paper [21]. In addition, some parameters are not alike. The following table shows the sources of the parameters, that we presented in the Table 3.1.

Table 3.2: Reference table for parameters

Sources	Parameters
[21]	$K, C_v, \lambda, \epsilon, \rho, h_m, h_e, \tau$
[23]	P_{S}
[6]	R
[16]	D



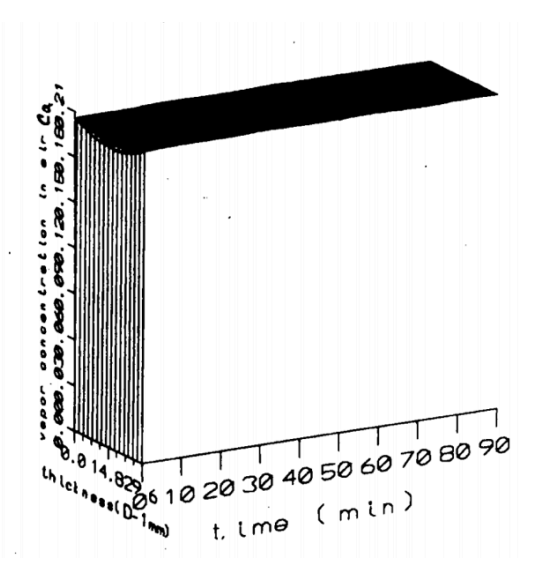


Figure 3.4: Moisture content of air in wool pores

The figure 3.4 demonstrates the moisture content in the air pores of the wool textile, from where we can conclude that the transportation of the water vapor in the air pores is extremely rapid. As mentioned before, initial condition for \mathcal{C}_A was zero. However, right after new surrounding was applied, water vapor concentration in the air pores arrived to the steady state solution sharply. Moreover, this behavior of the moisture content in air pores does not contradicts to the Wehner's result [21].

3.2. Case 1 19

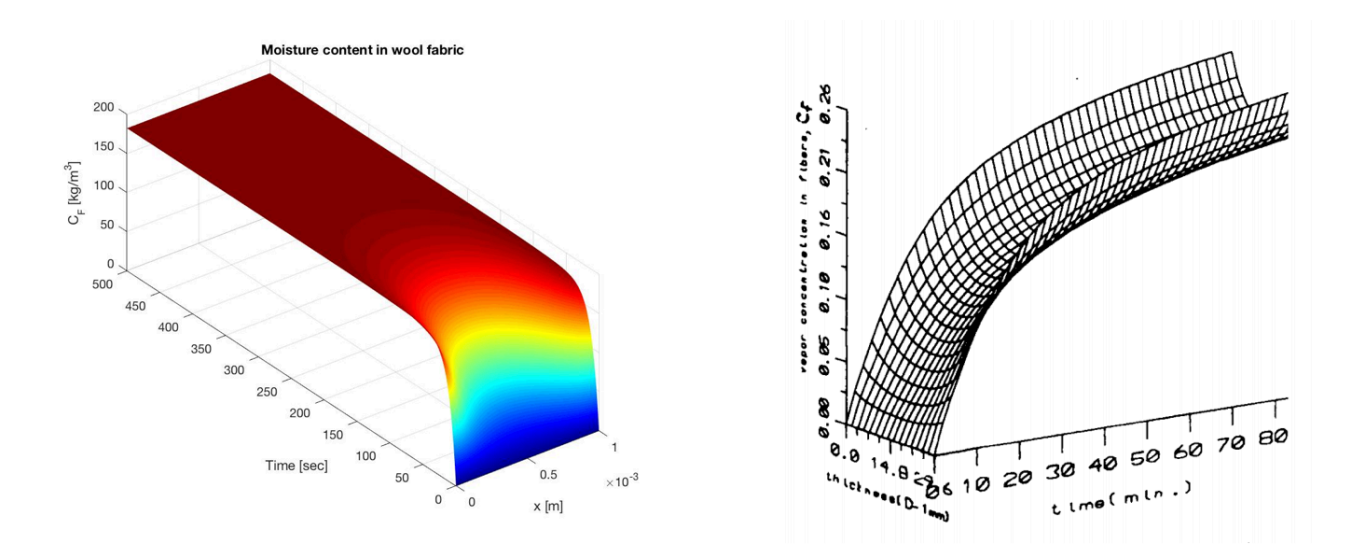


Figure 3.5: Moisture content in wool fabric

In the meantime, figure 3.5 presents the moisture content in the wool fibers. From the graphs above, we can say that the moisture diffusion in the fibers goes slower than in air pores. Nonetheless, we can see that the results are differ. The difference comes from Li and Luo [21] using two-stage sorption in wool fibers. While in this work was used simplified case of the rate equation as in Haghi [15].

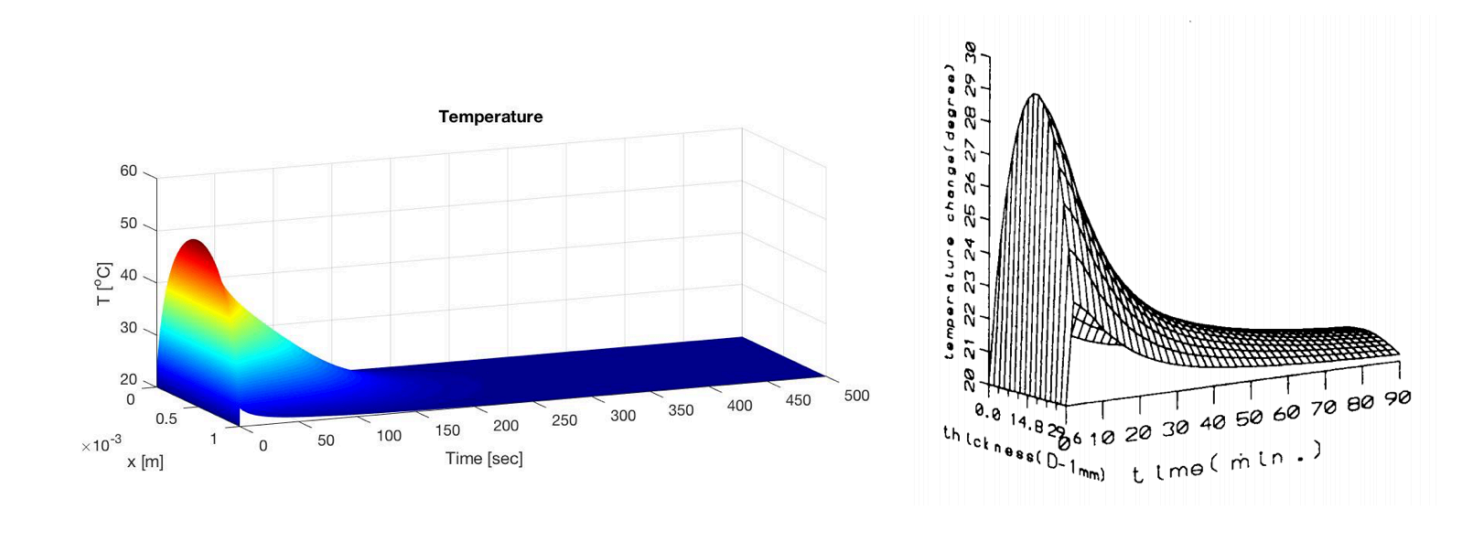


Figure 3.6: Temperature

In the Figure 3.6 the temperature profile is given. According to temperature graph, the heat distribution is not uniform. The reason of this non-uniformity could be non-uniform behavior of the moisture content in the fibers. When dispersion of heat is difficult it makes moisture sorption by wool fibers slow [21].

20 3. Drying of Textile

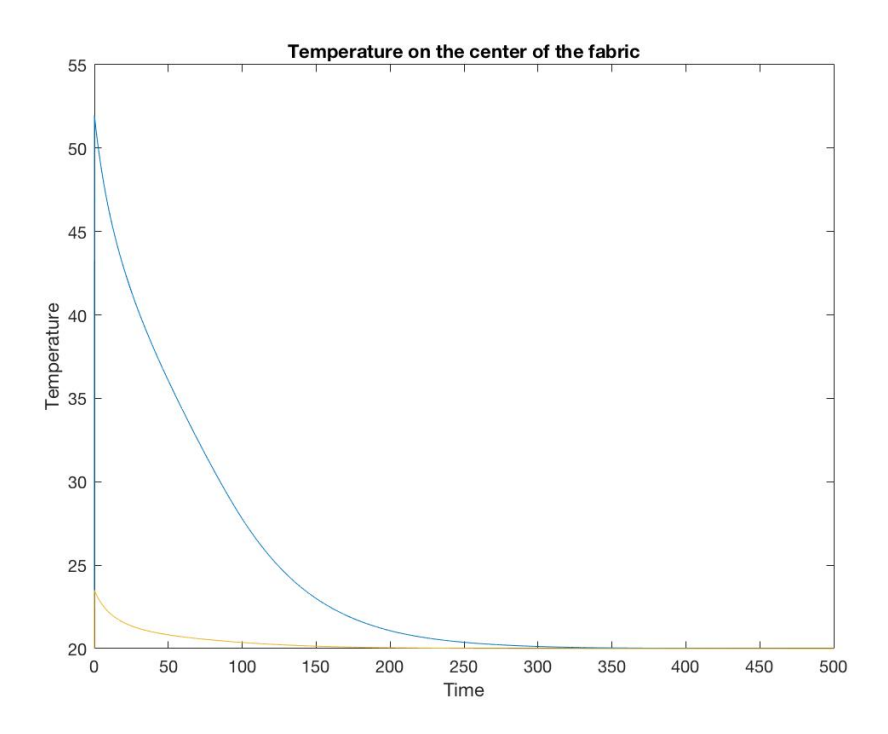


Figure 3.7: $T[{}^{\circ}C]$ - Temperature (time in seconds)

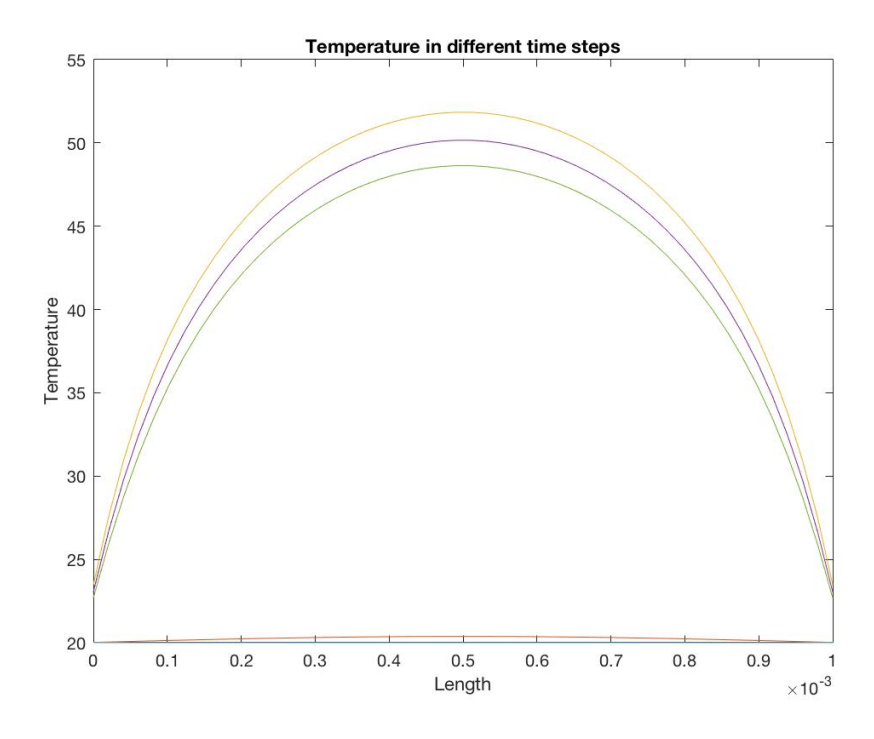


Figure 3.8: $T[^{\circ}C]$ - Temperature (length in meters)

The Figure 3.9 shows the influence of the thermal conductivity on temperature profile. Where small stands for $(38.493-0.72W_c+0.113W_c^2-0.002W_c^3)\times 10^{-6}$, actual is $(38.493-0.72W_c+0.113W_c^2-0.002W_c^3)\times 10^{-3}$ and large is $38.493-0.72W_c+0.113W_c^2-0.002W_c^3$. As we can see, the larger thermal

3.2. Case 1 21

conductivity the faster diffusion process takes place. Hence, the shape of temperature profile is more rectangular. Which means temperature spreads fast.

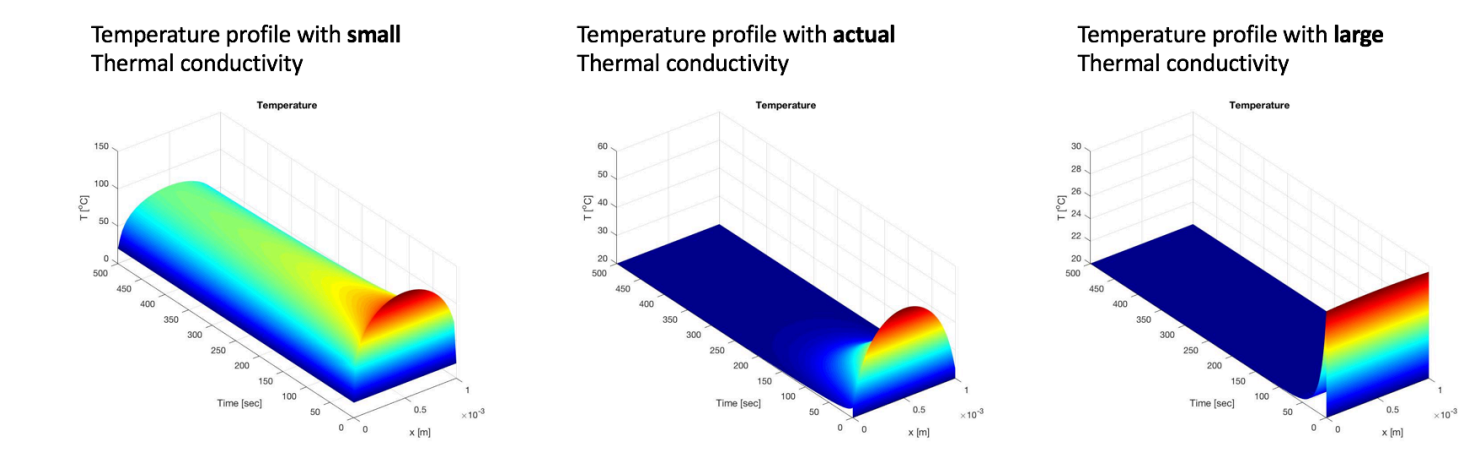


Figure 3.9: Temperature profile with different Thermal conductivity

The Figures 3.10-3.12 shows the influence of the rate constant k from 2.2. From here we can conclude that, the temperature profile goes to the steady state solution faster with higher rate constant. Which make sense, due to the fact that the rate equation plays the role of the heat source (like a sink).

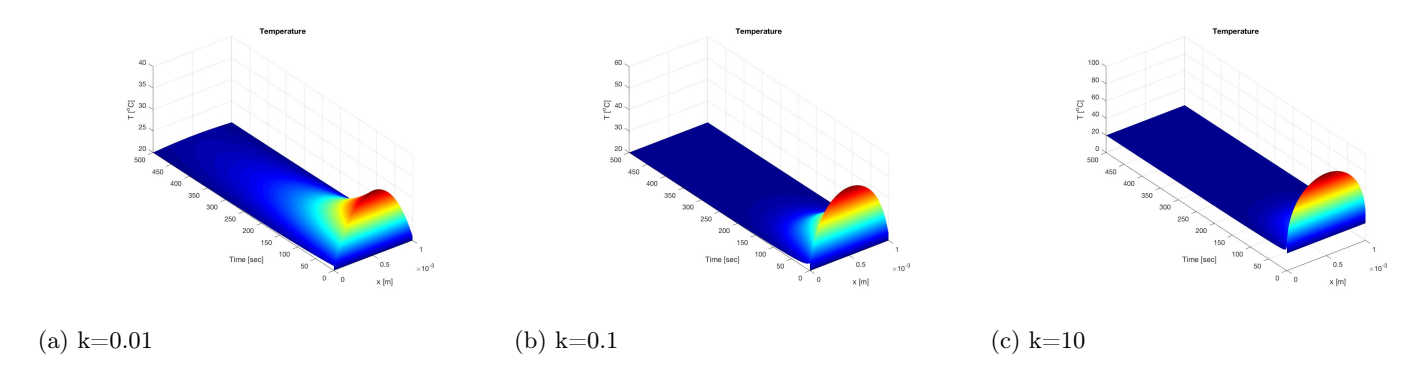


Figure 3.10: Temperature profile with different rate constants

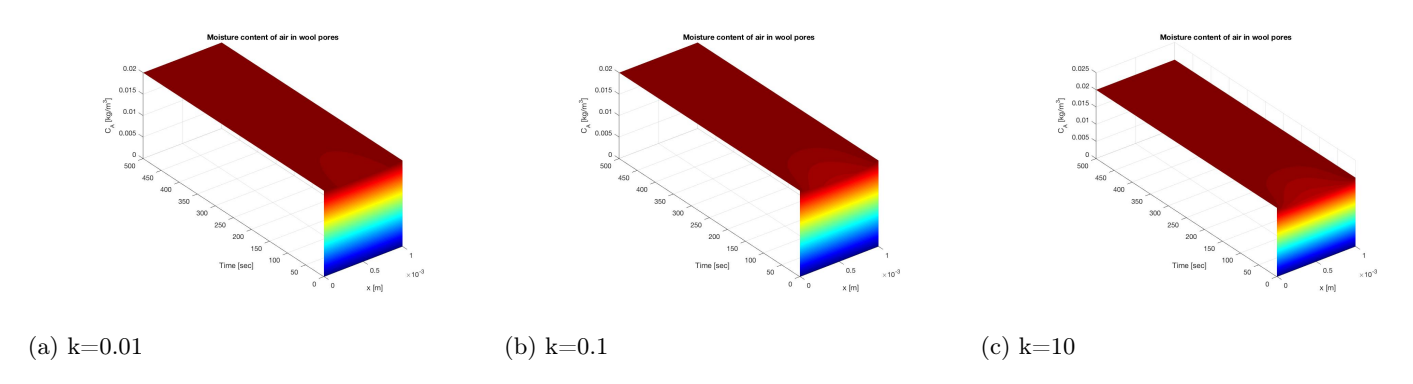


Figure 3.11: Moisture content of air in wool pores with different rate constants

22 3. Drying of Textile

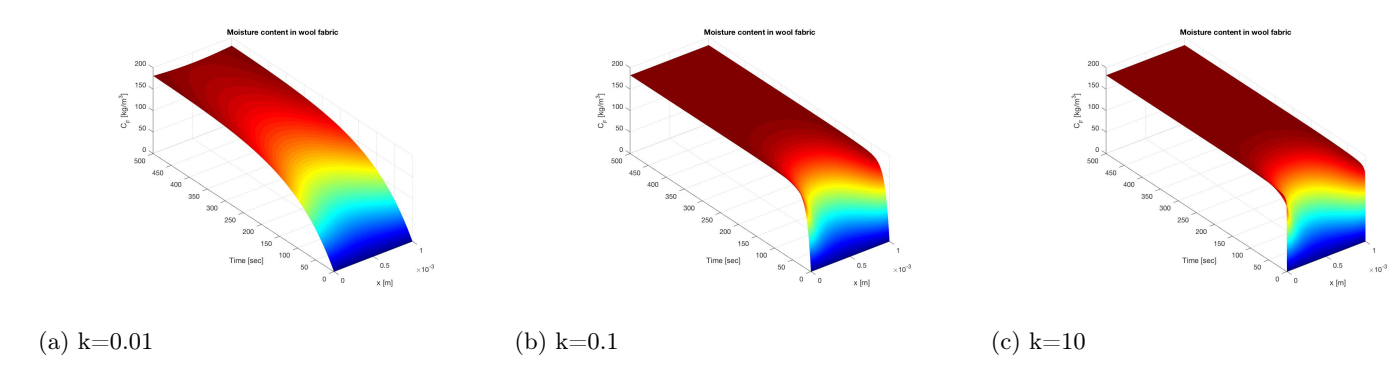


Figure 3.12: Moisture content in wool fabric with different rate constants

The Moisture content in wool fabric also behaves predictably. With small rate constant it reaches steady state solution slowly.

3.3. Case 2

Now, let us try Dirichlet boundary conditions for temperature equation. Suppose there are hot walls on each boundary. Additionally, the advective flux was added to C_A .

$$\begin{cases} \epsilon \frac{\partial C_A}{\partial t} = \frac{D\epsilon}{\tau} \frac{\partial^2 C_A}{\partial x^2} + v \frac{\partial C_A}{\partial x} - (1 - \epsilon) \frac{\partial C_F}{\partial t} \\ C_v \frac{\partial T}{\partial t} = K \frac{\partial^2 T}{\partial x^2} + \lambda \frac{\partial C_F}{\partial t} \\ \frac{1}{\rho(1 - \epsilon)} \frac{\partial C_F}{\partial t} = k(y_A - y_F) \end{cases}$$
(3.1)

where $v=10^2\times(x-x_{center})^3$ is velocity field. For boundary conditions at x=L:

$$\begin{cases} \frac{\partial C_A(L,t)}{\partial x} = -h_m(C_A - C_e) \\ T(L,t) = T_{wall} \\ \frac{\partial C_F(L,t)}{\partial x} = 0 \end{cases}$$
 (3.2)

For boundary conditions at x = 0:

$$\begin{cases} \frac{\partial C_A(0,t)}{\partial x} = h_m(C_A - C_e) \\ T(0,t) = T_{wall} \\ \frac{\partial C_F(0,t)}{\partial x} = 0 \end{cases}$$
 (3.3)

3.3. Case 2

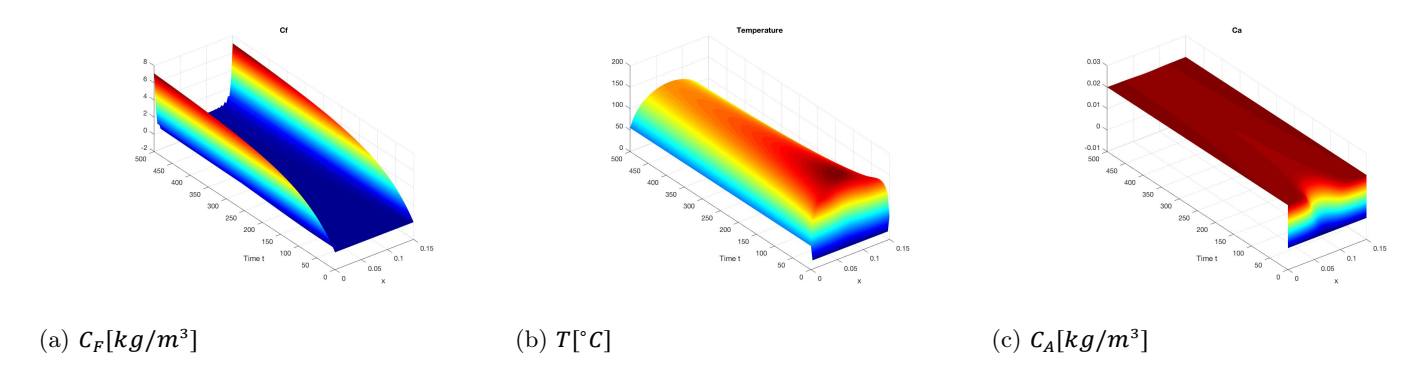


Figure 3.13: Results with Dirichlet B.C.

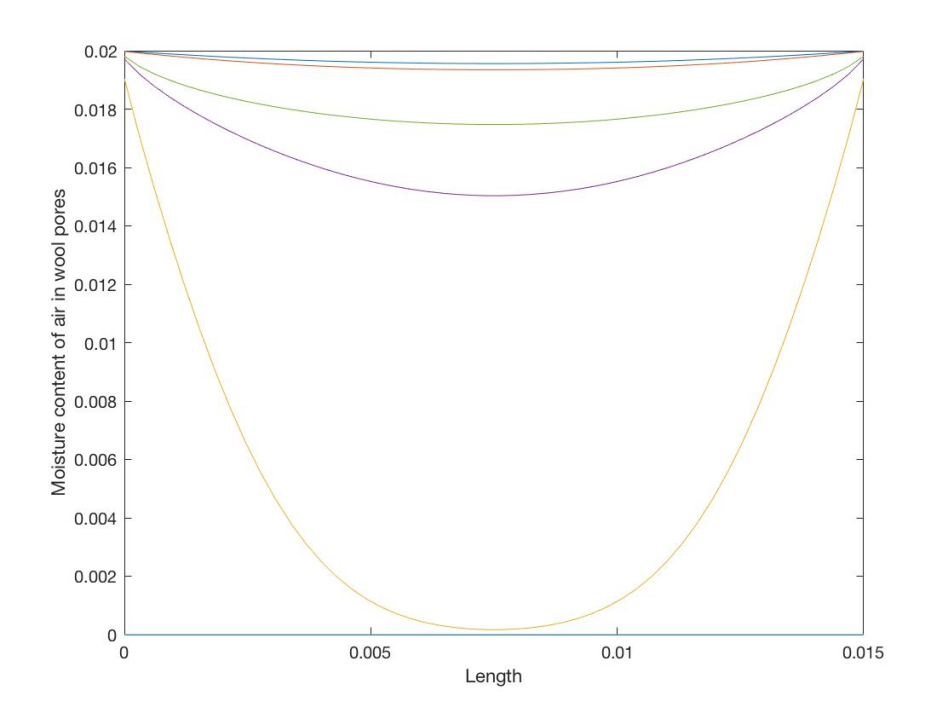


Figure 3.14: $C_A[kg/m^3]$ - Moisture content of air in wool pores (length in meters)

The next case is almost like previous one. Except the fact that, the heat source removed. Now, even if equation for temperature looks like independent, it is not. Due to the fact that the parameters K and C_{v} are depends on C_{F} .

$$\begin{cases} \epsilon \frac{\partial C_A}{\partial t} = \frac{D\epsilon}{\tau} \frac{\partial^2 C_A}{\partial x^2} + v \frac{\partial C_A}{\partial x} - (1 - \epsilon) \frac{\partial C_F}{\partial t} \\ C_v \frac{\partial T}{\partial t} = K \frac{\partial^2 T}{\partial x^2} \\ \frac{1}{\rho(1 - \epsilon)} \frac{\partial C_F}{\partial t} = k(y_A - y_F) \end{cases}$$
(3.4)

24 3. Drying of Textile

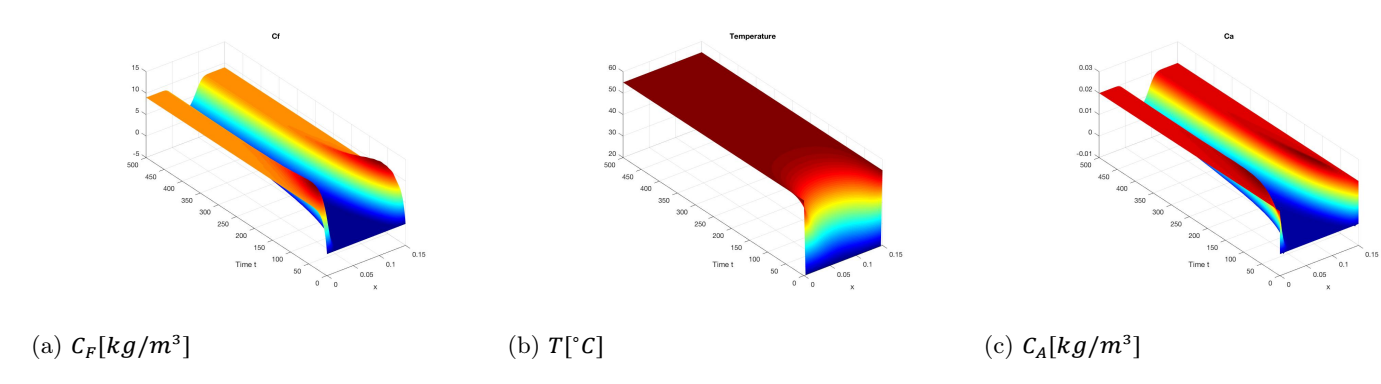


Figure 3.15: Results with Dirichlet B.C. and removed heat source

This temperature profile make sense more, due to the shape of the temperature profile. As we said before, there are two hot walls on the boundaries. So, it is obvious that the boundary temperatures goes to the wall temperature very fast, while temperature in the middle part approaches to the wall temperature with time.

Overall, re-doing paper [21] was good start in understanding the drying process. Even if our numerical values do not matched perfectly, visually the shapes of all three parameters are the same.

Heat Equation

4.1. Analytical solution

Anode baking occurs because of heat allocation in anode block through conduction. The energy diffusion is stationary. Accordingly, the temperature in the middle of the anode block is lower than on the boundaries. This kind of temperature spreading depends on anode's size (length, width, height) and physical parameters, such as thermal conductivity. However, if there is a plenty of time, temperature distribution in the anode body will be uniform. The furnaces build such that, in each pit, there are several layers of anode blocks and baked through the heat generated in the hot walls. Mostly, the angel between the heat flow and fuels is approximately 90 degrees. As a result, the temperature transmission that is normally stable is approximated with one dimensional model. Which is parabolic pde that characterizes heat diffusion. [2]

$$\frac{\partial T}{\partial t} = \alpha \frac{\partial^2 T}{\partial x^2} \tag{4.1}$$

where T(x,t) is the temperature, α is some mathematical parameter. The equation 4.1 is the core of the mathematical model for anode baking. Thus, it is essential to solve and analyze the heat equation. First, let us start with the finding analytical solution of the equation above. Additionally, considering the anode block between two hot walls, Dirichlet boundary condition will be used. Hence, T(0,t) = T(L,t) = 1473 Kelvin and T(x,0) = 350 Kelvin.

$$\frac{\partial T}{\partial t} = \alpha \frac{\partial^2 T}{\partial x^2} \qquad T(0,t) = T(L,t) = 1473, \quad T(x,0) = 350 \tag{4.2}$$

Usually, this type of partial differential equations can be solved by separation of variables. However, it requires homogeneous boundary conditions. While, the equation 4.2 has non-homogeneous boundary conditions, the method of separation of variables no longer works on this problem. Fortunately, there

26 4. Heat Equation

is a way how to deal with these boundary conditions. There are no heat or sink source in the equation 4.2. Moreover, the temperature on the boundaries are fixed and not going to change with time. This means, after sufficiently long time the temperature distribution should reach its steady state solution and no longer depend on time. By way of explanation, as time goes to infinity, T(x,t) should be as follow

$$\lim_{t \to \infty} T(x, t) = T_E(x) \tag{4.3}$$

where T_E is steady state solution [10]. Moreover, it must satisfy equation 4.2 and boundary conditions. Nevertheless, it will not satisfy initial conditions, because we are considering time in infinity, and initial conditions show the time zero. Then, we get new differential equation:

$$0 = \alpha \frac{\partial^2 T_E}{\partial x^2} \qquad T_E(0) = T_E(L) = 1473 \tag{4.4}$$

which is just 2nd order ordinary differential equation and can be solved by two times integrating.

$$T_E(x) = c_1 x + c_2 (4.5)$$

Applying boundary conditions from equation 4.4, we have $c_1 = 0$ and $c_2 = 1473$. Which gives $T_E(x) = 1473$. After, the result of T_E going to be used in solution of the equation 4.2. Then, let's define new function:

$$\bar{T}(x,t) = T(x,t) - T_E(x) \tag{4.6}$$

This can be rerouted as $T(x,t) = \bar{T}(x,t) + T_E(x)$. Next, let's look at partial derivatives:

$$\frac{\partial T}{\partial t} = \frac{\partial \bar{T}}{\partial t} + \frac{\partial T_E}{\partial t} = \frac{\partial \bar{T}}{\partial t} \qquad \frac{\partial^2 T}{\partial x^2} = \frac{\partial^2 \bar{T}}{\partial x^2} + \frac{\partial^2 T_E}{\partial x^2} = \frac{\partial^2 \bar{T}}{\partial x^2}$$
(4.7)

From the equations 4.7, it is obvious that both T(x,t) and $\bar{T}(x,t)$ must satisfy the same the same partial differential equation.

$$\bar{T}(x,0) = T(x,0) - T_E(x) = 350 - 1473$$
 (4.8)

$$\bar{T}(0,t) = T(0,t) - T_E(0) = 1473 - 1473 = 0$$
 (4.9)

$$\bar{T}(L,t) = T(L,t) - T_E(L) = 1473 - 1473 = 0$$
 (4.10)

Finally, we get homogeneous boundary conditions. Besides, the partial differential equation for $\bar{T}(x,t)$ is:

$$\frac{\partial \bar{T}}{\partial t} = \alpha \frac{\partial^2 \bar{T}}{\partial x^2} \qquad \bar{T}(0, t) = \bar{T}(L, t) = 0, \quad \bar{T}(x, 0) = 350 - 1473 \tag{4.11}$$

Equation 4.11 can be solved by separation of variables and have general solution [10]

$$\bar{T}(L,t) = \sum_{i=1}^{n} B_n \sin\left(\frac{n\pi x}{L}\right) e^{-\alpha(\frac{n\pi}{L})^2 t}$$
(4.12)

where

$$B_n = \frac{2}{L} \int_0^L (350 - 1473) \sin\left(\frac{n\pi x}{L}\right) dx = \frac{2}{L} \frac{(350 - 1473)L(1 - \cos(n\pi))}{n\pi}$$
(4.13)

$$T(x,t) = T_E(x) + \bar{T}(x,t) = 1473 + \sum_{i=1}^{n} B_n \sin\left(\frac{n\pi x}{L}\right) e^{-\alpha(\frac{n\pi}{L})^2 t}$$
(4.14)

Now, when the analytical solution is found, it can be run in Matlab (the script given in Appendix) and solution may be presented in the Figure 4.1. The next Figure 4.2 represents comparison between analytical result and result received from Matlab toolbox. Fortunately, they are identical. It gives confidence that both methods are working properly.

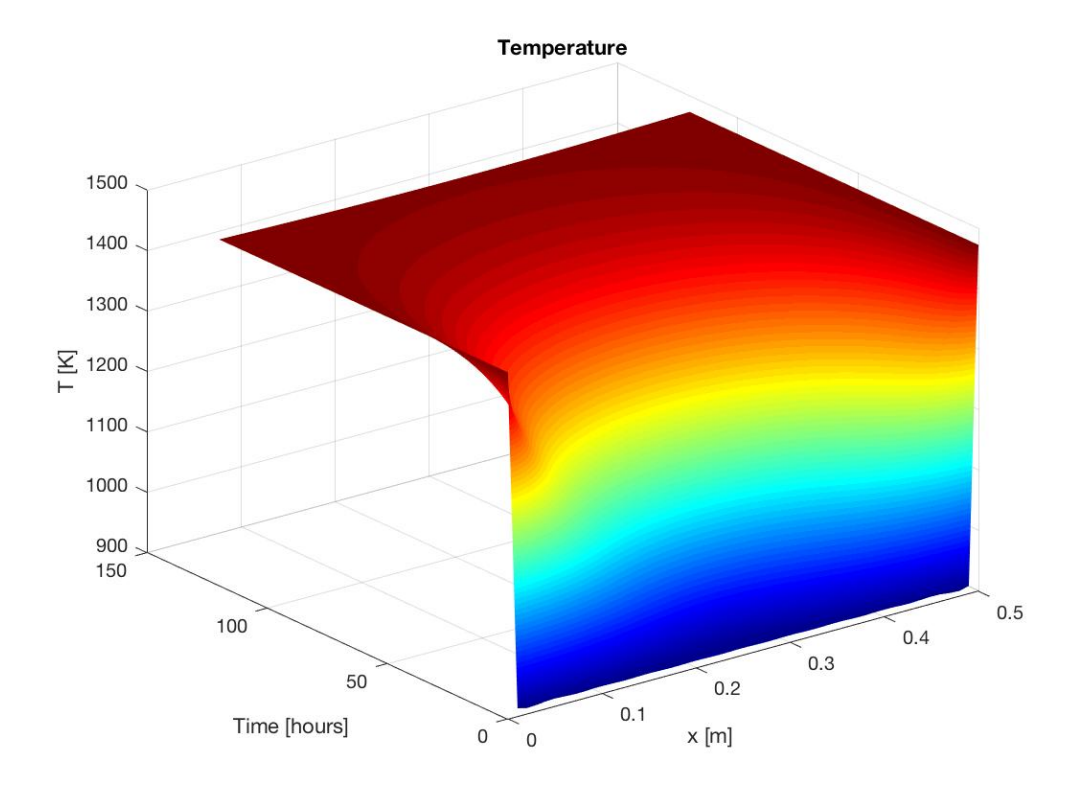
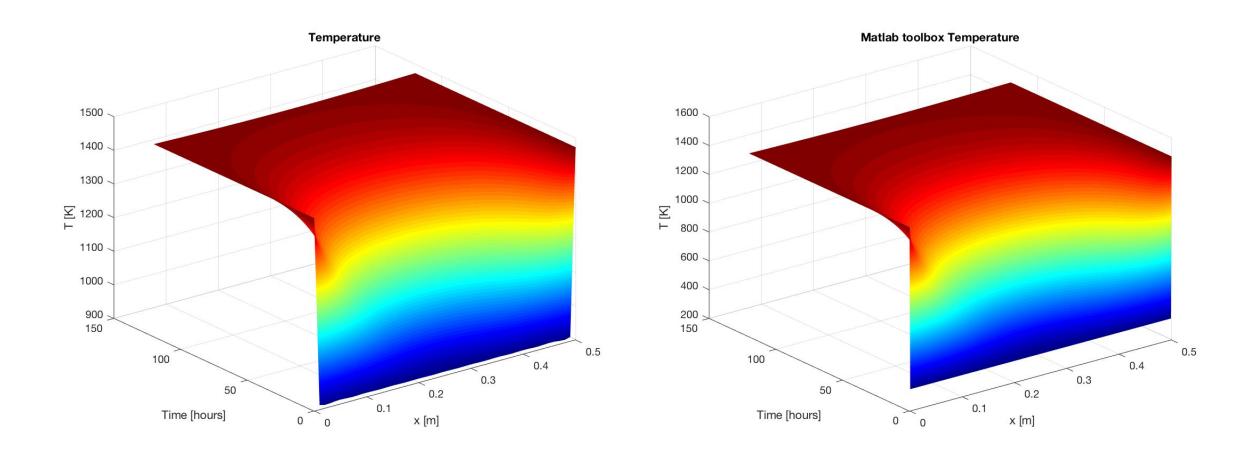


Figure 4.1: Temperature distribution according to analytic solution

28 4. Heat Equation



(a) Temperature distribution according to analytic so-(b) Temperature distribution according to Matlab toollution box solution

Figure 4.2: Temperature distribution according to analytic solution and Matlab toobox.

4.2. Thermal diffusivity

Further, let us consider the physical parameters of the heat equation. α form the equation 4.1 called thermal diffusivity, which is actually $\frac{K}{\rho C_{v}}$. Where K is thermal conductivity, ρ is density and C_{v} is specific heat capacity of the body. Assuming that we used constant values of these parameters, we also had constant thermal diffusivity. Subsequently, we wish to see the cases of non-constant thermal diffusivity and its effect on the temperature profile. We are going to estimate thermal diffusivity by two functions. First is a polynomial of order 6, and second is sinusoidal-exponential [5]. Also, lest use small k instead of α . Then the fists assumption of thermal diffusivity will look as follow:

$$k = k_1 + k_2 \frac{T}{k_8} + k_3 (\frac{T}{k_8})^2 + k_4 (\frac{T}{k_8})^3 + k_5 (\frac{T}{k_8})^4 + k_6 (\frac{T}{k_8})^5 + k_7 (\frac{T}{k_8})^6$$
 (4.15)

where $k_1=0.00005,\,k_2=k_3=k_4=k_5=k_6=k_7=0.0007$ and $k_8=2455.$

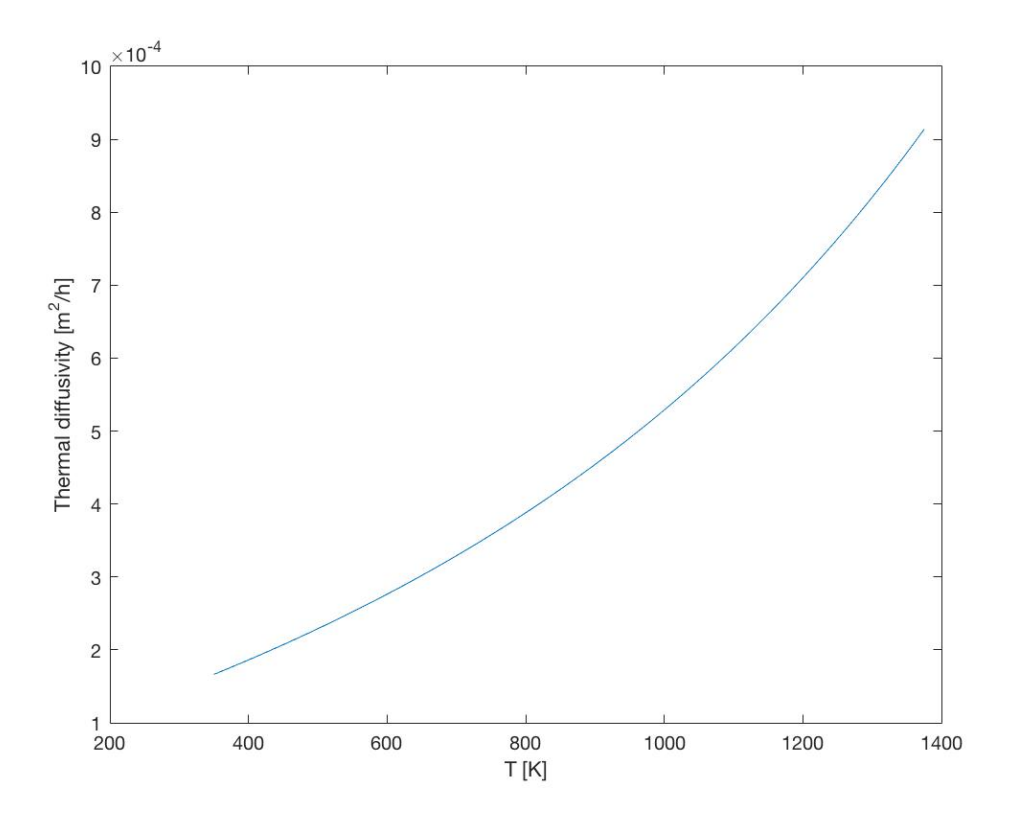


Figure 4.3: Polynomial thermal diffusivity

The Figure 4.3 shows relation between thermal diffusivity and temperature change. As we can see, it increases as temperature grows. Then, it is obviously will effect on temperature profile. We expect that convergence to the uniform temperature distribution will be slower. Due to, when thermal diffusivity was constant valued, it was greater than k in Figure 4.3. Then, the following graph expresses expected behaviour of the temperature distribution.

30 4. Heat Equation

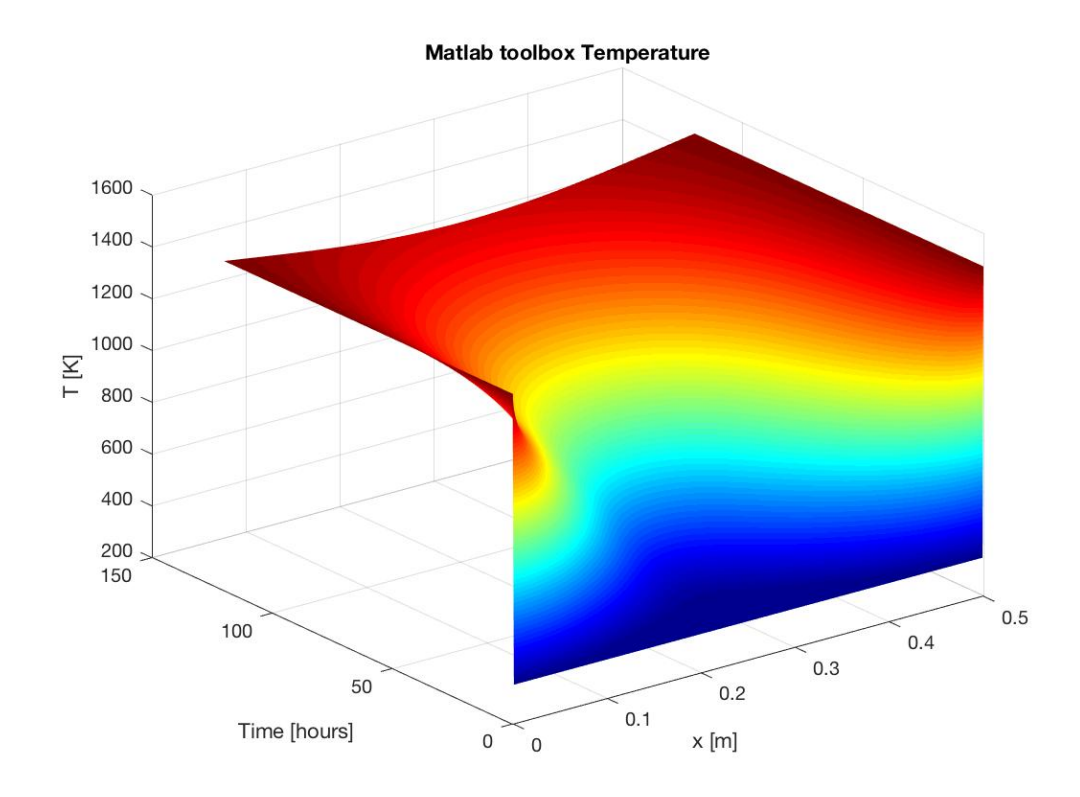


Figure 4.4: Temperature distribution after using polynomial thermal diffusivity

Our second choice was sinusoidal-exponential function for expression of thermal diffusivity.

$$k = k_1 + k_2 e^{\frac{T}{k_3}} + k_4 \sin\left(\frac{T}{k_5}\right) \tag{4.16}$$

where $k_1 = 0.0004,\, k_2 = 0.0001,\, k_3 = 10000,\, k_4 = 0.0004$ and $k_5 = 150$

The Figure 4.5 illustrates sinusoidal-exponential thermal diffusivity. However, it could be that, behind this case there is no physical explanation. Thus, is it purely mathematical assumption. Nevertheless, it is good to see how it effects on temperature spreading. Of course, it does not mean that temperature takes negative values, when thermal diffusivity at its minimum. Just, diffusion of the heat will slow down, so it is not too different from the case of polynomial thermal diffusivity.

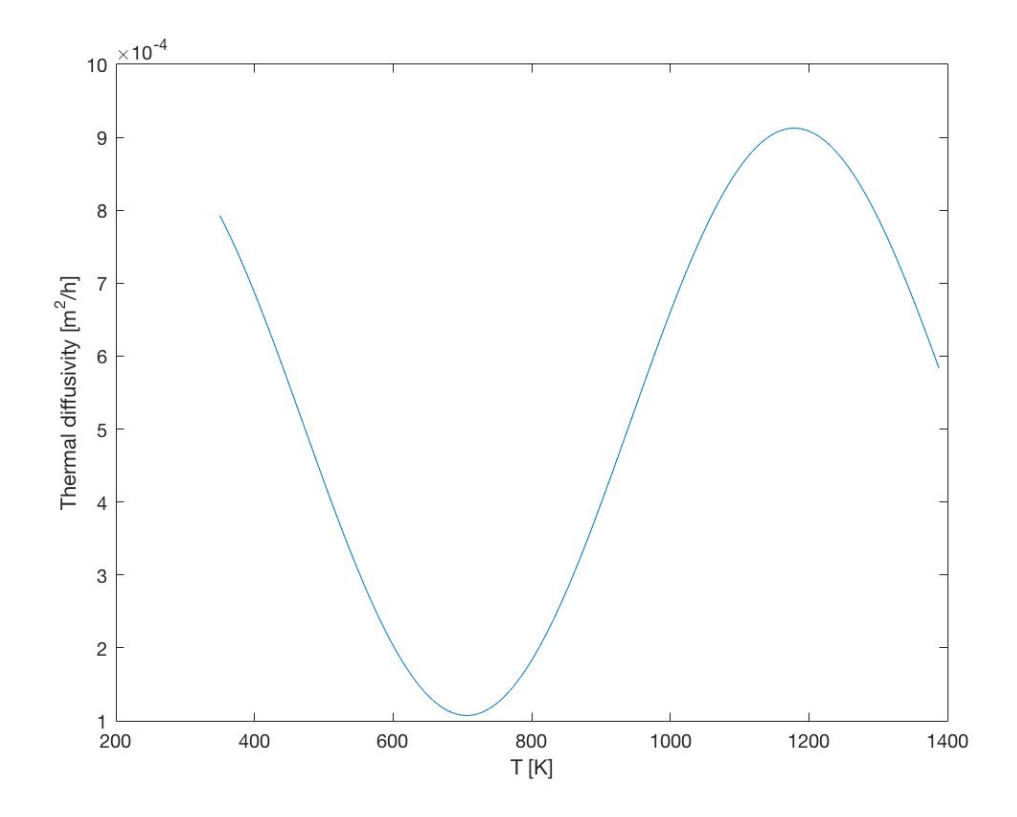


Figure 4.5: sinusoidal-exponential thermal diffusivity

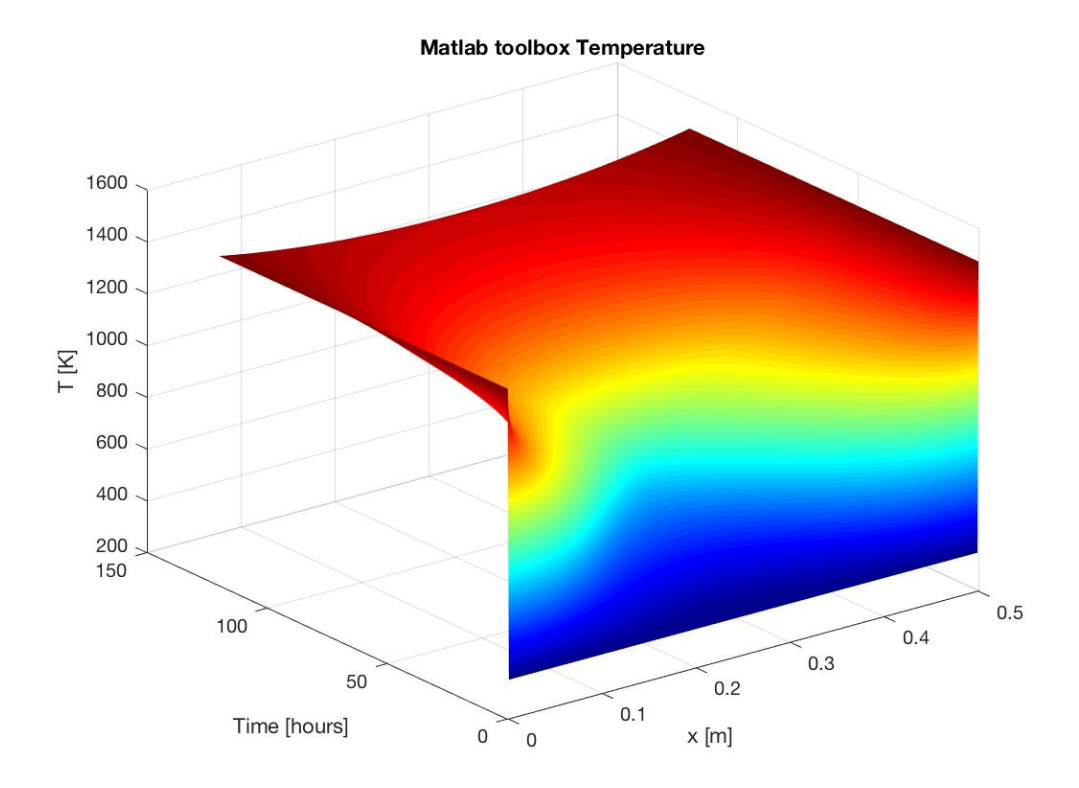


Figure 4.6: Temperature distribution after using sinusoidal-exponential thermal diffusivity

32 4. Heat Equation

From the other hand, we can change number of waves by changing coefficient $k_5 = 400$. So, the thermal diffusivity will start from its maximum value, decreases with temperature raise.

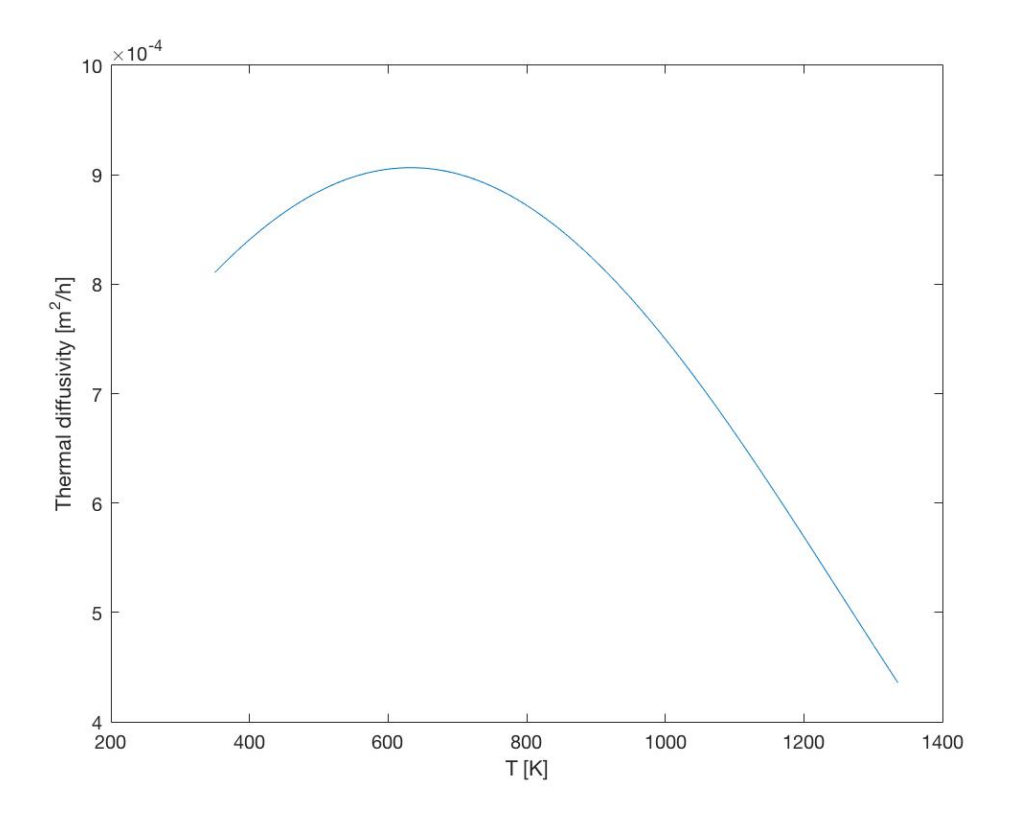
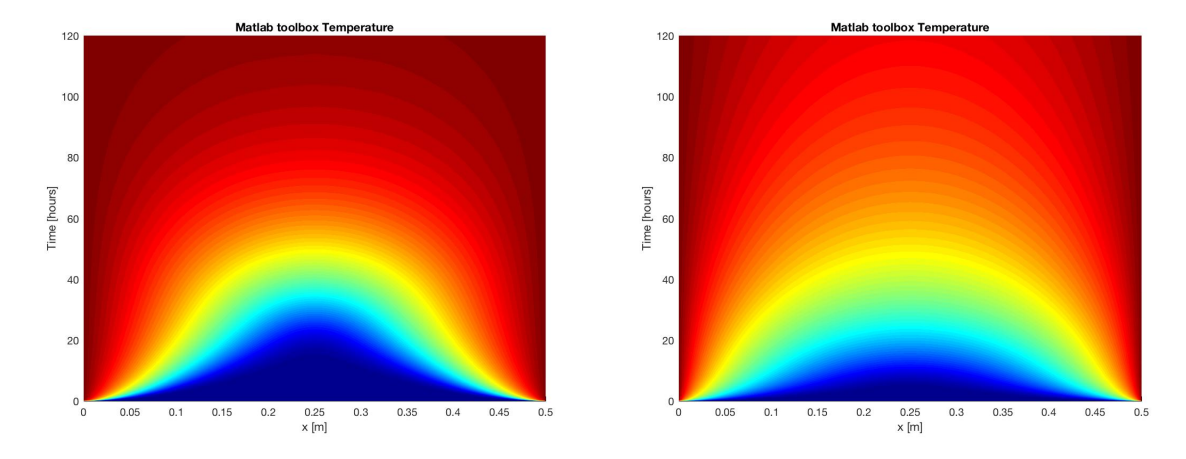


Figure 4.7: Thermal diffusivity



(a) Temperature distribution with polynomial \boldsymbol{k}

(b) Temperature distribution sinusoidal-exponential \boldsymbol{k}

Figure 4.8: Temperature distribution

The Figure 4.8 illustrates temperature distribution (view from the top) with two different thermal diffusivity. As a result of decreasing thermal diffusivity, the graph 4.8b represents that the heat diffusion in this case is quite slow. While, in the case of polynomial and increasing thermal diffusivity, heat

spreading is faster, which is shown in graph 4.8a.

One of the important parameters in a node baking model is saturation pressure P_s . In a node baking baking case, we took it as $P_s = e^{20.386 - \frac{5132}{T}}$ [7]. Accordingly, we can check P_s results by applying the values of temperature, those we already have. As reported in Figure 4.9, chosen formula behaves properly.

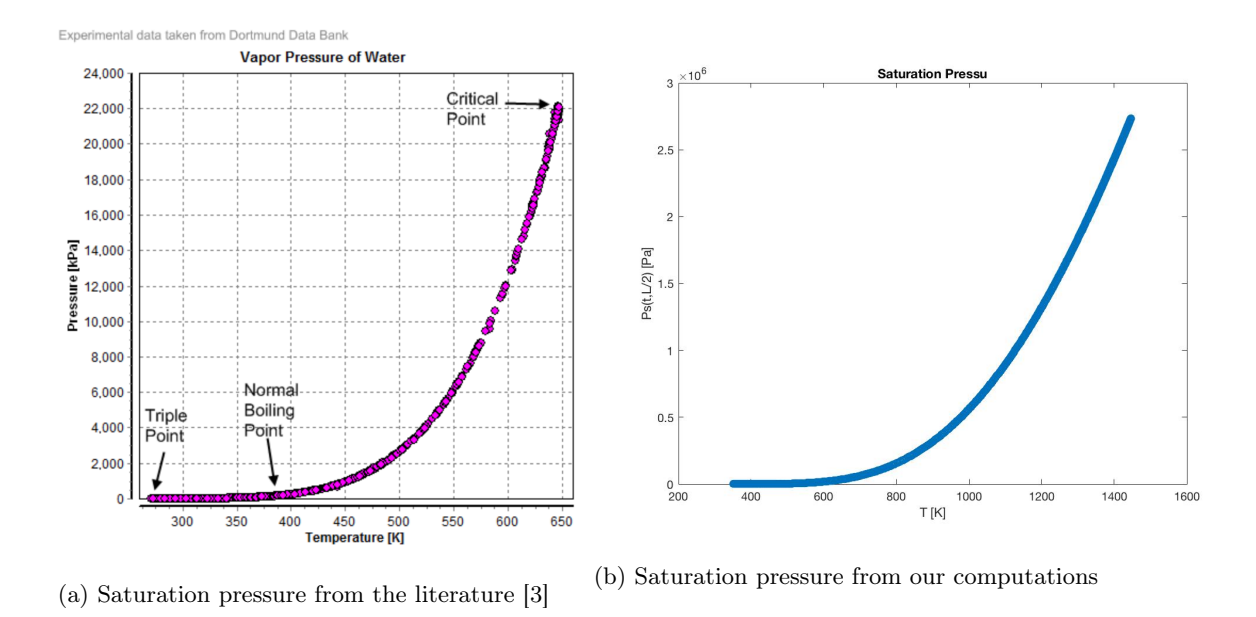


Figure 4.9: To be confident in behavior of Saturation Pressure, we compare it with independent source.

The results for main parameters such as temperature given as a matrix of length and time domain. Thus, the simulation of P_s was taken by using the temperature values from the middle of the x and all time points.

4.3. Sigmoid Function

Up to this point we took diffusion coefficient as a constant values. However, we understand that diffusion coefficient depends on temperature. In other words, gases starts released from raw anode material after some temperature reached up. Thus, instead of constant diffusion coefficient, we are going to use Sigmoid function.

$$S(T) = \frac{D}{1 + \exp(-k(T - T_0))}$$
(4.17)

where D is diffusion coefficient and maximum value of the function S(T). k is the steepness of the functions curve.

34 4. Heat Equation

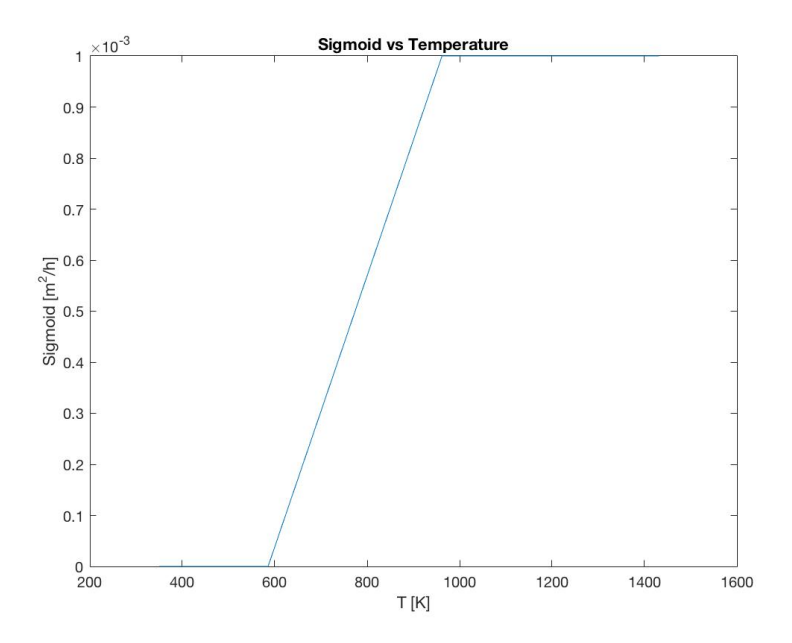


Figure 4.10: Sigmoid as a function of temperature.

The figure above shows relation between Temperature and Sigmoid function (diffusion coefficient). Obviously, up to some temperature point, diffusion coefficient is zero. Furthermore, after specific temperature reached up, the diffusion coefficient is equal to D, which maximum value of the sigmoid function.

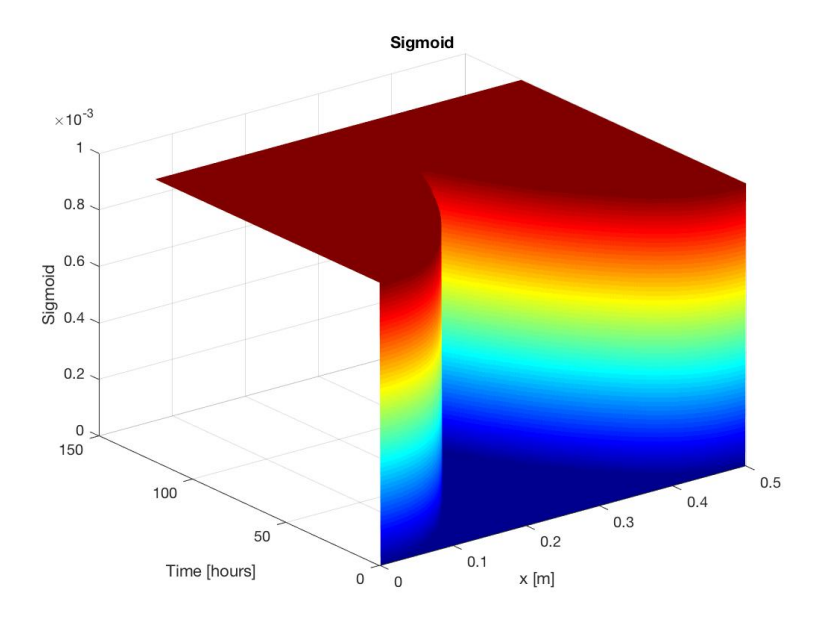


Figure 4.11: 3D Profile of sigmoid function

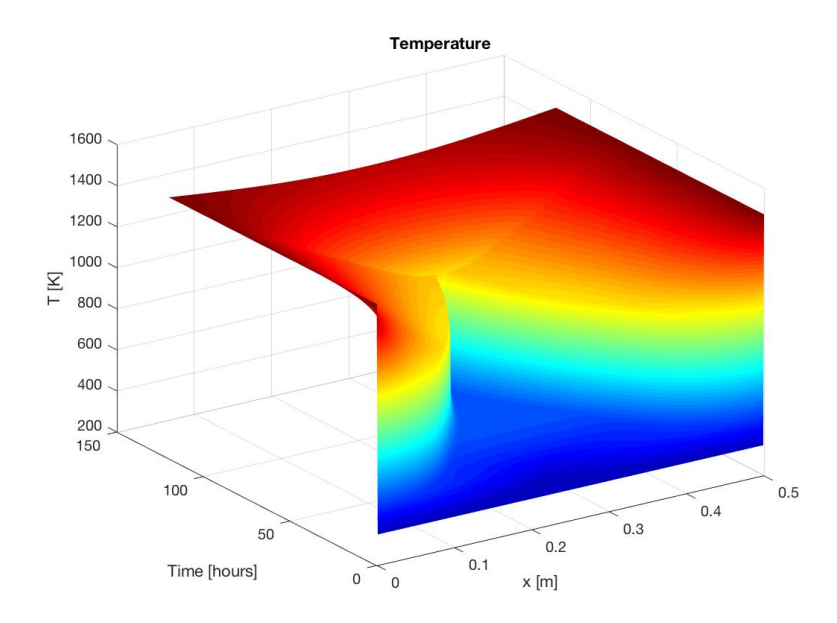


Figure 4.12: Temperature profile after using sigmoid function.

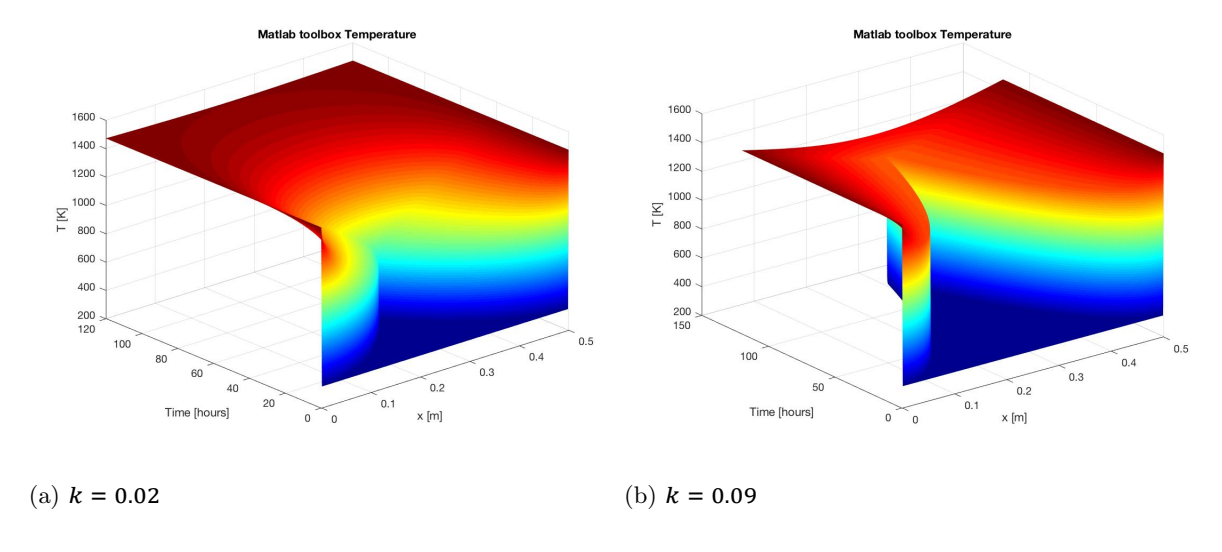


Figure 4.13: Temperature distribution with two different values of steepness.

Here, it may be noticed that the use of sigmoid function and the polynomial as a thermal diffusivity results on similar temperature profile. First, even if thermal diffusivity stays constant or decreases (cases when it is not increasing), temperature will not drop. Second, the similarity of the results can be explained by the behavior of the both functions. Sigmoid and polynomial functions growth with temperature linearly.

36 4. Heat Equation

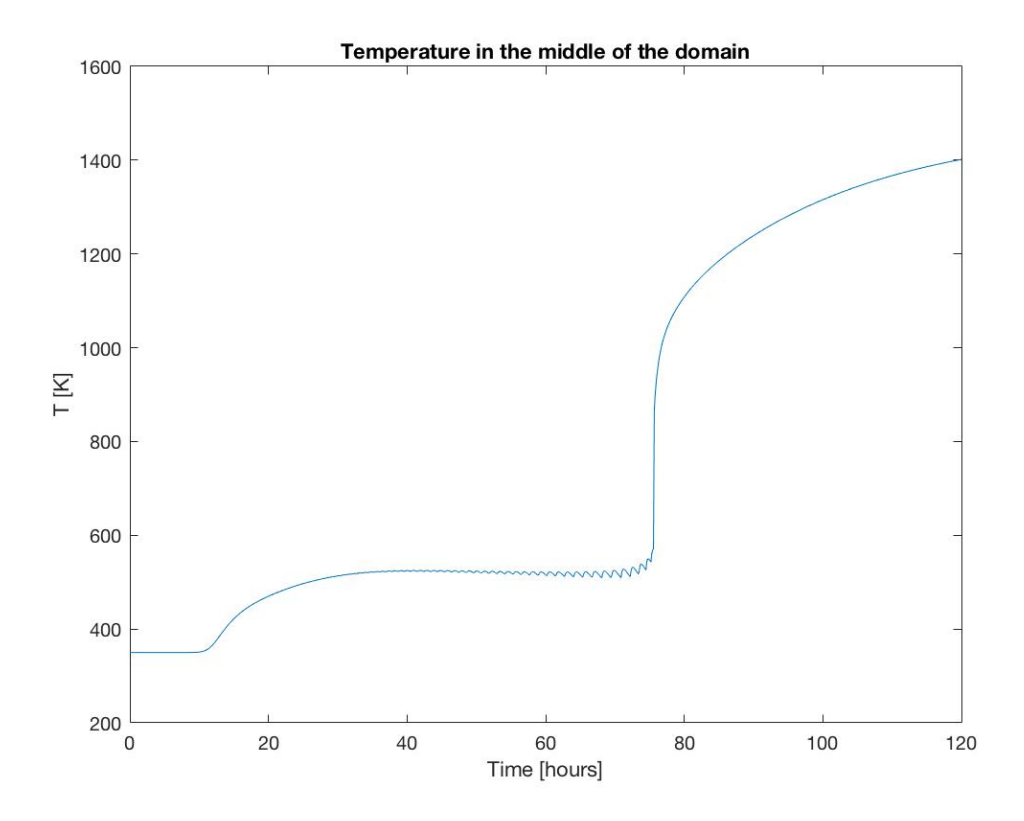


Figure 4.14: Temperature profile with sigmoid function

At this moment, hard to conclude is the sigmoid function mandatory part of the model or not. Moreover, using sigmoid instead of constant diffusion coefficient reduced volume of the released gases. That can be explained by the fact that whenever we use constant diffusion coefficient, it was taken as its maximum value. However, good to see that it works as expected.

Heat Transfer through Anode Material

The introduced model in this project shows the diffusion of heat and moisture in porous media, for estimation of thermal state and calculation of mass and energy carrying [20]. The advantage of this mathematical model among other 1D models is that, here a lot of physical parameters of the material considered. Which gives freedom of applying exactly this model into other materials [11]. As a consequence, in this section we will use this mathematical model of drying process for anode baking, due to the fact that anode is a porous media too [14]. Which means, actual physical parameters of the anode material going to be used. Heat and mass conservation equations will be given in terms of unit volume of the air-material mixture. Released gases accumulates in pores and material, simultaneously. Thus, in front of $\frac{\partial C_A}{\partial t}$ factor ϵ , and $\frac{\partial C_F}{\partial t}$ has a factor $1 - \epsilon$.

$$\begin{cases} \epsilon \frac{\partial C_A}{\partial t} = \frac{D\epsilon}{\tau} \frac{\partial^2 C_A}{\partial x^2} + v \frac{\partial C_A}{\partial x} - (1 - \epsilon) \frac{\partial C_F}{\partial t} \\ \rho C_v \frac{\partial T}{\partial t} = K \frac{\partial^2 T}{\partial x^2} + \lambda \frac{\partial C_F}{\partial t} \\ \frac{1}{\rho(1 - \epsilon)} \frac{\partial C_F}{\partial t} = k(y_A - y_F) \end{cases}$$
(5.1)

where $v=10^{-4}\frac{m}{s}$ is velocity field. For boundary conditions at x=L:

$$\begin{cases} \frac{\partial C_A(L,t)}{\partial x} = C_A - C_e \\ T(L,t) = T_{wall} \\ \frac{\partial C_F(L,t)}{\partial x} = 0 \end{cases}$$
 (5.2)

For boundary conditions at x = 0:

$$\begin{cases} \frac{\partial C_A(0,t)}{\partial x} = C_A - C_e \\ T(0,t) = T_{wall} \\ \frac{\partial C_F(0,t)}{\partial x} = 0 \end{cases}$$
 (5.3)

Also, $T_{wall}=1473$ and $C_e=0$. Initial conditions are $T=350,\,C_A=0$ and $C_F=0.15$

5.1. Numerical solutions

$$\begin{cases}
\frac{\partial C_A}{\partial t} = \frac{D}{\tau} \frac{\partial^2 C_A}{\partial x^2} + \frac{v}{\epsilon} \frac{\partial C_A}{\partial x} - \frac{(1 - \epsilon)}{\epsilon} \frac{\partial C_F}{\partial t} \\
\frac{\partial T}{\partial t} = \frac{K}{\rho C_v} \frac{\partial^2 T}{\partial x^2} + \frac{\lambda}{\rho C_v} \frac{\partial C_F}{\partial t} \\
\frac{\partial C_F}{\partial t} = k\rho (1 - \epsilon) (y_A - y_F)
\end{cases}$$
(5.4)

The system can be solved by finite difference discretization in the domain $x \in (0, L)$ and $t \in (0, t_{max})$ [21].

$$\frac{CA_{i}^{n+1} - CA_{i}^{n}}{\Delta t} = \frac{D}{\tau} * \frac{CA_{i-1}^{n} - 2CA_{i}^{n} + CA_{i+1}^{n}}{(\Delta x)^{2}} + \frac{v}{\epsilon} * \frac{CA_{i+1}^{n} - CA_{i-1}^{n}}{2\Delta x} - \frac{1 - \epsilon}{\epsilon} * \frac{CF_{i}^{n+1} - CF_{i}^{n}}{\Delta t}$$

$$\frac{T_{i}^{n+1} - T_{i}^{n}}{\Delta t} = \frac{K}{\rho C_{v}} * \frac{T_{i-1}^{n} - 2T_{i}^{n} + T_{i+1}^{n}}{(\Delta x)^{2}} + \frac{\lambda}{\rho C_{v}} * \frac{CF_{i}^{n+1} - CF_{i}^{n}}{\Delta t}$$

$$\frac{CF_{i}^{n+1} - CF_{i}^{n}}{\Delta t} = k\rho(1 - \epsilon)(\frac{CA_{i}^{n}T_{i}^{n}R}{PS_{i}^{n}} - \frac{CF_{i}^{n}}{\rho(1 - \epsilon)})$$

Further, we will get the following system of equations:

$$\begin{split} CA_{i}^{n+1} &= CA_{i}^{n} + \frac{D\Delta t}{\tau(\Delta x)^{2}} \left(CA_{i-1}^{n} - 2CA_{i}^{n} + CA_{i+1}^{n} \right) + \frac{v\Delta t}{\epsilon 2\Delta x} \left(CA_{i+1}^{n} - CA_{i-1}^{n} \right) - \\ &- \frac{\Delta t(1-\epsilon)}{\epsilon} * k\rho(1-\epsilon) \left(\frac{CA_{i}^{n}T_{i}^{n}R}{Ps_{i}^{n}} - \frac{CF_{i}^{n}}{\rho(1-\epsilon)} \right) \\ T_{i}^{n+1} &= T_{i}^{n} + \frac{K\Delta t}{\rho C_{v}(\Delta x)^{2}} \left(T_{i-1}^{n} - 2T_{i}^{n} + T_{i+1}^{n} \right) + \frac{\lambda \Delta t}{\rho C_{v}} k\rho(1-\epsilon) \left(\frac{CA_{i}^{n}T_{i}^{n}R}{Ps_{i}^{n}} - \frac{CF_{i}^{n}}{\rho(1-\epsilon)} \right) \\ CF_{i}^{n+1} &= CF_{i}^{n} + \Delta k\rho(1-\epsilon) \left(\frac{CA_{i}^{n}T_{i}^{n}R}{Ps_{i}^{n}} - \frac{CF_{i}^{n}}{\rho(1-\epsilon)} \right) \end{split}$$

However, the most of the explicit difference methods needs sufficiently small Δt , in order to provide stability and convergence. Thus, Matlab PDE-solver was chosen for solving these system of nonlinear partial differential equations.

Next, we will check the units.

$$\epsilon \frac{\partial C_A}{\partial t} = \frac{D\epsilon}{\tau} \frac{\partial^2 C_A}{\partial x^2} + v \frac{\partial C_A}{\partial x} - (1 - \epsilon) \frac{\partial C_F}{\partial t}$$

$$\frac{kg}{m^3 s} = \frac{m^2}{s} \frac{kg}{m^3 m^2} + \frac{m}{s} \frac{kg}{m^3 m} - \frac{kg}{m^3 s}$$

$$\frac{kg}{m^3 s} = \frac{kg}{m^3 s} + \frac{kg}{m^3 s} - \frac{kg}{m^3 s}$$

$$\rho C_v \frac{\partial T}{\partial t} = K \frac{\partial^2 T}{\partial x^2} + \lambda \frac{\partial C_F}{\partial t}$$

$$\frac{kg}{m^3} \frac{m^2}{s^2 K} \frac{K}{s} = \frac{kg * m}{s^3 K} \frac{K}{m^2} + \frac{m^2}{s^2} \frac{kg}{m^3 s}$$

$$\frac{kg}{s^3 m} = \frac{kg}{s^3 m} + \frac{kg}{s^3 m}$$

$$\frac{1}{\rho(1-\epsilon)}\frac{\partial C_F}{\partial t} = k(y_A - y_F)$$

$$\frac{m^3}{kg} \frac{kg}{m^3 s} = \frac{1}{s} (\frac{kg}{m^3} K \frac{m^2}{s^2 K} \frac{s^2 m}{kg} - \frac{kg}{m^3} \frac{m^3}{kg})$$

$$\frac{1}{s} = \frac{1}{s}$$

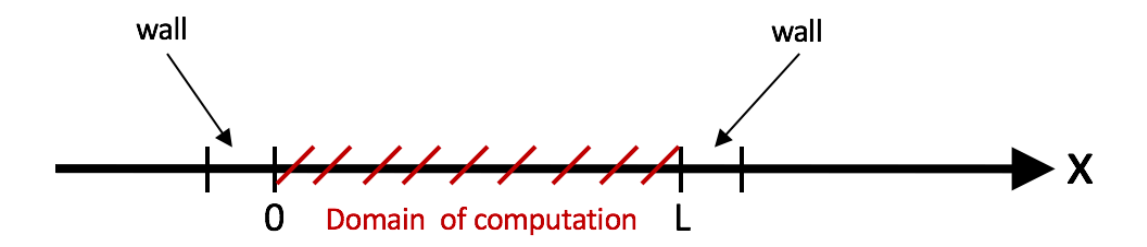


Figure 5.1: Anode baking furnace schematic view

Table 5.1: Numerical values and the physical units of the anode material [13]

Parameter	Formula	Unit
K	3.5 – 5	$kg * m/s^3K$
C_v	$175.03 + 20.04T - 6 * 10^{-4}T^2$	m^2/s^2K
λ	2260	m^2/s^2
ϵ	0.2	-
ρ	1600	kg/m^3
τ	1.5	_
D	2.49 <i>e</i> – 5	m^2/s
P_{S}	$exp(20.386 - \frac{5132}{T})$	m^{2}/s $kg/m * s^{2}$ $m^{2}/K * s^{2}$
R	461	$m^2/K * s^2$

Using the parameters for the anode material and domain of computation as in figure above, where length is L=0.5m and time is t=120h. We will get the profiles as below.

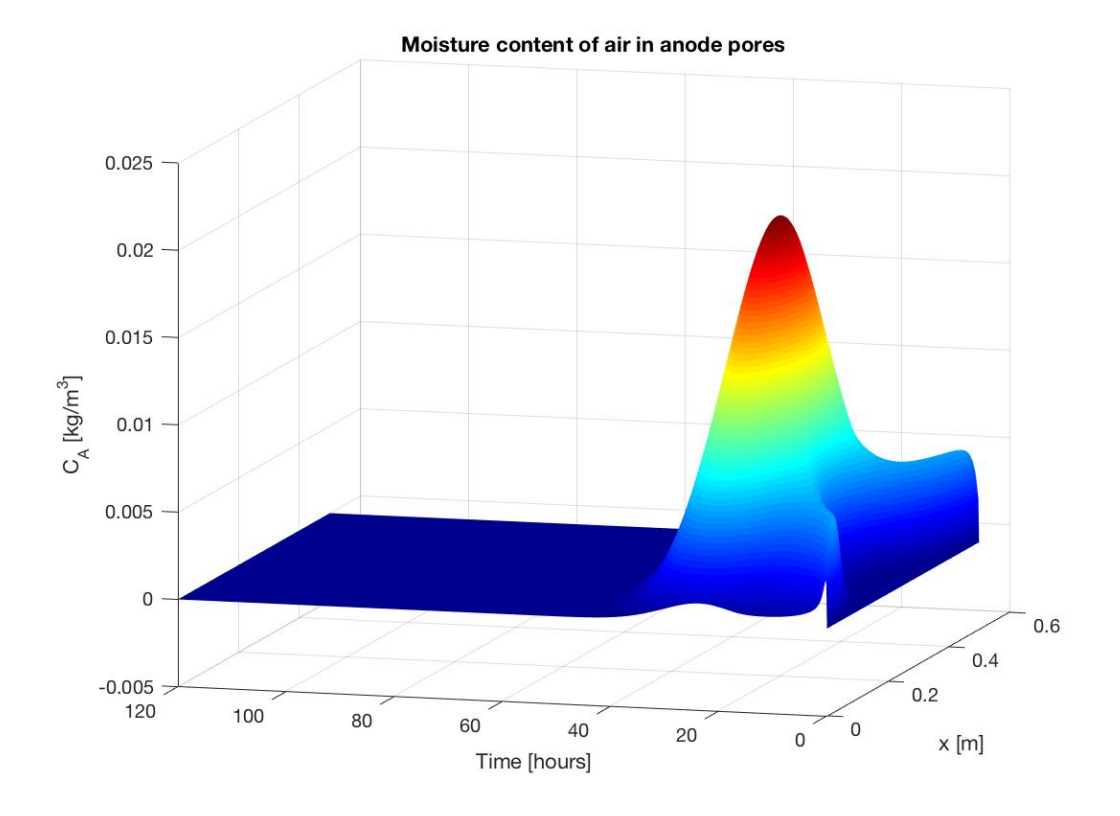


Figure 5.2: Moisture content of air in anode pores

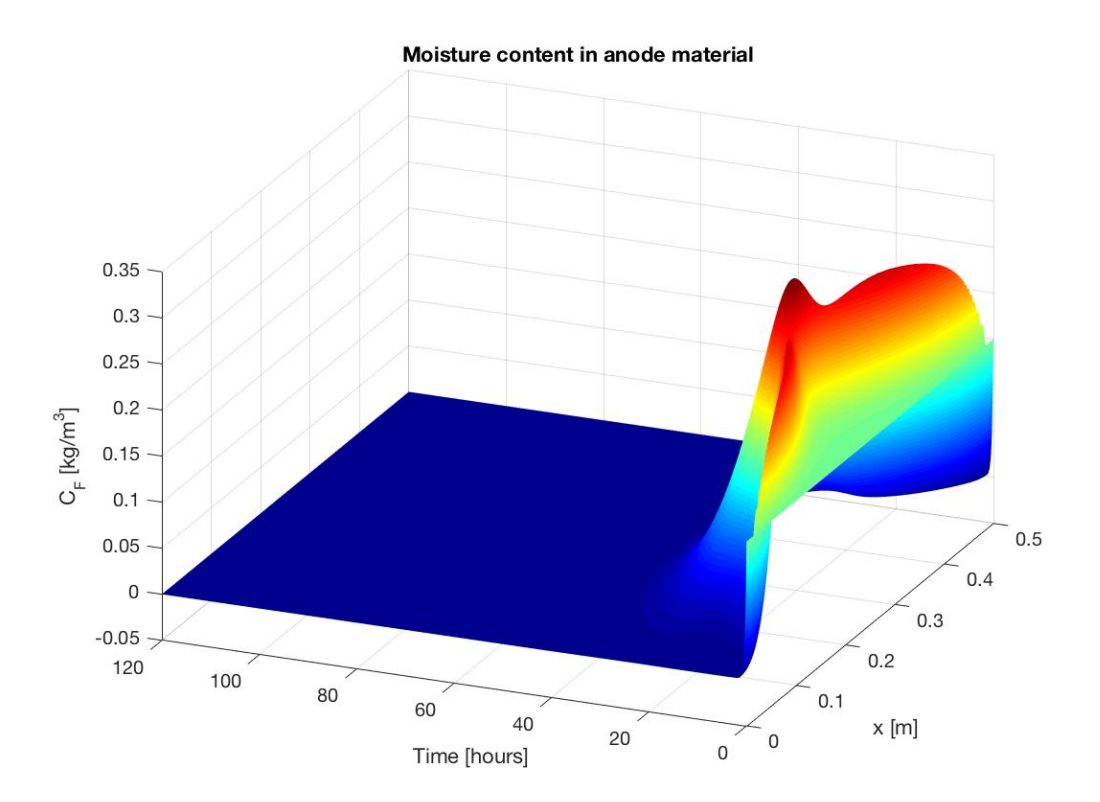


Figure 5.3: Moisture content in anode material

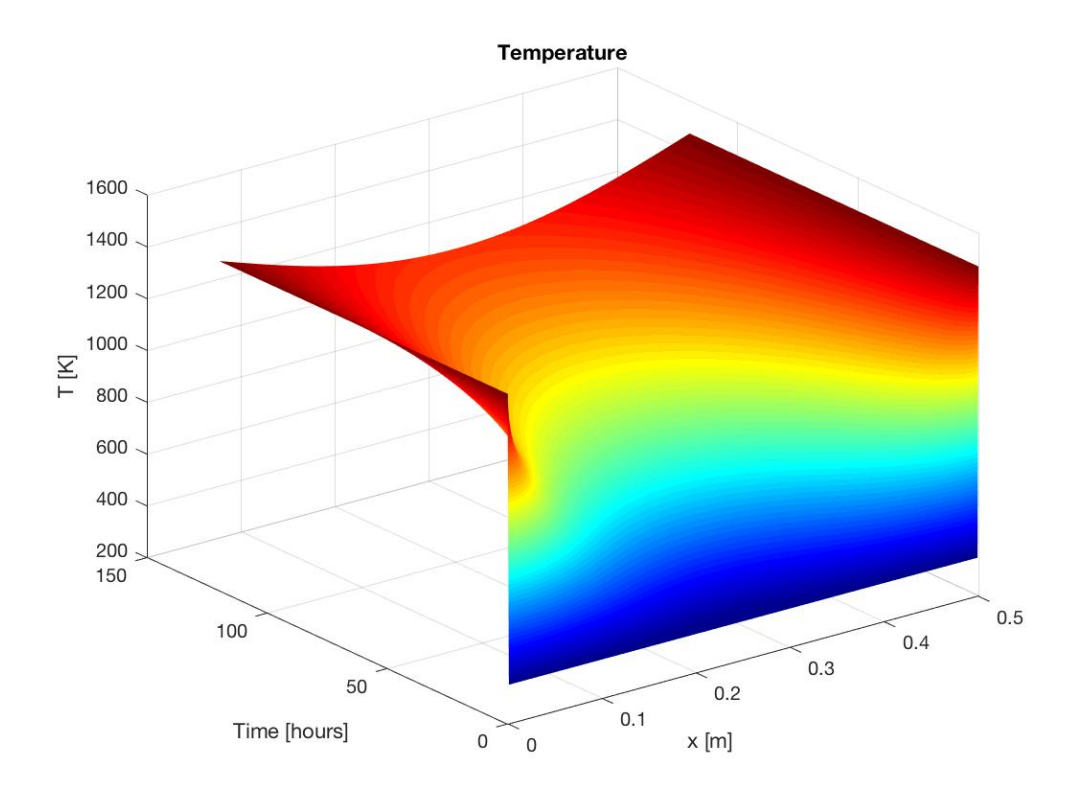


Figure 5.4: Temperature profile of the anode

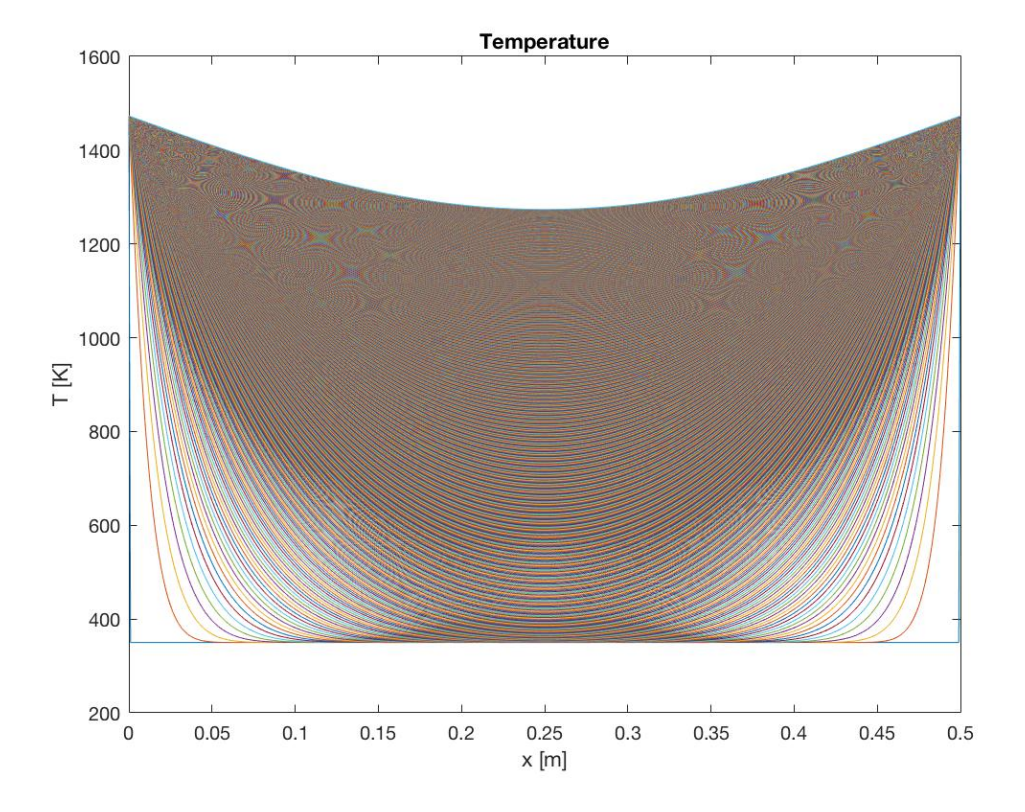


Figure 5.5: Temperature profile of the anode

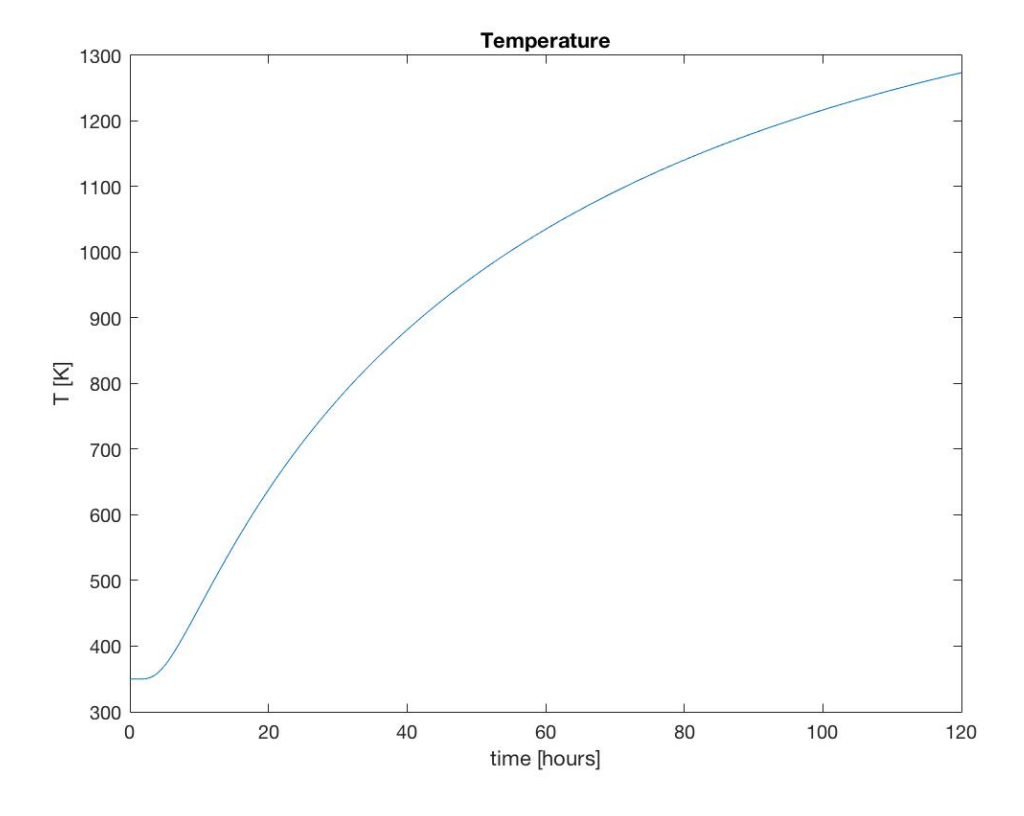


Figure 5.6: Temperature of the anode in the middle of the domain

However, if we change heat capacity by the constant value $C_v = 1500$, as a result, we get too sharp graphs. Given in Figures 5.7 - 5.9.

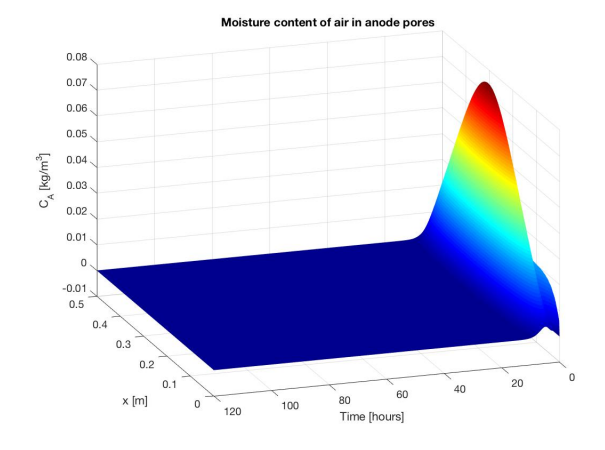


Figure 5.7: Moisture content in air pores

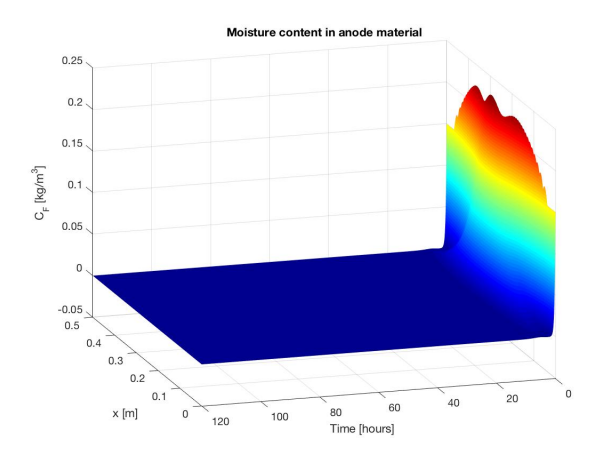


Figure 5.8: Moisture content in anode material

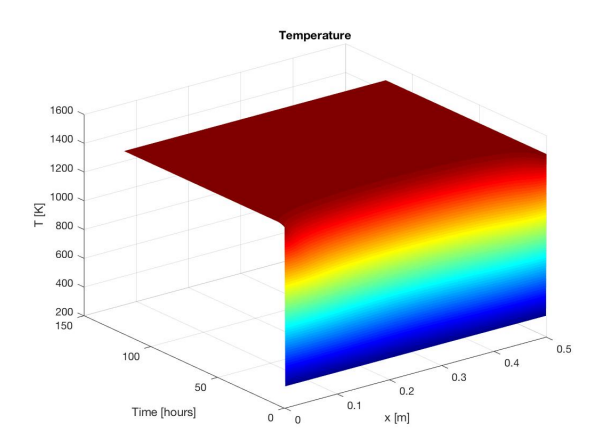


Figure 5.9: Temperature graph

According to picture above, we can make a conclusion about role of the heat capacity C_{ν} . Constant valued C_{ν} forced the exchange of moisture to occur very fast. Thus, it is not the best representative case of the reality. While, function valued heat capacity gave more realistic shape for both moisture in air-pores and in material.

Other interesting fact that, if we will change boundary condition for C_A , making $C_e = 1$. We can see how air-pores and material became even wet than it was.

$$\frac{\partial C_A(L,t)}{\partial x} = h_m(C_A - C_e) \tag{5.5}$$

$$\frac{\partial C_A(0,t)}{\partial x} = h_m(C_A - C_e) \tag{5.6}$$

 $T_{wall}=1473,\,C_e=1$ and $h_m=1.$ Initial conditions are $T=350,\,C_A=0$ and $C_F=0.15$

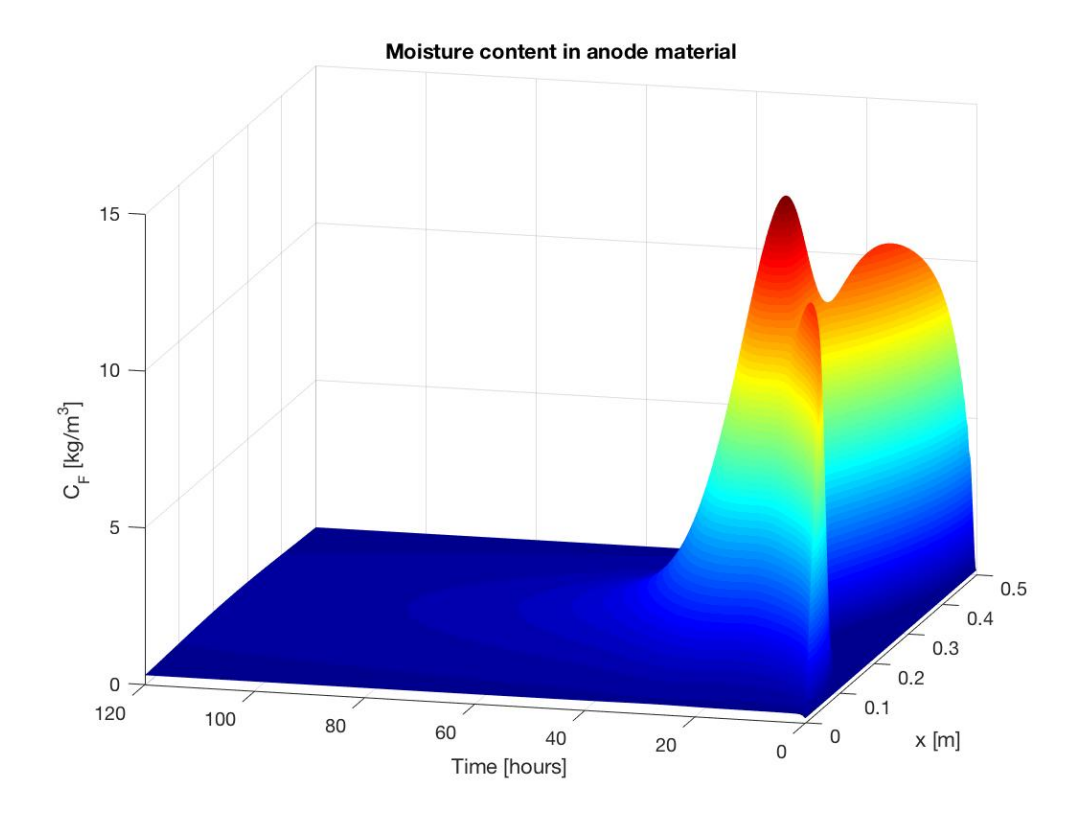


Figure 5.10: Moisture content in anode

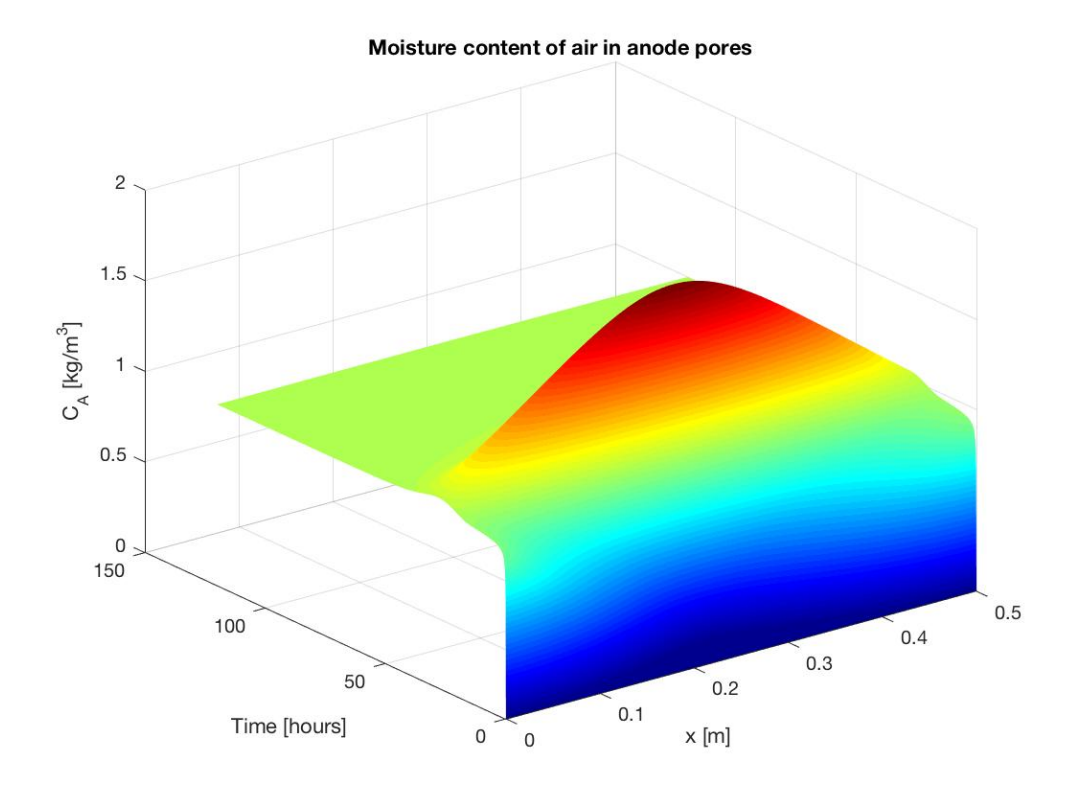


Figure 5.11: Moisture content in pores

As shown above, we did not bake the anode paste, but we made it even more wet than it was. Also, the mass of released gases are $4.4647*10^4$ kg, more than the mass of material in the pit. Thus, $C_e = 0$ is the best choice if material need to be baked.

The Figures 5.12 - 5.15 are the flux multiplied by the area of outflow (in our case area of anode block) and integrated over time. Where flux is $-D * \nabla C_A + \nu * C_A$.

According to the flux profile, the mass of gas leaving from the left boundary is 25 kg. Taking account that there are two boundaries, the total mass of gas going out from anode to fuel part of the furnace is 50 kg. From the literature [1], in each pit (one furnace contains 9 flues and 8 pits,and we are looking into one pit) 7 green blocks of anode with weight 1155 kg. After baking process, from 1 green block they get 1100 kg of baked anode. Thus, from 1 pit (1155*7 - 1100*7) 385 kg of gas cross over the wall. In our computations the amount of that gas is 49.6 kg per anode block, which is quite close to experimental value. While we took initial moisture of the material as a 15 percent. If material is more wet than our choice, moisture release will be grater. Also, our assumption about area of holes could be smaller or bigger than the real one.

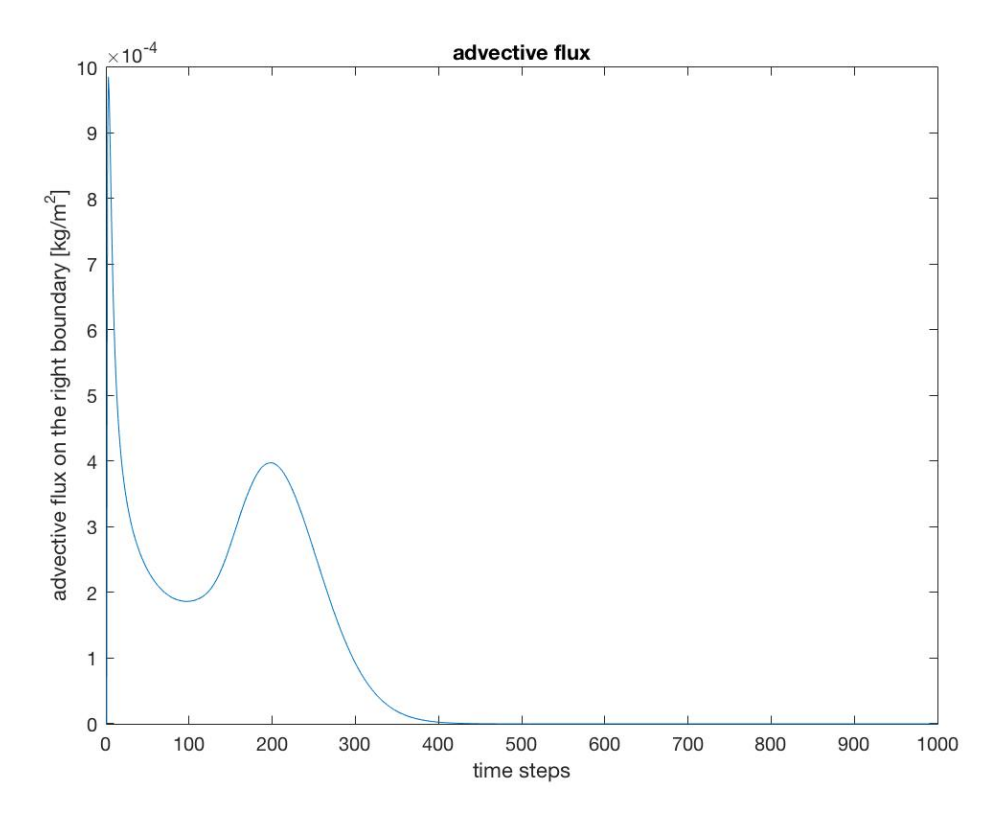


Figure 5.12

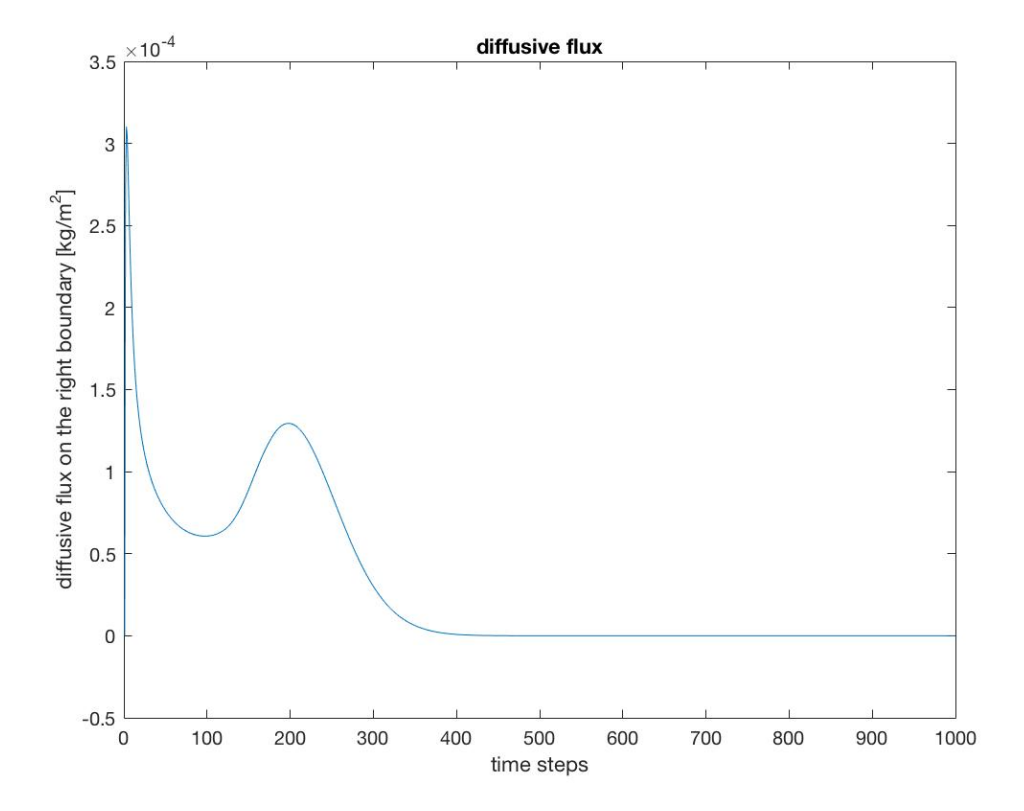


Figure 5.13

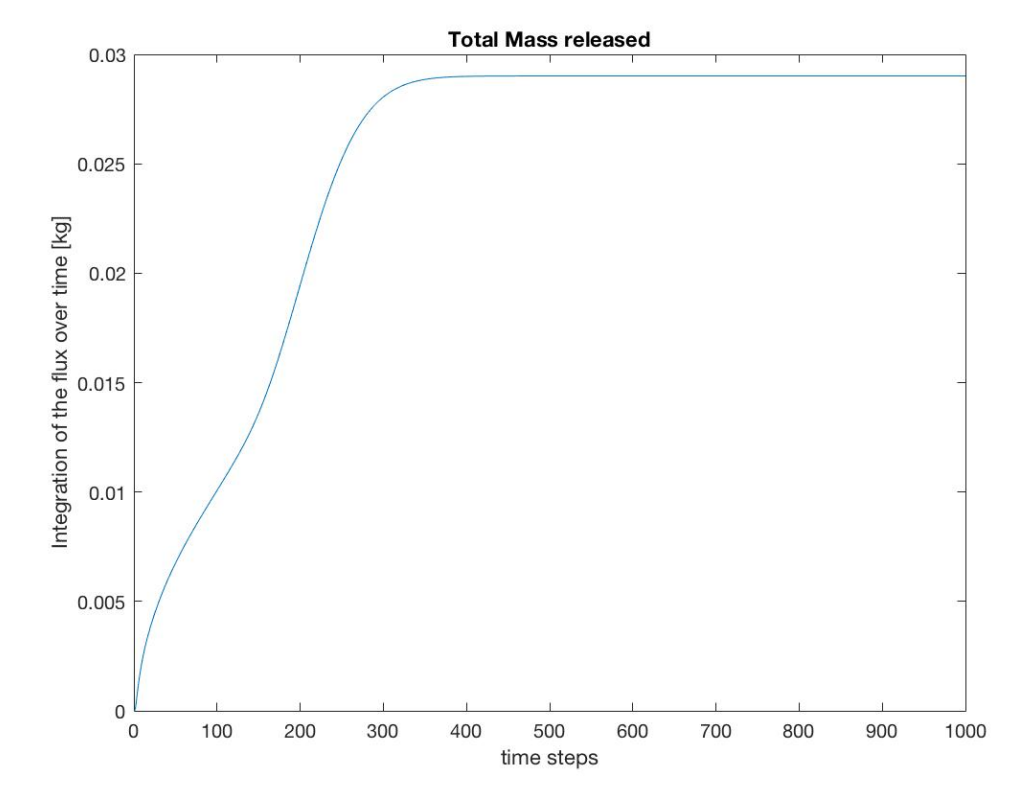


Figure 5.14: Integration of the flux over time at the left boundary

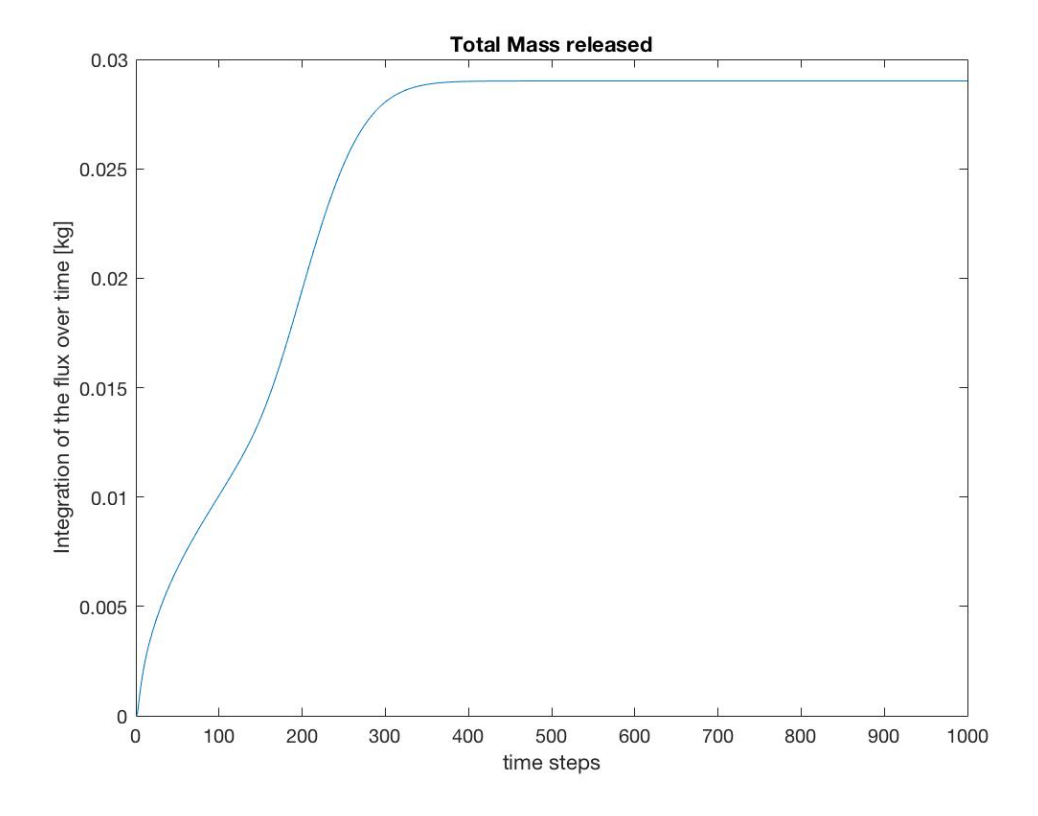


Figure 5.15: Integration of the flux over time at the right boundary

5.1.1. Robin Boundary Condition

In this section Robin Boundary Conditions for Temperature will be given.

$$\begin{cases} \frac{\partial C_A(L,t)}{\partial x} = -h_m(C_A - C_e) \\ \frac{\partial T(L,t)}{\partial x} = -h_{heat}(T - T_e) \\ \frac{\partial C_F(L,t)}{\partial x} = 0 \\ \frac{\partial C_A(0,t)}{\partial x} = h_m(C_A - C_e) \\ \frac{\partial T(0,t)}{\partial x} = h_{heat}(T - T_e) \\ \frac{\partial C_F(0,t)}{\partial x} = 0 \end{cases}$$

$$(5.7)$$

Where $T_e=1473,\ C_e=0,\ h_m=1$ and $h_{heat}=50.$ Initial conditions are $T=350,\ C_A=0$ and $C_F=0.15$

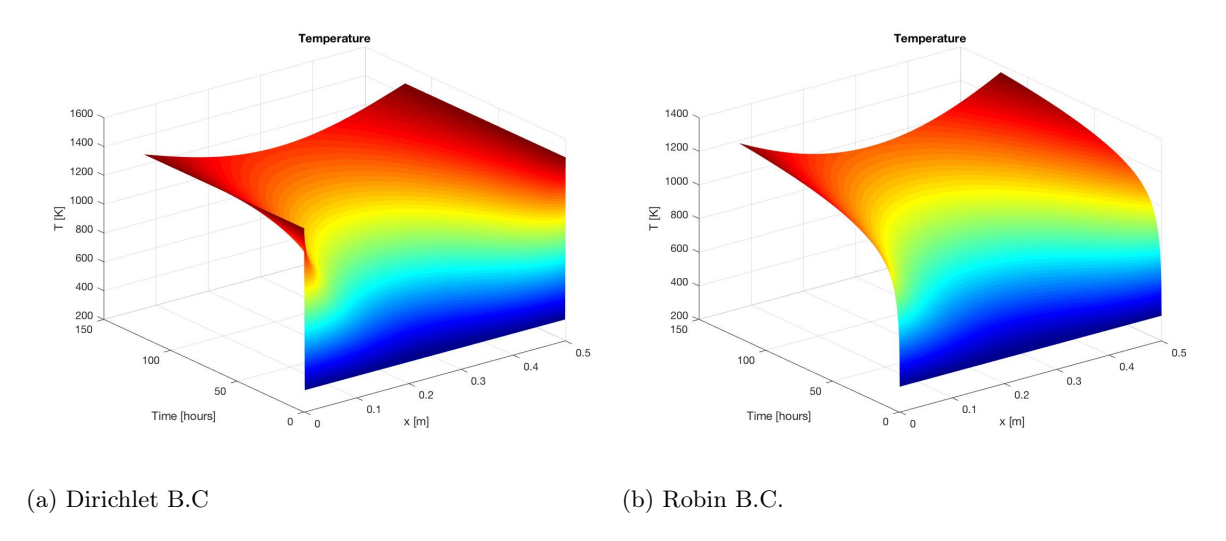


Figure 5.16: Difference between two boundary conditions

In Figure 5.16 two graphs of temperature given. The Figure 5.16a shows temperature profile with Dirichlet boundary condition, in this situation, it is assumed that anode placed between two hot walls. Thus, in comparison with the Robin boundary condition, in 5.16a temperature on the boundaries are sharp and from the beginning the same as wall temperature. While, in the Figure 5.16b we see that temperature on the boundaries goes to it's final destination slowly. A little bit faster than in the middle, but still slow with comparison 5.16a.

For Robin boundary condition we used h_{heat} heat transfer coefficient. Also, different values of heat transfer coefficient made an obvious changes in the behavior of the humidity and temperature. Moreover, heat transfer coefficient had an effect on the amount of released gases. By increasing and decreasing the value of h_{heat} , we can see how the amount of released gases raise and decline, correspondingly.

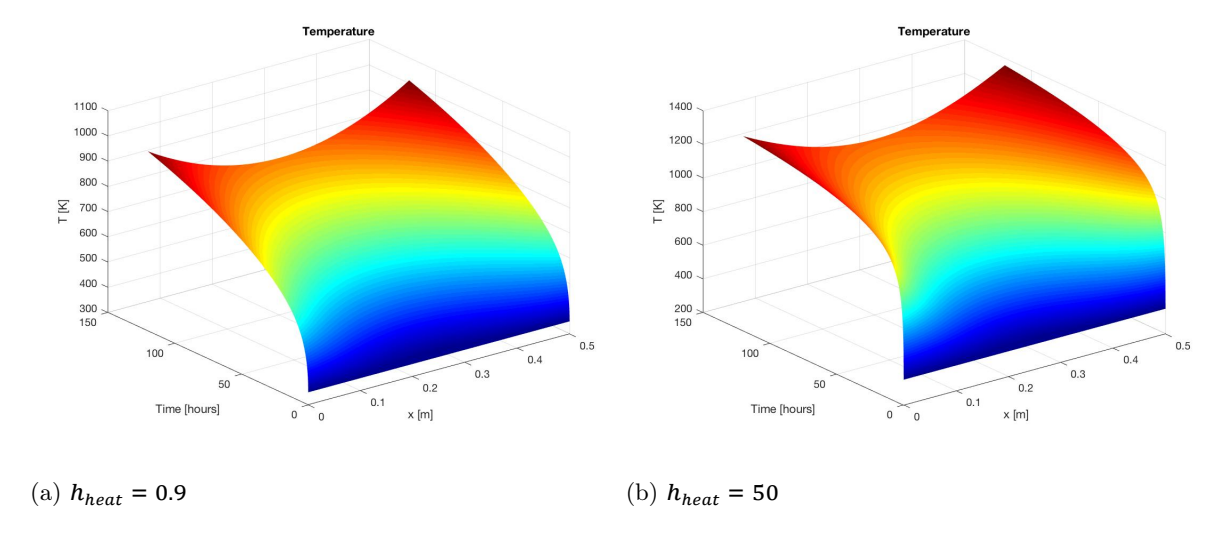


Figure 5.17: Temperature after using two different values of heat transfer coefficient

According to Figure 5.17 we may assume what is the role of the heat transfer coefficient. In the

Figure 5.17b temperature goes to the final value (wall temperature) faster than in Figure 5.17a. While, when $h_{heat} = 10$, temperature even could not reached wall temperature after 120h. Therefore, heat transfer coefficient works as pushing or stopping force of diffusion process. In other words, the higher the value of h_{heat} is, the faster heat diffusion is; the lower the value of h_{heat} is, the slower heat diffusion is.

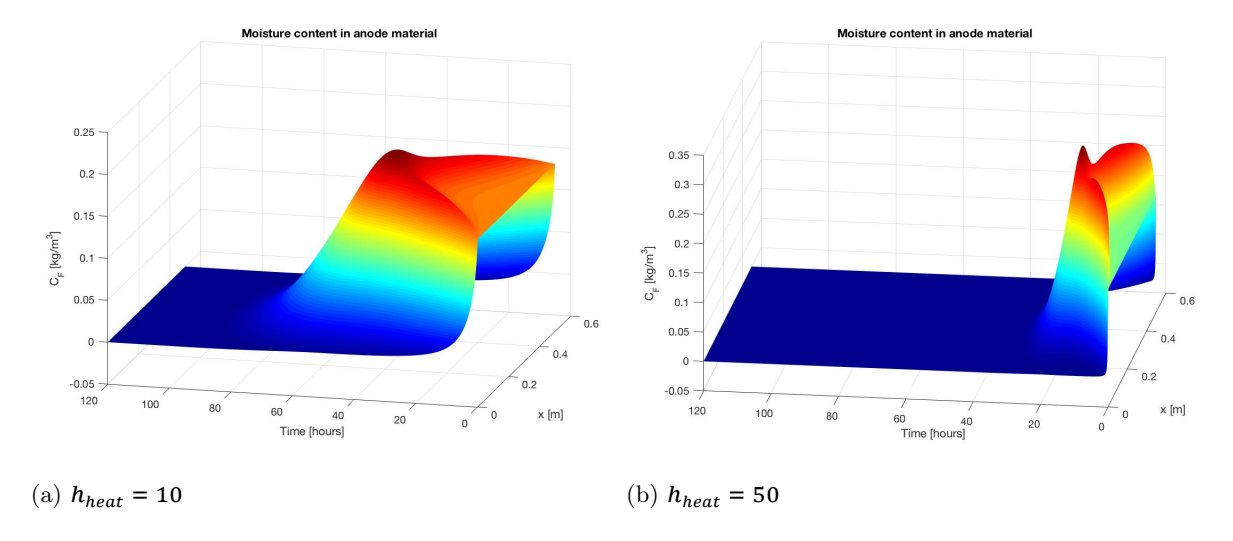


Figure 5.18: Moisture content in anode material after using two different values of heat transfer coefficient

Even if heat transfer coefficient appeared in the boundary condition of the temperature only, it has huge effect on moisture content of the material. The reason is that in this model mass and heat diffusion are related, and they are simultaneous processes. In consequence, the effect of h_{heat} on moisture content of the material is the same as the effect on the temperature behavior. Hence, if the value of h_{heat} is small, the moisture content of the material will change slowly; and if the value of h_{heat} is high, the moisture content of the material will change fast.

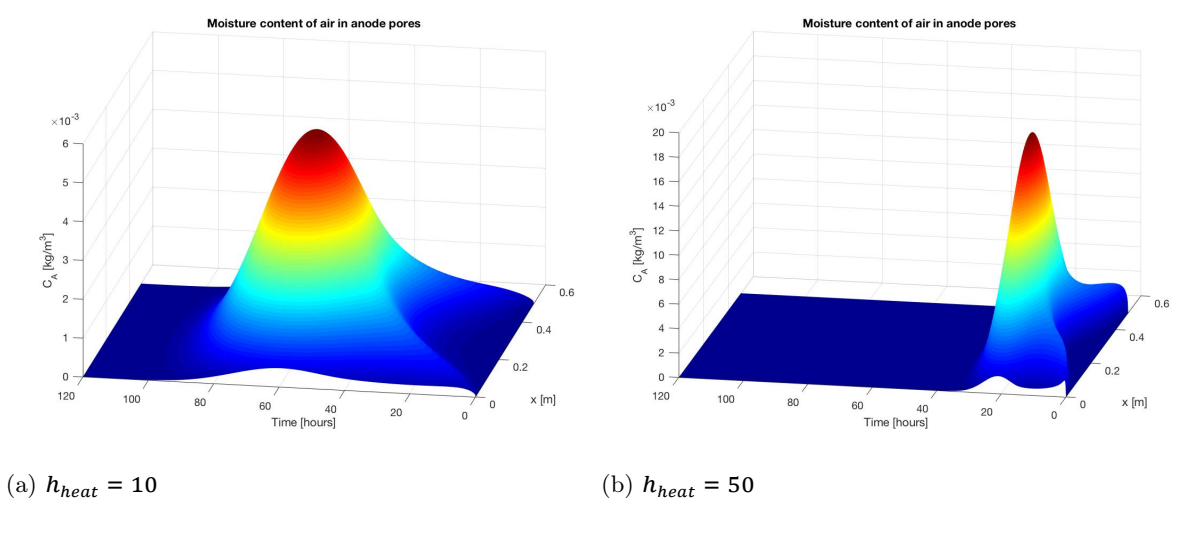


Figure 5.19: Moisture content in air pores after using two different values of heat transfer coefficient

Certainly, the moisture transportation in the air pores also felt change of heat transfer coefficient. The result of switch of the value of h_{heat} is as expected. For $h_{heat} = 10$ we got slow diffusion of water vapor in the air pores. Overall, different values of heat transfer coefficient gave reasonable changes in moisture and heat transport.

Further, the amount of released gases should be considered. Due to the fact that, by calculating the moisture diffusion in the air pores we found the amount of volatile gases. Here, one more thing must be noticed. By looking at Figures 5.18 and 5.19, it can be seen that in both graphs the peak values are different. For example, in 5.18a and 5.18b the max values of the moisture content in the material are 0.25 and 0.35, accordingly. It implies that, the high value of h_{heat} is the cause of releasing of more moisture. Likewise, in Figure 5.19 the graphs of moisture content in air pores has different peaks.

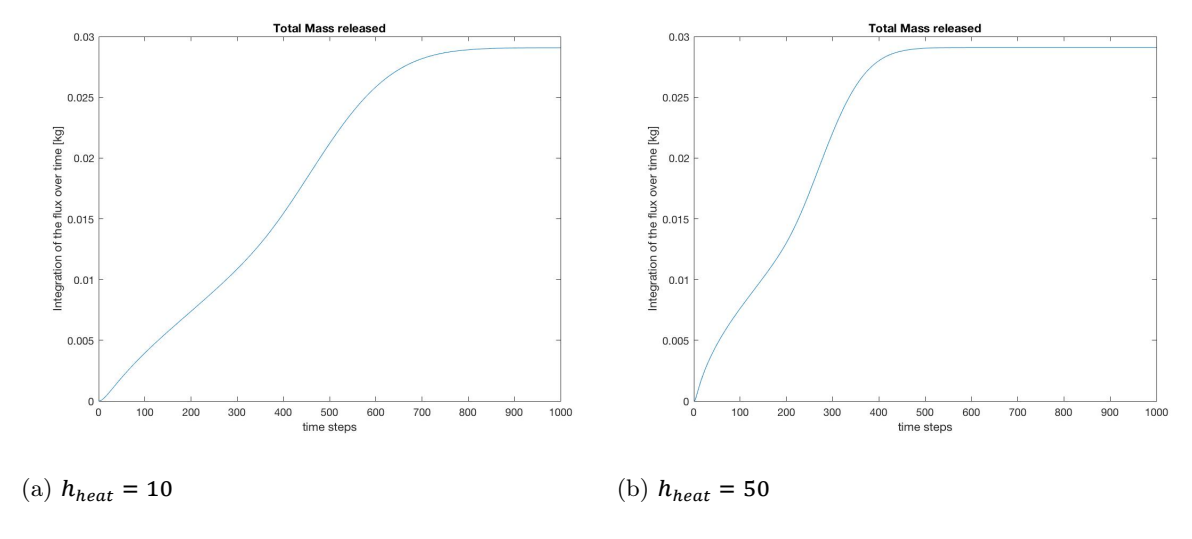


Figure 5.20: Mass released

According to the graph 5.20, it is obvious that with small value of heat transfer coefficient, the amount of mass released (the amount of volatile gases) are less than the amount of mass released with high h_{heat} . Even if two graphs has the same maximum value, in Figure 5.20b the curve reached the maximum value very fast and continued having that value till the end of the given time. Whereas, in Figure 5.20a maximum value of the curve captured after some time left. As a result, in case of $h_{heat} = 10$ the total amount of released gases is 37 kg, and in case of $h_{heat} = 50$ the total amount of released gases is 46 kg.

Further, we would like to back to rate equation from the model.

$$\frac{1}{\rho(1-\epsilon)}\frac{\partial C_F}{\partial t} = k(y_A - y_F)$$
 (5.8)

Where $y_A = \frac{C_A RT}{P_S}$ is a relative humidity of the air, $y_F = \frac{C_F}{\rho(1-\epsilon)}$ is the equilibrium relative humidity of the fiber and k is so called the constant between 0.01 and 10. We know that, with time difference between two humidities goes to zero and two surrounding comes to equilibrium. Now, let us think, what if y_A will be multiplied by some factor. For instance $\frac{1}{\rho(1-\epsilon)} \frac{\partial C_F}{\partial t} = k(10 * y_A - y_F)$.

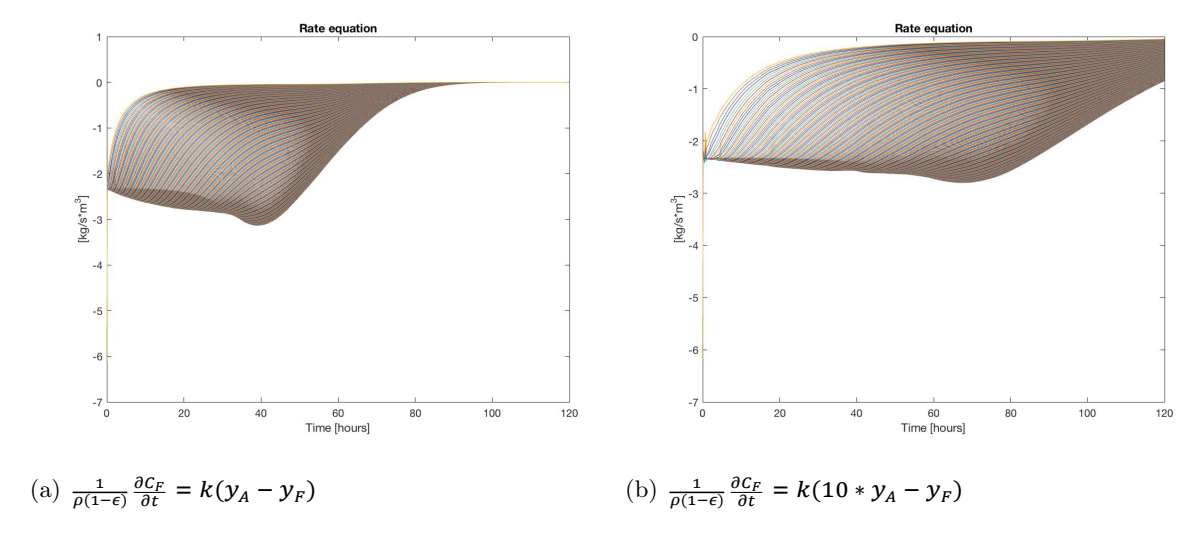


Figure 5.21: Rate equation without and with factor term

From the Figure 5.21 it can be concluded that graph 5.21b with factor term does not come to zero, and equality between air pores and material will not be achieved. We may assume that it leads to non-steady state solution for other variables.

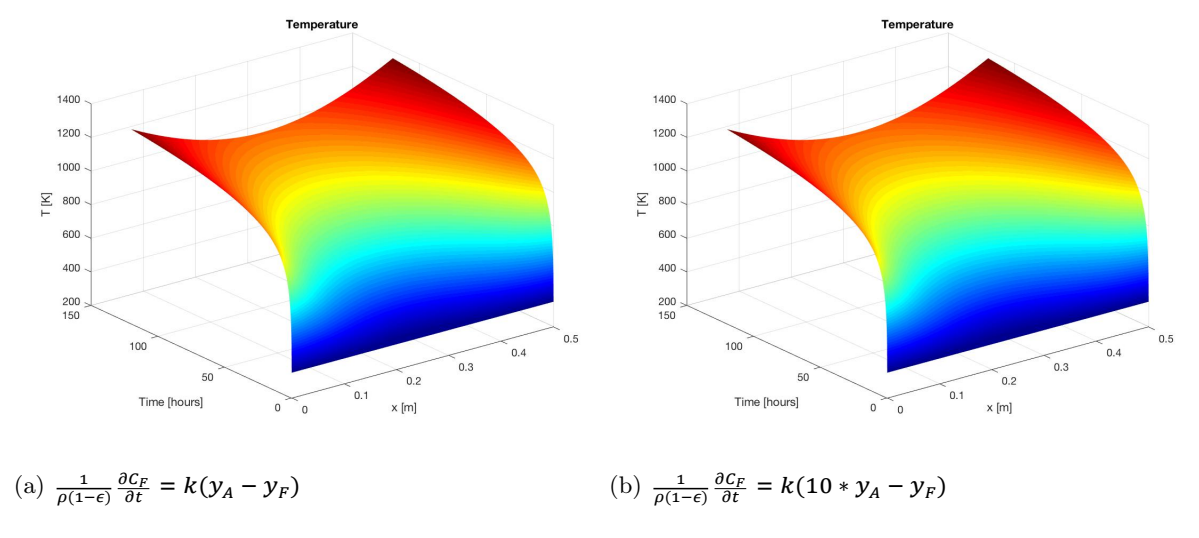


Figure 5.22: Temperature without and with factor term

In the Figure 5.22 temperature represented. However, there is no obvious difference between two graphs. Hence, at this point any conclusion for temperature distribution can be done.

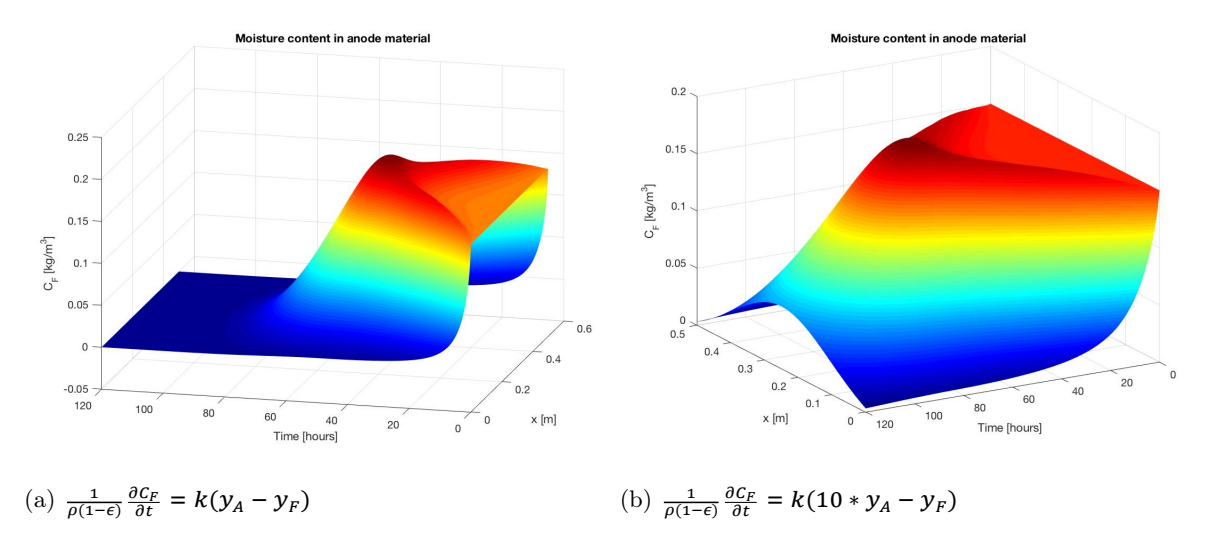


Figure 5.23: Moisture content in anode material without and with factor term

While, moisture content in the material shows huge contrast. The expected non-steady state solution is visible. In the end of 120 hours, the moisture content in anode material still deviating along x-axis.

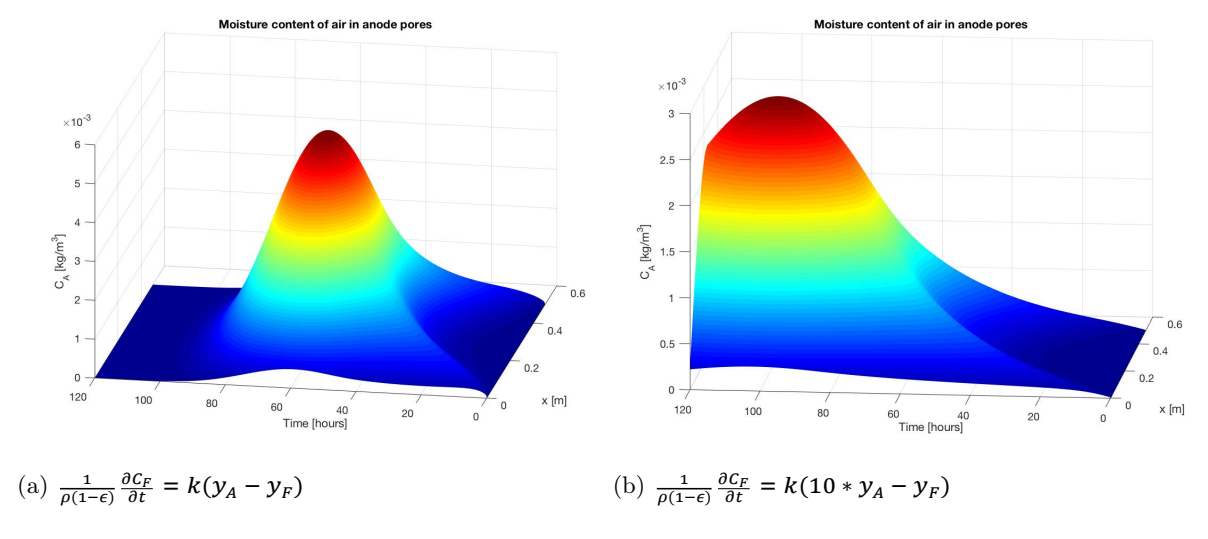


Figure 5.24: Moisture content in air pores without and with factor term

Results form the Figure 5.24 even stops on the peak. On the other hand, we know that C_A converges to C_e 's value.

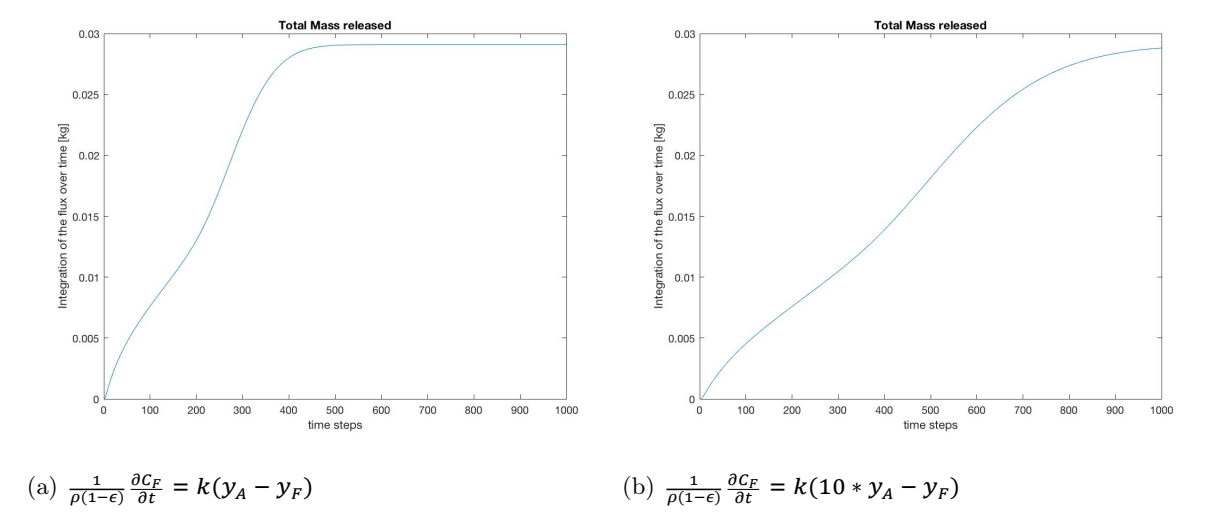


Figure 5.25: Mass released without and with factor term

Finally, this factor term has significant effect on the amount of released gases. Which make sense, because transport of moisture content was slower than in the case without multiplication to some factor. To be specific, in graph 5.25a amount of gases is 46 kg, in graph 5.25b that amount is 34 kg.

5.1.2. Homogeneous Neumann Boundary Condition

In this section we would like to look at the effect of the latent heat of evaporation (λ) in heat diffusion. From the equation below, we know that the term $\lambda \frac{\partial C_F}{\partial t}$ is considered as a additional heat source or so called sink term.

$$\rho C_v \frac{\partial T}{\partial t} = K \frac{\partial^2 T}{\partial x^2} + \lambda \frac{\partial C_F}{\partial t}$$
heat source

However, there are one more heat source, which are hot walls. Moreover, hot walls are the dominating heat source. Thus, the effect of the sink term can be visible only if we will remove from the boundary conditions the hot walls. Hence, the new boundary conditions will be as follow:

$$\begin{cases} \frac{\partial C_A(L,t)}{\partial x} = -h_m(C_A - C_e) \\ \frac{\partial T(L,t)}{\partial x} = 0 \\ \frac{\partial C_F(L,t)}{\partial x} = 0 \\ \frac{\partial C_A(0,t)}{\partial x} = h_m(C_A - C_e) \\ \frac{\partial T(0,t)}{\partial x} = 0 \\ \frac{\partial C_F(0,t)}{\partial x} = 0 \end{cases}$$

$$(5.9)$$

The Figure 5.26 represents temperature behavior with two different latent heat of evaporation (λ). Here, we can see how temperature decreases. On the other hand, you may ask why temperature declined even if there is a sink term. At this point, we would like to remind you that the rate equation (difference of two relative humidities) has always negative and zero values. As a result, sink term works as flowing

out sink. Thus, amount of decreased temperature, it is an energy what was used for drying. As there are no heating term, the material uses its own energy. In consequence, high value of the latent heat of evaporation leads to dramatic loss of temperature.

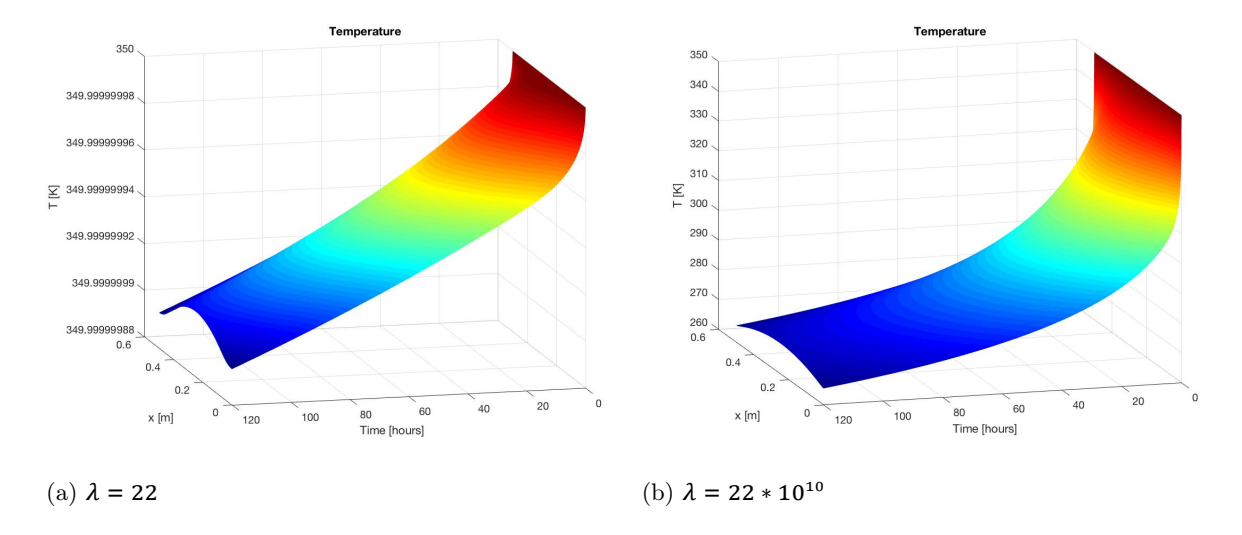


Figure 5.26: Effect of λ on Temperature profile

5.1.3. Radiation factor

Up to this point, we did not consider radiation factor (or existence of radiation). To be specific, here we are talking about thermal radiation, due to high temperature during the anode baking process. Previously, we have not consider radiation, because textile drying does not require heating up to high temperature, thus effect of radiation was negligible. However, thermal radiation can appear in any medium, as a result of temperature increase. It occurs due to the chaotic movement of the atoms and molecules in the material. Hence, we also decide to add the effect of radiation into the drying model. The radiation appears in the boundary condition of the heat equation. It describes radiative heat transfer between the given surface and external heat source of the model.

$$\begin{cases} \frac{\partial C_A(L,t)}{\partial x} = -(C_A - C_e) \\ \frac{\partial T(L,t)}{\partial x} = -(h_{heat}(T - T_e) + h_e(T^4 - T_e^4)) \\ \frac{\partial C_F(L,t)}{\partial x} = 0 \\ \frac{\partial C_A(0,t)}{\partial x} = (C_A - C_e) \\ \frac{\partial T(0,t)}{\partial x} = h_{heat}(T - T_e) + h_e(T^4 - T_e^4) \\ \frac{\partial C_F(0,t)}{\partial x} = 0 \end{cases}$$

$$(5.10)$$

Where h_e stands for radiation constant. The different values of h_e will be considered further.

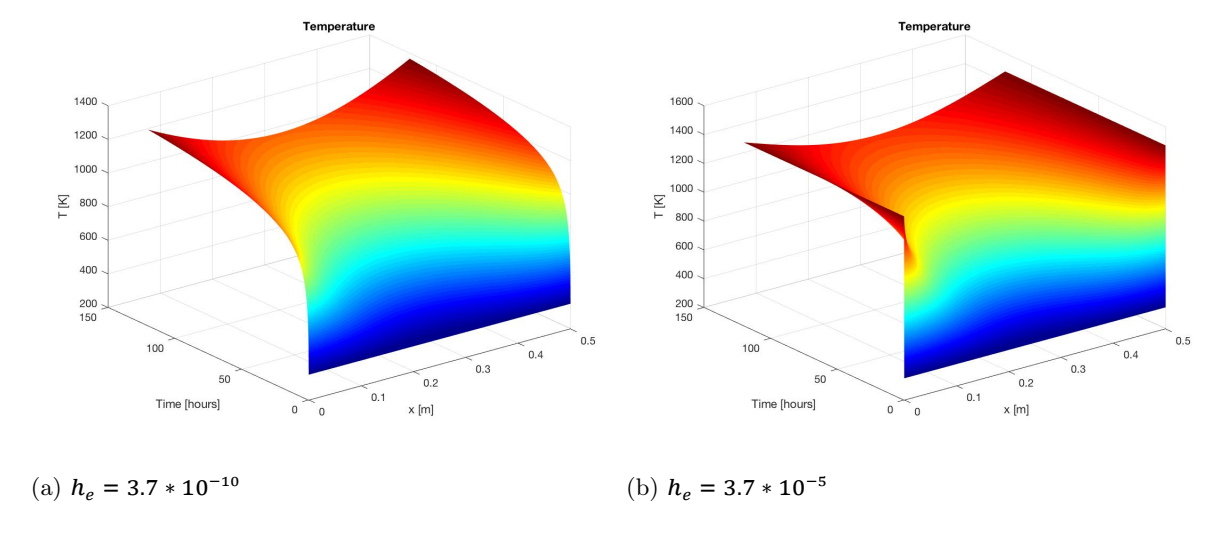


Figure 5.27: The effect of radiation constant

Interesting discovery from Figure 5.27 is that when we use small radiation constant (left picture), the result is similar to what we get when we apply Robin boundary condition. On the other hand, for $h_e > c$, where $c \approx 3.7 * 10^{-8}$, we get similar result as in case of using Dirichlet boundary condition.

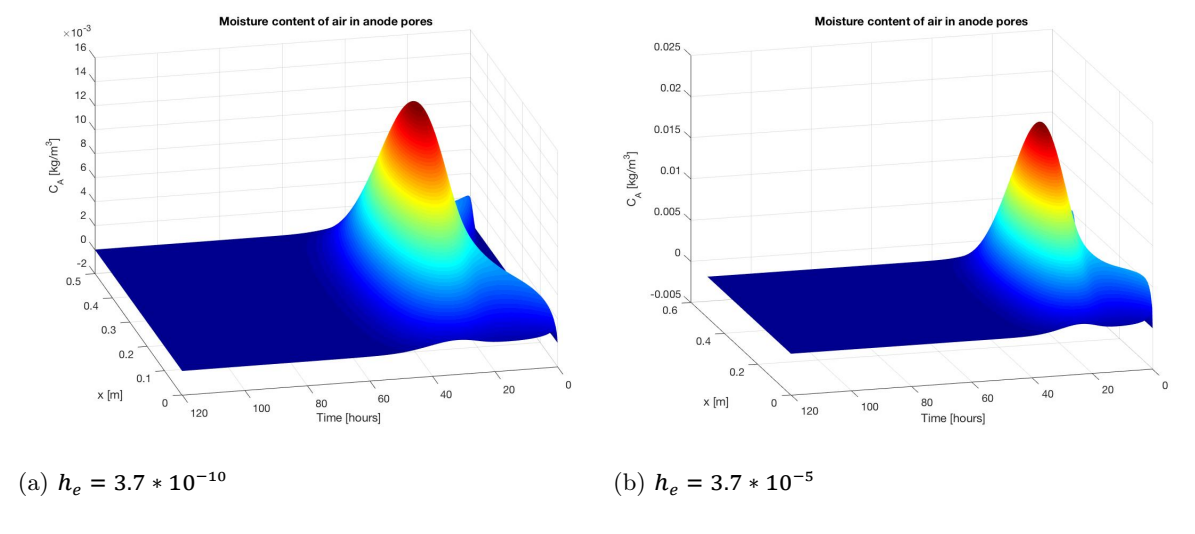


Figure 5.28: The effect of radiation constant

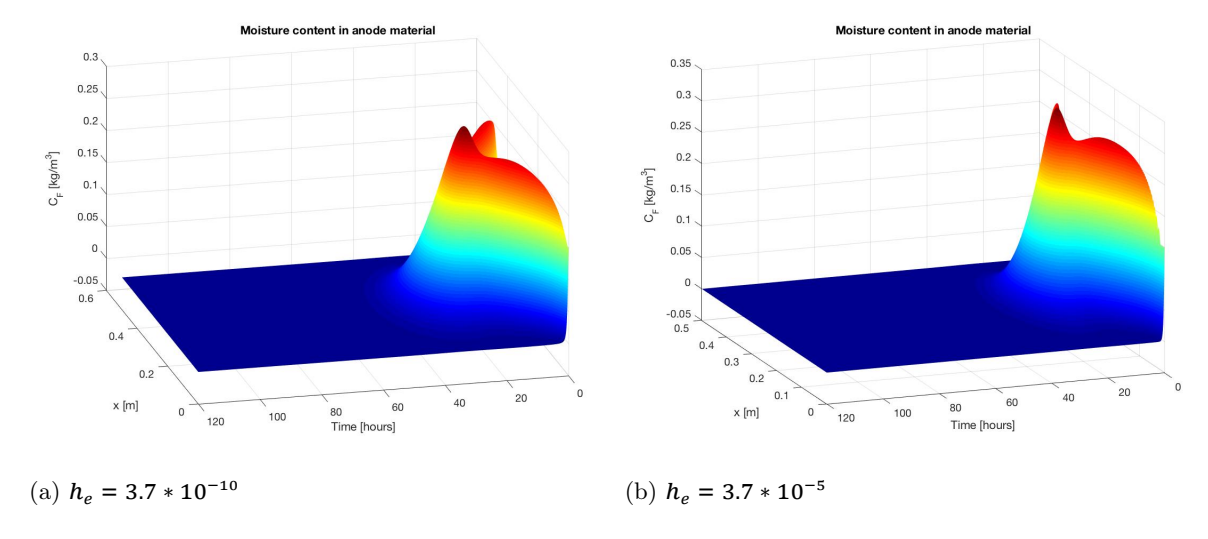


Figure 5.29: The effect of radiation constant

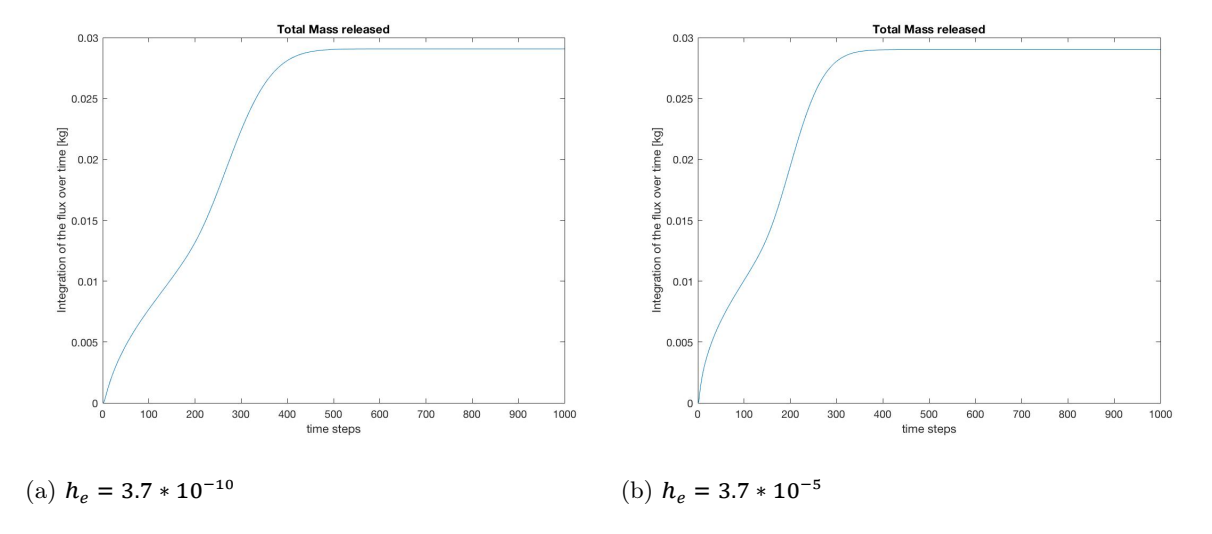


Figure 5.30: The effect of radiation constant

As shown above, radiation heat transfer coefficient has effect on the baking process. However, the effect of the radiation heat transfer coefficient diminishes on solution. Thus, we decide to chose small values, in order to see how exactly it effects. From the Figure 5.30a we can conclude that the amount of released gases are less than in the case 5.30b.

5.1.4. Non-constant boundary condition

Thus far, we consider only heating phase, where temperature in the furnace was fixed on its maximum value. However, the anode placed in a room temperature oven, and only then the pre-heating process begins. Hence, we assume that now, boundary conditions for temperature profile will be non-homogeneous

Dirichlet.

$$\begin{cases} \frac{\partial C_A(L,t)}{\partial x} = -h_m(C_A - C_e) \\ T(L,t) = -T_{wall} \\ \frac{\partial C_F(L,t)}{\partial x} = 0 \\ \frac{\partial C_A(0,t)}{\partial x} = h_m(C_A - C_e) \\ T(0,t) = T_{wall} \\ \frac{\partial C_F(0,t)}{\partial x} = 0 \end{cases}$$
(5.11)

where T_{wall} is a function as in Figure 5.31. This function was built to show the temperature acceleration in the combustion section. First, it started at room temperature, then the process of fuel burning began, so temperature increases with time.

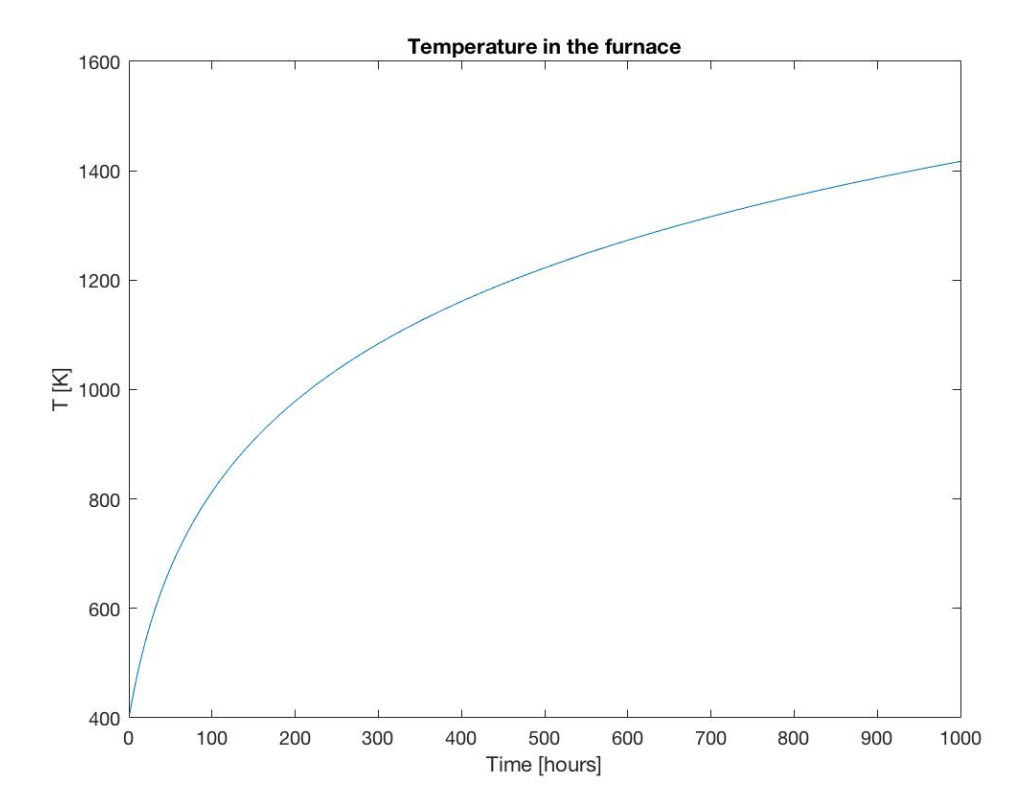
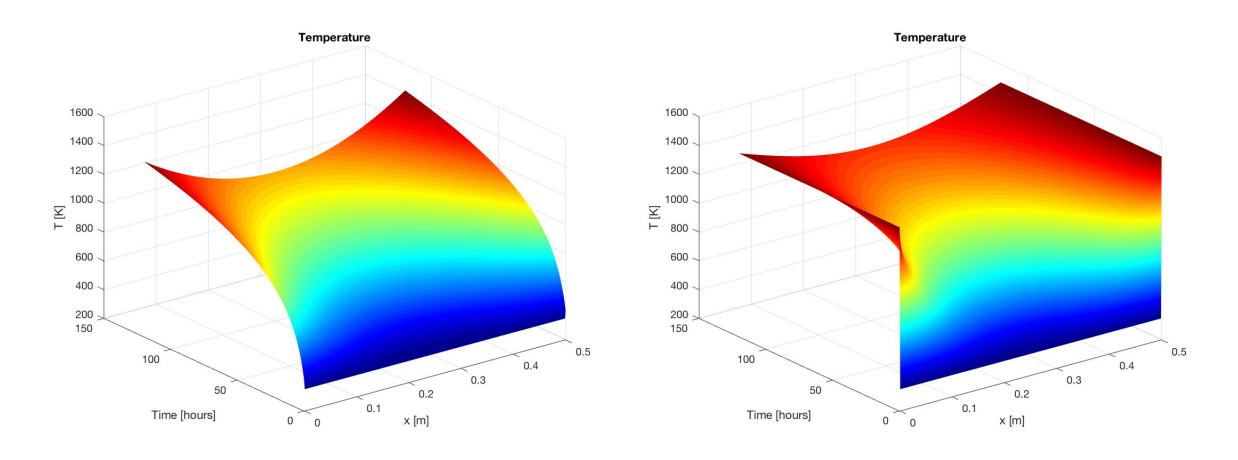


Figure 5.31: Temperature distribution starts at the room temperature and increases up to $1400~\mathrm{K}$

Now, we can not expect that temperature profile on the boundaries will reach maximum temperature at time zero. The Figure below shows comparison between constant valued Dirichlet boundary condition and function valued one.



- (a) Function valued Dirichlet B.C.
- (b) Constant valued Dirichlet B.C.

Figure 5.32: Different boundary conditions

From the Figure 5.32, it can be concluded that with new boundary conditions, it is needed more time for anode baking process. Thus, it can be considered as a pre-heating phase. Pre-heating plus heating phases should continue 280 hours.

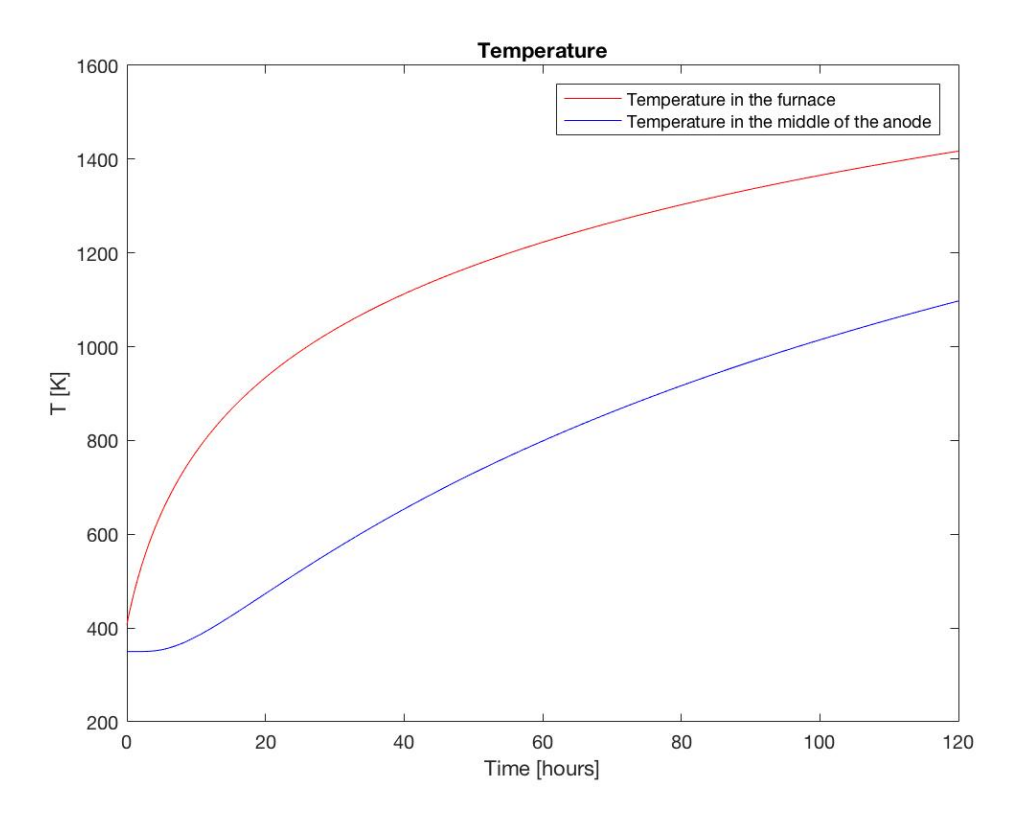


Figure 5.33: Temperature in the middle of the anode and in the furnace

The graph above 5.33 shows that the temperature in the middle of the anode has a maximum at 1000 Kelvin, in the given time. While, when we used constant valued Dirichlet boundary condition,

temperature in the middle of the anode reaches almost 1200 Kelvin, as in the Figure 5.34. Important thing that here, in Figure 5.34, accelerating furnace temperature does not included into boundary conditions, it is for comparison only.

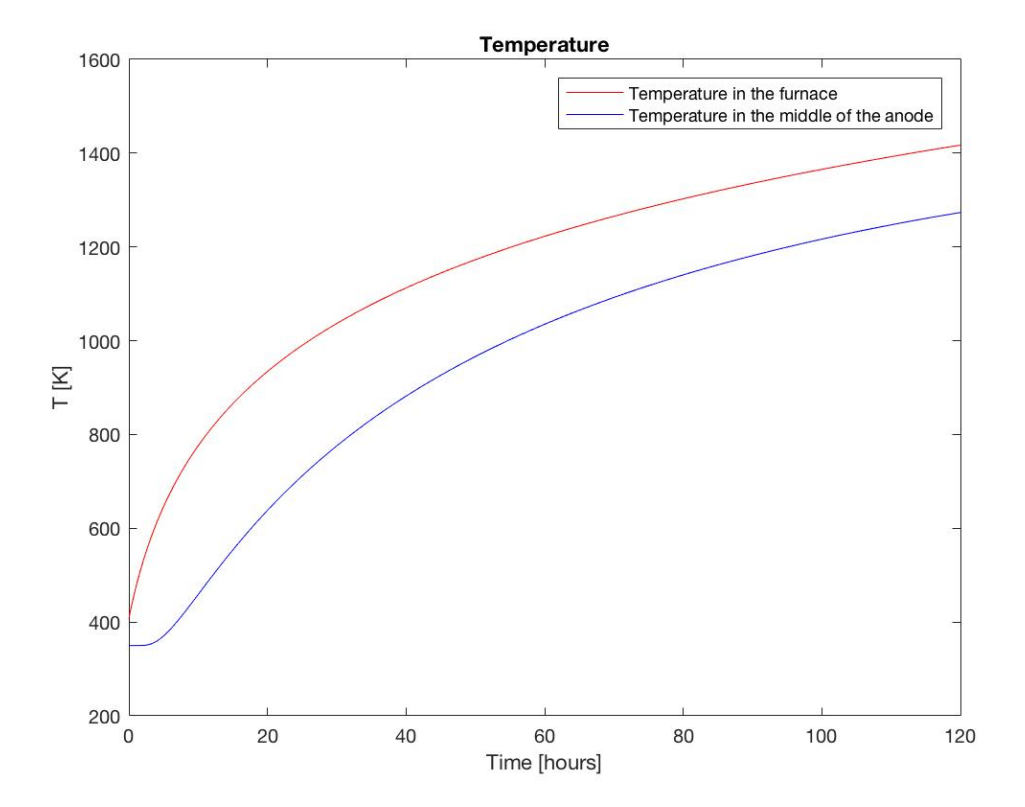


Figure 5.34: Temperature in the middle of the anode and in the furnace



Conclusion - Discussion - Recommendation for Future Work

In conclusion, the aim of this work is to construct mathematical model for evaporated gases from the anode material, and solve for the volume of the evaporated gases. Thus, understanding the heat and moisture diffusion during the drying process was essential. As a literature study, we try to replicate the results of [21]. After investigation of the mass and heat diffusion of the textile, it can be concluded that the moisture transportation in the textile during the volatile humidity conditions can be described by the following equations: moisture diffusion in the air pores of the material and heat transfer in the material.

Consequently, mathematical model of the textile drying was applied to the anode in the furnace. This is simply because of the common sense that in both processes (baking and drying) heat is applied gradually to evaporate excess moisture from the material without burning it. The system of equations of drying process can be customized by changing material parameters. Moreover, into the equation of moisture content in the void space the advective term with velocity field was added, to consider the movement of of the water drops. This allowed us to transform it to anode baking. After that, real sizes of the furnace, baking time and characteristics of the anode material were used. Moreover, according to the literature, experimental observations showed that the typical anode loses 55 kg out of 1155 kg of initial weight, after baking process, which is 4.8% [1]. Furthermore, our computations based on the given mathematical model gave approximately 40 - 50 kg of weight loss out of approximately 1047 kg (3.8% - 4.8%). The result gives us good confirmation about the way of calculation the volatile gases and choice of the system of equations.

In simple words, the importance of this work is to calculate the amount of released gases from the anode that accounts for 30% - 40% of the total energy consumption. Most of the literature in describing anode baking used only heat equation. The novelty of this thesis is in using more advanced textile drying model with the total flux definition. This means that the huge part of energy consumption was not investigated properly. Moreover, in our work, we also considered the dependencies between the volume of volatiles and the parameters of the material. For example, change of thermal diffusivity by sigmoid function led to less amount of emitted gases. Meantime, the sigmoid is a function of temperature, which means people can control the volume of volatiles by simply changing the temperature. This can help us in optimizing energy consumption, i.e. more efficient use of energy.

In this study, we simplified several parts of the model. Thus, if someone wants to further research this topic, there are a number of recommendations we would like to make.

- 1. Obviously, first advise is enlarge the dimension of the computational domain. If now it is in 1D, in future it can be done in 2D, or even better in 3D. Where all the dimensions (height, length, width) of the furnace and anode will be taken into account. In this case, the directions of the heat, moisture and other flows will be visualized.
- 2. Second recommendation is going to be about density parameter. We assumed that density parameter is constant during the whole process. However, if we take a simple example of pottery making, we can see that the pottery roasting process changes the density of the clay. The same principle applies in our case. Therefore, density has to be taken as a varying parameter. For example, one can take density as a function of moisture content of the air pores and fibers (C_A, C_F) .
- 3. Next, to reduce the complexity, in our work we omitted existence of the packing coke between hot walls and anode. Thus, to get more precise results, existence of the packing coke should appear in the equations, as a two different diffusion coefficients.
- 4. Fours recommendation is to consider the pore capacity. For instance, the regular dish washing sponge can absorb some fixed amount of water, but no more. We can assume the same situation, when humidity is high and all spores are occupied. This means when we apply heat, the movement of water drops towards the center of anode is not possible. This will slow down the baking process. Here, we does not consider the situation above. Consequently, in some sense, this work is linear representation of the drying process. In future, more complex model can be build.
- 5. Final recommendation is about the chemical reactions during the baking process. Certainly, the paste of raw anode consists of different chemical ingredients. As a result, under the high temperature they will enter into chemical reactions with air and water, which is the cause of volatile gases (known

as secondary fuel). In this work, we assumed that the resulting gases are only water vapors. Hence, one could extend this for possible chemical reactions and consider different vapors. It will help to make more precise modelling and to understand ecological consequences of anode baking.

Appendix

A1. Nomenclature

 $D[m^2/s]$ - diffusion coefficient

 $C_A[kg/m^3]$ - moisture content of air in fabric pores

 $C_F[kg/m^3]$ - moisture content of fibers in a fabric

T[K] - temperature

 ϵ - porosity

K[kJ/mK] - thermal conductivity

 $\rho[kg/m^3]$ - density

 $C_v[kJ/kgK]$ - heat capacity of fabric

 $\lambda[kJ/kg]$ - latent heat of evaporation

 $q[W/m^2]$ - convective heat transfer rate

 $h_{heat}[kJ/m^2K]$ - heat transfer coefficient

 $h_e[kJ/sm^2K]$ - radiation heat transfer coefficient

 $T_e[K]$ - external air temperature

 $m[kg/m^2s]$ - mass transfer rate

 $h_m[m/s]$ - mass transfer coefficient

 $C_e[kg/m^3]$ - moisture content of external air

R[kJ/kgK] - gas constant

 $P_s[kg/m^2]$ - saturation pressure

 τ - effective tortuosity of fabric

 $W_c = C_F/\rho$

 $k[s^{-1}]$ - rate constant

A2. Matlab PDE solver

In Matlab there is a function pdepe, which can solve initial-boundary value problems for parabolic and elliptic partial differential equations in 1D. Even the system of non-linear differential equations may be solved by this function. The pdepe solves PDEs of the form

$$c(x,t,u,\frac{\partial u}{\partial x})\frac{\partial u}{\partial t} = x^{-m}\frac{\partial}{\partial x}\left(x^m f\left(x,t,u,\frac{\partial u}{\partial x}\right)\right) + s\left(x,t,u,\frac{\partial u}{\partial x}\right) \tag{6.1}$$

where m = 0, initial and boundary conditions need to satisfy the following forms:

$$u(x, t_0) = u_0(x) (6.2)$$

$$p(x,t,u) + q(x,t)f(x,t,u,\frac{\partial u}{\partial x}) = 0.$$
 (6.3)

PDE Toolbox from Matlab solves initial-boundary value problems for parabolic and elliptic partial differential equations using the finite element analysis [22].

Matlab script

```
x = linspace(0,0.5,500);
t = linspace(0,120,1000);
m = 0;
sol = pdepe(m, @pdefun ex2, @icfun ex2, @bcfun ex2, x, t);
c1 = sol(:,:,1);
c2 = sol(:,:,2);
c3 = sol(:,:,3);
% -----
figure
surf(x,t,c1)
shading interp;
colormap(jet);
title('Moisture content of air in anode pores')
xlabel('x [m]')
ylabel('Time [hours]')
zlabel('C_A[kg/m^3]')
% -----
figure
surf(x,t,c2)
shading interp;
colormap(jet);
title('Temperature')
xlabel('x [m]')
ylabel('Time [hours]')
zlabel('T [K]')
% -----
figure
surf(x,t,c3)
shading interp;
colormap(jet);
title('Moisture content in anode material')
xlabel('x [m]')
ylabel('Time [hours]')
{\rm zlabel}({}^{,}C_F[kg/m^3]{}^{,})
% -----
function [g,f,s] = pdefun_ex2(x,t,c, DcDx)
```

```
ka = 5 * 3600^3;
Ca = (175.03 + 20.04 * c(2) - 6 * 10^{-4} * c(2)^{2}) * 3600^{2};
pa = 1600;
tau = 1.5;
epsilon = 0.2;
lambda = (2.2 * 1e0) * 3600^2;
Da = (2.49*1e-5)*3600;
g = [epsilon; pa*Ca; 1];
f = [Da*epsilon/tau;ka; 0].* DcDx;
k prime = 12.8*3600;
Ps = \exp(20.386 - (5132/c(2))) * 133.322 * 3600^2;
R = 461 * 3600^2;
yA = (c(1)*c(2)*R)/(Ps);
yF = c(3)/(pa*(1-epsilon));
dCfdt = k prime*(yA-yF);
v = (1*1e-4)*3600;
s = [-(1-epsilon)*dCfdt; lambda*dCfdt; dCfdt] + [v*(x-(0.5)/2)^3; 0; 0].*DcDx;
end % -----
function c0 = icfun ex2(x)
c0 = [0;350;0.15];
end
function [pl, ql, pr, qr] = bcfun \exp(xl,cl,xr,cr,t)
Tw = 1473;
C_e = 0;
he = 0.08*3600;
hr = (3.7 * 1e - 8) * 3600^3;
hm = 5 * 3600^3;
pl = [-(cl(1)-C_e); -((cl(2)-Tw)*hm); 0];
ql = [1; 1; 0];
\mathrm{pr} = [(\mathrm{cr}(1)\text{-}\mathcal{C}_{\boldsymbol{e}});\,(\mathrm{cr}(2)\text{-}\mathrm{Tw})^*\mathrm{hm}\,\,;\,0];
qr = [1; 1; 0];
end
```

Matlab script

```
x = linspace(0,0.5,50);

t = linspace(0,120,1000);
```

```
[X,T] = meshgrid(x,t);
alpha=0.001;\\
L = 0.5;
T1 = 1473;
N = 1000;
u = 0;
for k=1:N
u = u + ((350 - T1) * (1 - (-1)^k)/(k * pi)) * sin(k * pi * X/L). * exp(-alpha * ((k * pi/L).^2) * T);
\operatorname{end}
u1 = T1 + u;
figure
\operatorname{surf}(X,T,u1)
shading interp;
colormap(jet)
title ('Temperature')
xlabel('x [m]')
ylabel('Time [hours]')
zlabel('T [K]')
```

Bibliography

- [1] Raja Javed Akhtar. Anode quality and bake furnace performance of emal. Light Metals, pages 1175-1179, 2012. URL https://www.rd-carbon.com/data/documents/research-development/RDC-3077-Anode-Quality.pdf.
- [2] M.N. Batoei S. Sadeghi B. Baharvand, M.A. Siahouei. Study on anode baking parameres in open-top and closed-type ring furnaces. Light Metals, pages 1145–1150–478, 2003. URL http://www.almahdi.ir/almahdi/uploads/2017/04/1-1.pdf.
- [3] D.D. Bank. Online ddb search, 2018. URL http://www.ddbst.com/ddb-search.html.
- [4] F. Becker and F. Goede. Ring pit furnaces for baking of high quality anodes an overview. Aluminium International Journal, pages 1–15, 2006. URL http://www.riedhammer.de/system/00/01/42/14219/633776329561250000_1.pdf.
- [5] Y. Ching-yu. Estimation of the temperature-dependent thermal conductivity in inverse heat conduction problems. Applied Mathematical Modelling, (23):469-478, 1999. URL https://ac.els-cdn.com/S0307904X98100938/1-s2.0-S0307904X98100938-main.pdf?_tid=e6483f4e-9e7d-468f-bc09-667e54badc2a&acdnat=1548951016_e0a0840c6919ef525e2751d208849481.
- [6] John M. Cimbala. The ideal gas constant, 2014. URL https://www.mne.psu.edu/cimbala/learning/general/gas_constant.pdf.
- [7] J. Current. Physics Related to Anesthesia. PediaPress, 2010.
- [8] A.K. Datta. Porous media approaches to studying simultaneous heat and mass transfer in food processes. i: Problem formulations. Journal of Food Engineering, 80, 2007.
- [9] A.K. Datta. Porous media approaches to studying simultaneous heat and mass transfer in food processes. ii: Property data and representative results. Journal of Food Engineering, 80, 2007.
- [10] P. Dawkins. Paul's online notes, 2019. URL http://tutorial.math.lamar.edu/Classes/ DE/HeatEqnNonZero.aspx.
- [11] D. Frydrych and P. Ralek. The solution of coupled heat and moisture diffusion with sorption for textiles. Proceedings of ALGORITMY, pages 53-63, 2005. URL http://pc2.iam.fmph.uniba.sk/amuc/_contributed/algo2005/frydrych-ralek.pdf.

70 Bibliography

[12] Fusiref. Anode baking furnace, 2019. URL https://www.fusiref.com/en/sectors/aluminium/anode-baking-furnace.

- [13] O. Gundersen. Modelling of structure and properties of soft carbons with application to carbon anode baking, 1998.
- [14] O. Gundersen and G. Balchen. Modeling and simulation of an anode carbon baking furnace. Modeling, Identification and Control, 16(1):3–33, 1995. doi: doi:10.4173/mic.1995.1.1.
- [15] A.K. Haghi. A mathematical model of the drying process. Acta Polytechnica, 41(3):20-23, 2001. URL https://ojs.cvut.cz/ojs/index.php/ap/article/view/226.
- [16] A.K. Haghi. Factors effecting water-vapor transport through fibers. Theoret. Appl. Mech., 30(4):277-309, 2003. URL http://www.ssm.org.rs/WebTAM/_private/V0L30_4/pdf_ format/hagh.pdf.
- [17] P. Henry and R. Pickard. Diffusion in absorbing media. Proceedings of the Royal Society of London. Series A. Mathematical and Physical Sciences., 171, 1939. ISSN 945. doi: https://doi.org/10.1098/rspa.1939.0062. URL https://royalsocietypublishing.org/author/ Pickard%2C+Robert+Howson.
- [18] J. White B. Khoo J. Peraire, A. Patera. Finite element methods for elliptic problems. variational formulation: The poisson problem, 2003. URL https://ocw.mit.edu/courses/aeronautics-and-astronautics/ 16-920j-numerical-methods-for-partial-differential-equations-sma-5212-spring-200 lecture-notes/lecs13_14_notes.pdf.
- [19] F. Keller and P.Sulger. Anode baking, 2008. Sierre, Switzerland, RD Carbon Ltd.
- [20] Y. Li and J. Fan. Transient analysis of heat and moisture transfer with sorption/desorption and phase change in fibrous clothing insulation. Numerical Heat Transfer, Part A: Applications, 51(7): 635–655, 2007. doi: 10.1080/10407780600936327.
- [21] Y. Li and Z. Luo. An improved simulation of the coupled diffusion of moisture and heat in wool fabric. Textile Research Journal, 10(69):760–768, 1998. doi: doi:10.1177/004051759906901010.
- [22] MathWorks. Partial differential equations, 2018. URL https://nl.mathworks.com/help/matlab/math/partial-differential-equations.html#brfhgfv-1.
- [23] P. Nordon and H.G. David. Coupled diffusion of moisture and heat in hygroscopic textile materials. International Journal of Heat and Mass Transfer, 10(7):853 866, 1967. ISSN 0017-9310. doi: https://doi.org/10.1016/0017-9310(67)90065-8. URL http://www.sciencedirect.com/science/article/pii/0017931067900658,.

Bibliography 71

[24] M. Meier et al W.Fischer, R.Perruchoud. Anodes for the aluminium industry, 1995. Sierre, Switzerland, RD Carbon Ltd.

[25] M. Meier et al W.Fischer, R.Perruchoud. Anodes for the aluminium industry, 1995-2005. Sierre, Switzerland, RD Carbon Ltd.